COMPOSITION OF ATMOSPHERE AT THE CENTRAL ANATOLIA

A THESIS SUBMITTED TO
THE GRADUATE SCHOOL OF NATURAL AND APPLIED SCIENCES
OF
THE MIDDLE EAST TECHNICAL UNIVERSITY

BY

EBRU YÖRÜK

IN PARTIAL FULFILLMENT OF THE REQUIREMENTS FOR THE DEGREE
OF MASTER OF SCIENCE
IN
THE DEPARTMENT OF ENVIRONMENTAL ENGINEERING

JANUARY 2004

Approval of the Graduate School of Natural and Applied Sciences

_____

Prof. Dr. Canan Özgen
Director

I certify that this thesis satisfies all the requirements as a thesis for the Degree of Master Science.

_____

Prof. Dr. Filiz B. Dilek
Head of Department

This is to certify that we have read this thesis and that in our opinion it is fully adequate, in scope and quality, as a thesis for the Degree of Master of Science.

_____

Prof. Dr. Gürdal Tuncel
Supervisor

Examining Committee Members

Prof. Dr. Ülkü Yetiş _____

Prof. Dr. Gürdal Tuncel _____

Prof. Dr. Celal F. Gökçay _____

Assoc. Prof. Gülen Güllü _____

Dr. İpek İmamoğlu _____

ABSTRACT

COMPOSITION OF ATMOSPHERE AT CENTRAL ANATOLIA

Yörük, Ebru

M. Sc., Department of Environmental Engineering

Supervisor: Prof. Dr. Gürdal Tuncel

January 2004,179 pages

Concentrations of elements and ions measured in samples collected between February 1993 and December 2000 at a rural site in central Anatolia were investigated to evaluate the chemical composition of atmosphere at central Anatolia, to determine pollution level of the region, to study temporal variability of the pollutants and to investigate the sources and source regions of air pollutants in the region.

Level of pollution at central Anatolia was found to be lower than the pollution level at other European countries and Mediterranean and Black Sea regions of Turkey.

Enrichment factor calculations revealed that SO_4^{2-}, Pb and Ca are highly enriched in the aerosol; whereas, soil component has dominating contribution on observed concentrations of V, Mg, Ca and K.

$SO_4^{2-}/(SO_2+SO_4^{2-})$ ratio observed in Çubuk station indicates that contribution of distant sources is more important than the contribution of local sources on observed SO_4^{2-} levels. SO_4^{2-}/NO_3^- ratio calculations showed that Central Anatolia is receipt of SO_4^{2-} from Eastern European countries.

Positive Matrix Factorization (PMF) analysis revealed 6 source groups, namely motor vehicle source, mixed urban factor, long range transport factor, soil factor, NO_3^- factor and Cd factor.

Distribution of Potential Source Contribution Function (PSCF) values showed that main source areas of SO_4^{2-}, NH_4^+ and Cd are western parts of Turkey, Balkan countries, central and western Europe, central Russian Federation and north of Sweden and Finland; NO_3^- are the regions located around the Mediterranean Sea; and there is no very strong potential source area observed for NH_3 and Pb.

Keywords: Aerosols, Central Anatolia, Enrichment Factors, Gaseous Pollutants, Pollution Level, Positive Matrix Factorization, Potential Source Contribution Function, $SO_4^{2-}/(SO_2+SO_4^{2-})$ Ratio, SO_4^{2-}/NO_3^- Ratio

ÖZ

ORTA ANADOLU'DA ATMOSFERİN KOMPOZİSYONUNUN BELİRLENMESİ

Yörük, Ebru

Yüksek Lisans, Çevre Mühendisliği Bölümü

Tez yöneticisi: Prof. Dr. Gürdal Tuncel

Ocak 2004, 179 sayfa

Orta Anadolu'da bulunan kırsal bir istasyonda Şubat 1993 - Aralık 2000 tarihleri arasında toplanan element ve iyon örnekleri incelenmiştir. Bu çalışma bölgenin kirlilik düzeyini tespit etmek, kirletici konsantrasyonlarının zaman içindeki değişimlerini incelemek ve bölgede tespit edilen kirleticilerin kaynak ve kaynak bölgelerini belirlemek üzere yapılmıştır.

Orta Anadolu'nun kirlilik düzeyinin diğer Avrupa ülkelerinden ve Türkiye'nin Akdeniz ve Karadeniz bölgelerinden daha düşük olduğu tespit edilmiştir.

Zenginleşme faktörleri hesapları SO_4^{2-}, Pb ve Ca element ve iyonlarının atmosferde toprağa göre oldukça zenginleştiklerini; V, Mg, Ca ve K

elementlerinin atmosferdeki konsantrasyonlarında toprak kaynağının belirleyici olduğunu göstermektedir.

Çubuk istasyonunda tespit edilen $SO_4^{2-}/(SO_2+SO_4^{2-})$ oranları uzun mesafeli taşınımın ölçülen SO_4^{2-} konsantrasyonları üzerinde yerel kaynaklardan daha etkili olduğunu göstermektedir. Hesaplanan SO_4^{2-}/NO_3^- oranları tespit edilen SO_4^{2-} konsantrasyonlarının bölgeye Doğu Avrupa üzerinden uzun mesafeli taşınımla taşındığını göstermektedir.

Pozitif Matriks Faktörizasyonu (PMF) analizi Orta Anadolu'da 6 ana kaynak belirlemiştir. Bunlar motorlu taşıtlar faktörü, karışık kentsel faktör,uzun mesafeli taşınım faktörü, toprak faktörü, NO_3^- faktörü ve Cd faktörüdür.

Potansiyel Kaynak Katkı Fonksiyonu (PKKF) değerlerinin dağılımı bölgede tespit edilen SO_4^{2-}, NH_4^+ ve Cd'un ana kaynaklarının Türkiye'nin batısı, Balkan ülkeleri, orta ve batı Avrupa, Rusya'nın orta bölgeleri ve İsveç ve Finlandiya'nın kuzey olduğunu göstermektedir. NO_3^-'ün hesaplanan PKKF değerleri bu elementin ana kaynaklarının Akdeniz çevresinde bulunduğunu göstermektedir. PKKF tekniği NH_3 ve Pb'nin hiçbir güçlü kaynak bölgeye sahip olmadığını göstermektedir.

Anahtar Kelimeler: Aerosoller, Gaz Fazlı Kirleticiler, Kirlilik Düzeyi, Orta Anadolu, Pozitif Matriks Faktorizasyonu, Potansiyel Kaynak Katkı Fonksiyonu (PKKF), $SO_4^{2-}/(SO_2+SO_4^{2-})$ Oranı, SO_4^{2-}/NO_3^- Oranı, Zenginleşme Faktörleri

To my dear family...

ACKNOWLEDGEMENTS

I would like to take this opportunity to extend my deepest gratitude to my supervisor, Prof.Dr. Gürdal TUNCEL, of the Department of Environmental Engineering, Middle East Technical University. His guidance and superb analytical skill have been instrumental in the success of this thesis.

Special acknowledgement is also given to Refik Saydam Hygiene Center for providing us with the data obtained from Çubuk station. I am also grateful to Mrs. Canan YEŞİLYURT in the Refik Saydam Hygiene Center for her assistance and companionship throughout the research.

Due recognition should also be given to Fatma ÖZTÜRK, Güray DOĞAN, Mihriban YILMAZ and Öznur OĞUZ from the Department Of Environmental Engineering, Middle East Technical University, for their understanding, co-operation and for being good friends.

Special thanks to my dear fiancé Bülent TUNA for his encouragement over the last one year.

Last but not least I am grateful to my wonderful parents that are giving me a great moral support.

TABLE OF CONTENTS

LIST OF TABLES

LIST OF FIGURES

CHAPTER 1

INTRODUCTION

1.1. Framework

Aerosols are of great concern in the last decay because of its effects on Earth's radiation budget and atmospheric chemistry. Aerosols are generally contained in the boundary layer and removed from the atmosphere in a short time due to both wet and dry deposition. Having such short residence time they can be transported only at a regional scale. On the other hand, some of the aerosols can reach upper troposphere. These aerosols have significantly longer residence times and can be long range transported to hundreds to thousands kilometers.

The international action on long range transport of air pollutants is first started with the 1972 United Nations Conference on the Human Environment in Stockholm which signaled the increasing acid rain problems in Europe. Long-range Transport of Air Pollutants (LRTAP) study conducted in 1972 is the first international study on the long-range transport. In this project, wet deposition of sulfur compounds in Western Europe is studied. This study points out that though the countries with the largest sulfur dioxide emissions received the largest acid deposition, five countries, namely Norway, Sweden, Finland, Austria and Switzerland imported more pollution from other countries than they received from their own sources (Elsom, 1987).

The findings of this project implied that cooperation at the international level was necessary to solve environmental problems such as acidification. In response to these acute problems United Nations Economic Commission for Europe (UNECE) initiated a special programme, namely Co-operative Programme for Monitoring and Evaluation of Long-range Transmission of Air Pollutants in Europe (EMEP), in 1977. Later, a High-level Meeting within the Framework of the Economic Commission for Europe (ECE) on the Protection of the Environment was held at ministerial level in November 1979 in Geneva. It resulted in the signature of the Convention on Long-range Transboundary Air Pollution by 34 Governments and the European Community (EC). After put into force in 1983, EMEP has become a sub-programme of the Convention.

Initially, the EMEP programme focused on assessing the transboundary transport of acidification and eutrophication; later, the scope of the programme has widened to address the formation of ground level ozone and, more recently, of persistent organic pollutants (POPs), heavy metals and particulate matter. The EMEP programme relies on three main elements: (1) collection of emission data, (2) measurements of air and precipitation quality and (3) modelling of atmospheric transport and deposition of air pollution. At present, about 100 monitoring stations in 24 ECE countries participate in the programme.

Turkey signed the Convention on Long-range Transboundary Air Pollution in 1984 and joined to the EMEP Network with Çubuk station in 1992.

1.2. Objectives of the Study

It is fairly well established in the literature that Mediterranean region is under strong influence of pollutants transported over industrialized European countries (Güllü et al., 2000; Luria et al.,1999; Molinaroli et

al., 1999). Consequently any data generated in this region is vitally important to understand levels and source regions of pollutants. Although some data are now available for the eastern Mediterranean, data is lacking for the central Anatolia and Black Sea regions.

The main objective of this study is to evaluate chemical composition of atmosphere at the central Anatolia and to determine levels, temporal variability, sources and source regions of air pollutants in this region.

The data used in this study was generated by the Ministry of Health, Refik Saydam Hygiene Center at a rural station located at Çubuk as a part of the EMEP monitoring program between 1993 – 2000. The work by the Ministry of Health, Refik Saydam Hygiene Center resulted in one of the largest data sets available in the whole Mediterranean region. The data was transmitted to the EMEP center, but not evaluated to understand chemical composition of the atmosphere. In the EMEP, the data is used to calibrate the models and to make general assessments for regional pollution through comparison between approximately 100 EMEP stations operating in different parts of Europe. The data used in this study is obtained through a protocol between the Ministry of Health and the Middle East Technical University for more detailed evaluation.

In this study, data averages were compared with corresponding data from known clean and polluted atmospheres around the world to assess the level of pollution in the Central Anatolia.

Temporal variations of pollutants were investigated in two levels. (1) Short-term (episodic) variations and reasons for observed episodic nature of the data were investigated. (2) Long-term (seasonal) variations and factors affecting seasonality in concentrations were investigated.

The source regions affecting Central Anatolia were investigated using the following approaches. (1) Enrichment factors were investigated to

asses the contribution of soil source on concentrations of pollutants. (2) correlations between pollutants were investigated to understand groups of measured parameters that show similar pollutants. (3) SO_4^{2-}/NO_3^- ratio, which is expected to be different at the Eastern and Western Europe, were investigated to determine regions in Europe that can be responsible for pollutants observed at the Central Antolia. (4) positive matrix factorization method were performed to data set to determine covariances in the data set, which can be due to similar sources of measured parameters or due to similar transport patterns. (5) potential contribution function approach were used to determine locations of sources in Turkey and elsewhere that affect observed concentrations at the Central Anatolia.

In the following chapter one can find the background information about the aerosols and gaseous pollutants and a literature survey of studies conducted in Mediterranean region. This chapter also reviews the receptor oriented models that are used in the source apportionment studies.

The general information about the materials and methods used in this thesis is given in the third chapter. Detailed information about site selection, sampling methods and analytical techniques are given in the Appendix part.

The results of statistical treatment of data are discussed in the fourth chapter. The sources and source regions of air pollutants reached at the region which were determined through application of various receptor modeling techniques are also given in this chapter.

In the fifth chapter, the main outcomes of this thesis and some suggestions about further research are given.

CHAPTER 2

BACKGROUND

2.1. Aerosols and Gaseous Pollutants

Aerosol is defined as the stable suspension of solid or liquid material in a gaseous medium. In atmospheric studies it can be named as particulate material instead.

Aerosols play an important role in atmospheric chemistry. They act as condensation nuclei in the formation of clouds and form a surface for some gas phase reactions. By absorbing and scattering light they affect the global climate. They may also cause haze formation and visibility degradation. Aerosols cause some respiratory and hearth problems in humans. Moreover, they may form a surface for transportation of toxic and carcinogenic pollutants from region to region. They can be removed from the atmosphere by wet and/or dry deposition. No matter wet or dry deposited they cause adverse effects on forestry ecosystems and biogeochemical cycles in aqueous environments.

The most important characteristic of aerosols is their sizes as the deposition, transportation and inhalation processes are controlled predominantly by the sizes of the aerosols. Figure 2.1 shows the mass distributions of particle sizes in the atmosphere. The particles can be divided into two groups according to their sizes. The particles which have particle diameter less than 2.5 μm are referred as fine particles and bigger than 2.5 μm are referred as coarse particles. Coarse

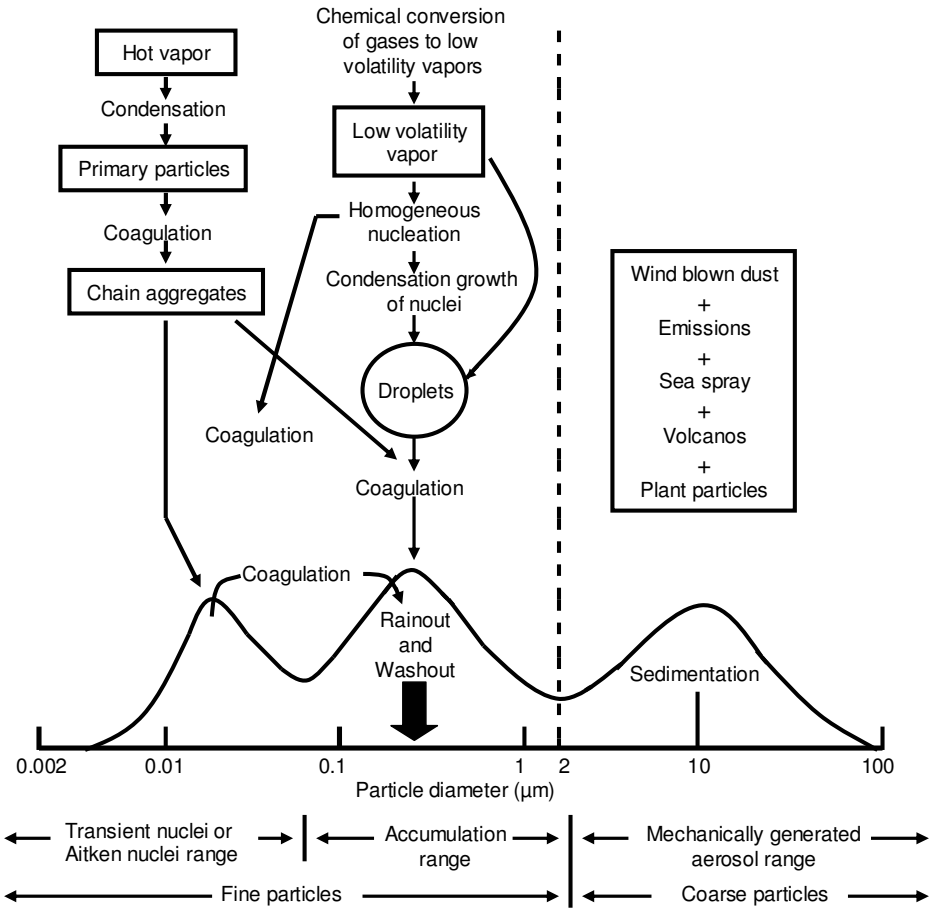

Figure 2.1. Schematic of atmospheric size distribution showing the three modes, the main source of mass for each mode, and the principle processes involved in inserting mass into and removing mass from each mode (Finlayson-Pitts, 1986)

particles include particles produced by mechanical processes and bubble-bursting process over the sea surface, crustal material, pollen and spores. As being large in size and mass, they removed from the atmosphere by gravitational settling. Fine particles divide into two ranges. First one is the “nucleation” range and the second is the “accumulation range. Particles smaller than 0.08 µm are fall into “nucleation” range and are produced by gas to particle conversion at ambient temperature or combustion processes. The lifetime of these particles is very short as they rapidly coagulate and form bigger particles. Particles which have particle sizes from 0.08 to 2.5 µm are fall into “accumulation” range. They are produced generally from condensation of low vapor pressure vapors from combustion process and coagulation of small particles. The residence time of these particles are longer than the particles in “nucleation” range.

2.2. Sources of Aerosols

Aerosols are composed of organic and inorganic compounds and biological debris like sulfates, nitrates, ammonia, ammonium, crustal material and trace metals. The discussion in this manuscript will be confined to trace elements and ions associated with particles, as these are the parameters studied in this work.

Trace metals are used as ideal tracers to determine the sources of aerosols as the sources of these elements are well documented**.** Figures 2.2 and 2.3 shows the global emissions of trace metals to the atmosphere from anthropogenic and natural sources, respectively.

Aerosols have both natural and man-made sources. Natural sources include lithosphere, biosphere, sea, and volcanic activities. Crustal particles and elements associated with these particles (so called crustal elements) are produced by weathering or mechanical grinding

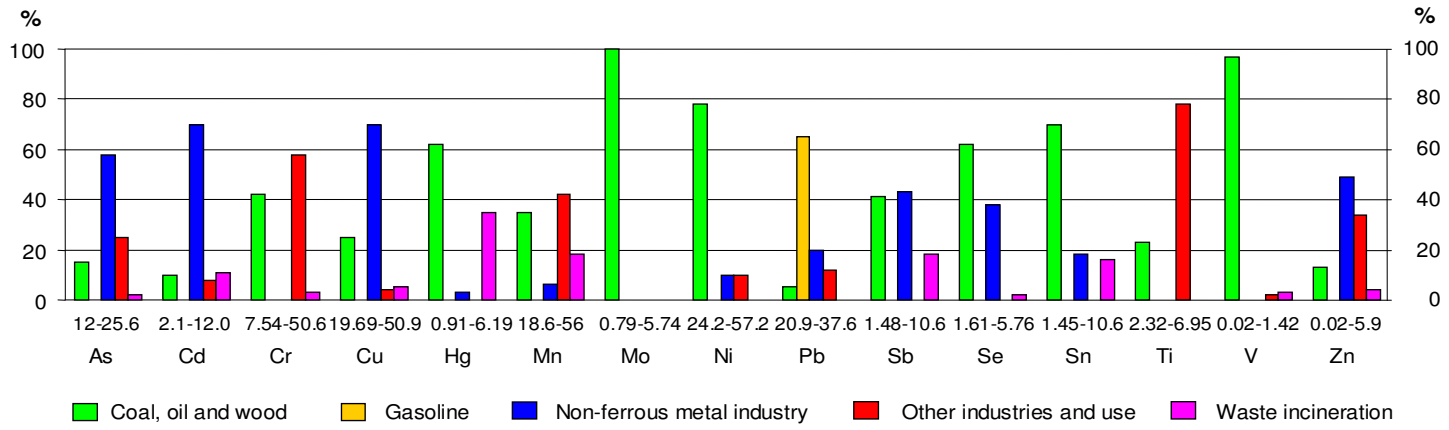

*Numbers under the columns are the range of estimates of the emissions in thousands of tonnes per year.

**The percentages shown by the bars are calculated using the maximum value of the range of the total and individual source category estimates.

Figure 2.2. Global emissions of trace metals to the atmosphere from anthropogenic sources (AMAP, 1998)

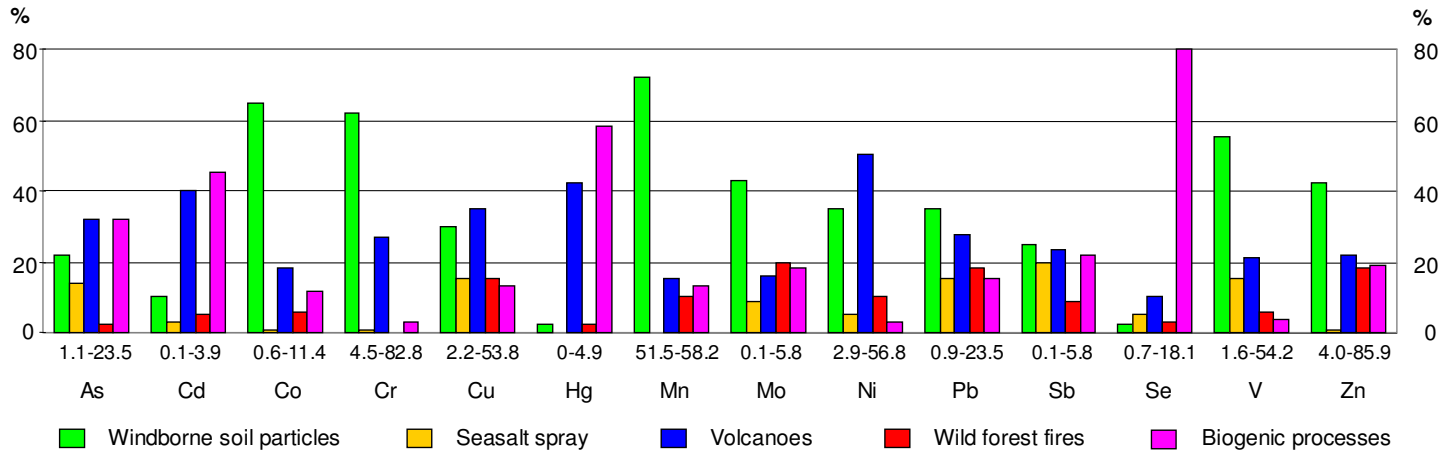

*Numbers under the columns are the range of estimates of the emissions in thousands of tonnes per year

**The percentages shown by the bars are calculated using the maximum value of the range of the total and individual source category estimates.

Figure 2.3. Global emissions of trace metals to the atmosphere from natural sources (AMAP, 1998)

processes with the action of the wind (Vega et al., 2002; Chow et al., 1994). Sea salt elements in the atmosphere are produced by bubble bursting over the sea surface (Cipriano et. al., 1983). Plants release some biogenic particles like pollens and spores, which are believed to contain some of the elements (Yin et. al., 2004). The only high temperature source in the nature is volcanic activity. Volcanic activity emits both particles and gases to the atmosphere. Volcanic particles do contain trace elements like As, Se, Zn etc. In addition, secondary contain trace elements like As, Se, Zn etc. In addition, secondary particles also form by gas-to-particle conversion of gases emitted from volcanoes (Faber et al., 2003; Tassi et al., 2003; Varrica et al., 2000). Anthropogenic sources of aerosols and trace elements associated with them include the products of combustion processes (particularly combustion of fossil fuels) and industrial activities. These processes emit both gases and particles to atmosphere. Some of the gases either condense on existing particles and some converts into particles with gas-to-particle conversion process (Charron and Harrison, 2003).

2.3. Sulfur and Nitrogen Compounds

Sulfur dioxide (SO_2) is a highly soluble gas in water, forming sulfuric acid which causes acidity in the rain. The SO_2 is also precursor of particulate sulfate (SO_4) by giving gas-to-particle conversion reaction on the surface of the aerosols. Atmospheric life of SO_2 is only a few days whereas SO_4 has nearly 10 days retention time in the atmosphere and can be transported over thousand kilometers (Luria et al., 1996) The major sources of sulfur compound emissions are fossil fuel burning, including coal and oil fired power plants and boilers (Okay et. al., 2001), ore smelters and oil refineries together with smaller stationary combustion sources (Kouvarakis et. al., 2002), such as space heating. Natural sources of sulfur compounds include release from volcanoes, biological decay, forest fires, sea spray and DMS (Kubilay et. al., 2002).

Nitrogen compounds in the ambient atmosphere include NO and NO_2, commonly referred as NO_x, NO_3, NH_3, NH_4^+ and HNO_3. Nitrogen oxides are released into the atmosphere mainly in the form of nitric oxide (NO) as a result of the reaction of atmospheric nitrogen and oxygen during high temperature combustion processes such as burning of fuel (coal, oil, gas) and internal combustion (motor vehicles) (Vitousek et al., 1997). Nitric oxide is readily oxidizes to form nitrogen dioxide (NO_2). Most of the nitrogen dioxide is formed from the oxidation of nitric oxide in this way, although some is released directly from source. Natural sources of nitrogen oxides include volcanoes (Mather et. al., 2004), oceans (Anderson et. al., 2003), biological decay and lightning strikes (Olivier et. al., 1998). As a strong oxidizing agent nitrogen dioxide reacts in the air to form nitric acid, which causes acidification of the environment together with sulfuric acid.

Ammonia (NH_3) is released to atmosphere mainly from fertilizing agents used in agricultural activities and from animal farms (Krupa, 2003). Ammonia is a very important gas in atmospheric chemistry as it is the main alkaline gas present in the atmosphere. In a very short time, the ammonia released from the source is transformed to ammonium (NH_4^+) containing aerosols, $(NH_4)_2SO_4$ and NH_4NO_3 by giving reaction with H_2SO_4 and HNO_3, respectively. Due to its high concentration near the source and high deposition velocity ammonia is removed from the atmosphere locally. However, ammonium aerosols are transported over long distances due to their low deposition velocity (Singles et al., 1998).

Atmospheric sources, transport and deposition of N-compounds have attracted special attention in recent years, as they are nutrients and can cause eutrophication in inland and coastal waters (Guerzoni et al., 1999).

2.4. Long-range Transport of Pollutants to Mediterranean Region

Atmosphere is a significant source of pollutants that reach both coastal and open seas. Atmospheric input of natural and anthropogenic sources strongly impact the biogeochemistry of semi-closed seas like Mediterranean Sea (Guerzoni et al., 1999).

Composition of atmosphere over eastern Mediterranean has been studied by various researchers from Israel, Greece and Turkey since late 70's (Chester et al., 1977; Bergametti et al., 1989; Bardouki et al., 2003; Luria et al., 1996; Danatalos and Glavas et al., 1995, 1999; Matvev et al., 2002; Herut et al., 2001; Ganor et al., 1997, 2000; Chabas and Lefèvre, 2000; Kouvarakis and Mihalopoulos, 2002; Erduran and Tuncel, 2001; Al-Momani et al, 1995; Güllü et al., 2000; Kubilay and Saydam, 1995).

Main ionic and organic species was studied by Bardouki et al. (2003). 30 size-resolved aerosol samples were collected to determine the chemical composition of atmosphere. Organic ionic mass contributed 1-2 % of the total mass fraction in which oxalate, acetate and formate ions formed the 90 % of the total organic ionic mass. Sulfate together with ammonium ion is found to account for 90 % of fine fraction of the total ion mass. Na^+, Cl^-, Ca^+, CO_3^{2-} and NO_3^- ions found to contribute 90 % of the ion mass in the coarse fraction.

Amount of sulfur compounds entering and leaving Israel is studied by Matvev et al. (2002) by analyzing data collected during research flights. 50 to 90 % of sulfur flux entering and 15 % of sulfur flux leaving was found to be composed of particulate sulfate. Sulfur emitted in Israel remains as sulfur dioxide till air masses leaves the Israel. Authors concluded that 15% of the sulfur compounds emitted from industrialized European countries reach to Israel and all sulfur emitted from Israel was transported eastward.

Kubilay et al. (2002) studied methanesulfanate (MSA) and non-sea-salt sulfate (nss-sulfate) concentrations in eastern Mediterranean region of Turkey. They observed high concentrations of MSA and nss-sulfate in summer months which they suggested to be due to high DMS production at Black Sea. During autumn and spring months the direction of air mass patterns over Black Sea shifted to westerlies which cause low concentrations of sulfate in the western Mediterranean region of Turkey. Authors concluded that observed MSA and nss-sulfate concentrations in autumn and winter are due to long-range transport of sulfate aerosols over European countries and in spring due to long-range transport of Saharan dust.

Luria et al. (1996) studied sulfur compounds over eastern Mediterranean by interpreting the data obtained from different parts of Israel. Authors observed that for all sampling sites the sulfate shows highest concentrations in summer and lowest in winter due to the high rate of photo-oxidation reaction that transform SO_2 to SO_4^{2-}. They concluded that SO_4^{2-} is long-range transported to Israel. This conclusion was based on poor correlation between particulate SO_4^{2-} and SO_2 and high sulfate to total sulfur ratio. They supported this idea by showing that observed SO_4^{2-} concentrations are comparable for different sites of the Israel and not affected due to the local changes of SO_2 concentrations.

Kubilay and Saydam (1995) studied trace metals collected at a coastal station located western Mediterranean region of Turkey. Order-of-magnitude higher concentrations of soil-related elements were observed when air masses come from North Africa and higher concentrations of pollution-derived elements were associated with air masses originating from Europe.

Temporal variability of concentrations of measured parameters depends on several factors like source strengths, transport patterns and

meteorological conditions. Temporal variability of concentrations of trace metals and major ions measured at Antalya station located at Mediterranean coast of Turkey is studied by Güllü et al. (2000). Authors observed high concentration of mineral aerosols in summer months. The intense activity of synoptic scale meteorological events enhances the uplift of crustal material over North Africa and Middle East desert regions in spring and autumn. The back trajectory analysis conducted by the Authors showed that this crustal material is then transported to eastern Mediterranean Basin. By using back trajectory analysis and studying the concentrations measured, the authors also observed that anthropogenic elements are transported over industrialized European countries to eastern Mediterranean and concentrations of these pollutants show summer high concentrations as they are scavenged out from the atmosphere during wet seasons along their long-range transport to Mediterranean Basin. Finally, Authors observed that sea salt elements show high concentrations during wet season as strong winds in this season enhance the bubble bursting over sea surface.

Researchers from Spain, Italy and France has been studied the atmosphere over western Mediterranean Basin since late 80's (Chester et al., 1984; Sanz et al., 2002; Avila et al., 1998; Molinaroli et al., 1999; Narcisi, 2000; Guerzoni et al., 1996, 1999; Migon et al., 1993, 1996, 2000, 2001; Remoudaki et al., 1991; Sandroni and Migon, 1997; Grousset et al., 1995; Despiau et al., 1995; Guieu et al, 1996).

Sandroni and Migon (1997) studied trace metal concentrations measured at six stations located at coastal sites of western Mediterranean. They observed that the stations located on the continental shore line are influenced by the industrial emissions from northern and central European countries more than the ones located on the shore line of the islands. Authors concluded that only fine-grained particles are medium-range transported to open western Mediterranean

Sea and coarse particles are deposited to the continental regions where they are emitted. Furthermore, they showed that despite the effect of local meteorological events, the spatial variability of trace metals concentrations is very low over the western Mediterranean Sea.

Atmospheric input of trace metals to the northwestern Mediterranean Basin is studied by Guieu et al. (1996). The results of the six year project conducted at six coastal sites of the northwestern Mediterranean showed that atmospheric trace metals like Al, Fe and Cr are mostly in particulate form and Co, Cu, Mn, Pb, Ni, and Zn in dissolved form in rain water. Authors compared the river input of trace metals with atmospheric input and concluded that more than 50 % of the dissolved input to the marine system originates from the atmosphere. The percentage was found particularly high for anthropogenic pollutants such as Pb, Cd, and Zn.

Studies conducted over western and eastern Mediterranean Basin showed that concentrations of anthropogenic and marine elements are comparable in eastern and western Mediterranean and concentrations of crustal elements are lower in western Mediterranean than eastern Mediterranean (Güllü et al., 2000; Kubilay and Saydam, 1995, Guerzoni et al., 1996; Erduran and Tuncel, 2001).

2.5. Receptor Oriented Models

Receptor oriented models have been applied in atmospheric studies to identify potential sources and to estimate the contributions of sources affecting the chemical composition of the atmosphere at the receptor site (Hopke, 1985). The most commonly applied multivariate statistical approaches used in the receptor modeling include Factor Analysis (FA) (Hopke, 1985), Chemical Mass Balance (CMB) (Miller et al., 1972), Principle Component Analysis (PCA) (Thurston and Spengler, 1985). These techniques have been used since 80's. A new multivariate

technique called Positive Matrix Factorization (PMF) (Paatero and Tapper, 1994) started to be applied to atmospheric data in recent years and it is gaining wide use nowadays.

Chemical Mass Balance (CMB) is a statistical method to determine the contributions of sources of atmospheric pollutants when the number of sources and source profiles are well defined (Quin et al., 2002). The problem of using CMB lies on the necessity of defined source profiles as in many cases of atmospheric studies the source profiles of the pollutants are not easily obtained because of the existence of many small sources with varying compositions (Quin et al., 2002).

Factor Analysis (FA) estimates the number and composition of the sources as well as their contributions to the samples taken at the receptor without any information about the source profiles as in the case of CMB. However, FA or Principle Component Analysis (PCA) which is the most common form FA has some drawback, too. First it needs further transformation or rotation to make the results statistically meaningful but no satisfactory rotation have yet been found (Ramadan et al., 2003). Furthermore, it cannot properly handle missing and below-detection-limit data, require fairly large data set and results are qualitative. Paatero and Tapper (1994) have also showed that factor analysis produces poor fits of the data matrix, when variability in the data is small and when unique variances are high.

A new technique, called Positive Matrix Factorization is developed to overcome these difficulties encountered in the FA. Positive Matrix Factorization (PMF) is the only multivariate statistical technique that produces quantitative results to explain possible sources of pollutants. As the name implies PMF integrates non-negativity constraints to solve bilinear models which means there should be no negative value in the source composition or source strengths (Quin et al., 2002). It also utilizes the error estimates of the data matrix. PMF approach is

applicable to both 2-way and 3-way bilinear models. Recently, it has been extended to arbitrary multilinear models (Paatero, 1999).

All of the receptor models mentioned above determine the sources and contributions of these sources; however, they cannot give the locations of the sources at regional scale problems. To overcome this problem Potential Source Contribution Function (PSCF) which uses chemical, geographical and meteorological data in order to identify the locations of the problems can be used. Enrichment factors and correlation matrix are the other statistical methods to obtain more information about sources of the pollutants.

2.5.1. Positive Matrix Factorization

Positive Matrix Factorization (PMF) is developed by Paatero and Tapper (1994) as a new approach to factor analysis. PMF determines the sources and contributions of these sources on the pollution level of the receptor site. Unlike factor analysis PMF produces quantitative non-negative solutions to the classical factor analysis model given below;

$$X = GF + E$$

or in component form;

$$X_{ij} = \sum_{p=1}^{p} G_{ip} F_{pj} + e_{ij}$$

where X is the data matrix of measured species to be analyzed with n rows and m columns, G and F are the factor matrices to be determined with dimensions n x p and p x m, respectively, and E is the matrix of residuals with n rows and m columns. Here, n represents the number of pollutants measured at the receptor site, m represents the number of samples, and p represents the number of factors.

In PMF, sources are constrained to have non-negative values which mean there would be no negative source contribution to the samples. PMF also computes individual error estimates for each observed data point. These estimates are based on the standard deviation values of each data point and also on the non-negativity criteria. This feature of PMF makes the missing and below-detection-limit data to be handled by adjusting the corresponding error estimates.

The task of the PMF can be presented as;

$$\text{minimize } Q = \sum_{i=1}^{n}\sum_{j=1}^{m}\frac{E_{ij}^2}{s_{ij}^2} \text{ with } G_{ik} \geq 0,\ F_{kj} \geq 0,\ k = 1,2,...,p$$

where g_{ik} and f_{kj} are elements of G and F, respectively. The residuals, e_{ij}, are defined by;

$$e_{ij} = X_{ij} - \sum_{k=1}^{p} G_{ik}F_{kj}$$

and s_{ij} is the standard deviation of X_{ij}. Analysis of this weighted Least Squares fit, Q, of PMF can be used to determine the optimum number of the factors as theoretical Q must be equal to the number of individual data points of the matrix X. Number of factors may be determined by changing its number to obtain this theoretical number and also by looking at the changes occurred to the profiles of factor loadings and temporal variations of the factors obtained from the result matrices of G and F of PMF, respectively.

One other advantage of PMF is that it produces another result matrix of rotation estimates which indicates if the solution can be rotated and in what way to produce other possible solutions. However, 2 dimensional PMF model has some special problems. First, it is slower than the factor analysis as the algorithms used are more complicated. Secondly in

some cases the sum-of-squares expression to minimize Q gives more than one local minima and the “right” minimum may not be the deepest one.

2.5.2. Potential Source Contribution Function

Potential Source Contribution Factor (PSCF) receptor model is commonly used in the studies of long range transport of atmospheric pollutants (Güllü, 1996; Çetin, 2002) as it combines geographical (backtrajectories) and chemical data to determine geographical locations that have higher probability of being source areas of pollutants at the receptor site. In many applications geographical data are combined with the results of multivariate statistics on the data set (Lupu and Maenhaut, 2002). This had increased the use of trajectory statistics in regional source apportionment studies.

The methods that combine geographical and chemical information are commonly called as “trajectory statistics”. Potential source contribution function (PSCF) (Malm et al., 1986) is the most widely used technique in trajectory statistics; however, other techniques, such as, concentration fields (Seibert et. al., 1994) and redistributed concentration fields (Stohl, 1996) are also available, but not used as widely as the PSCF. The PSCF uses meteorological data taken from the air mass back trajectories. In order to calculate the PSCF value first the whole geographical region that trajectories pass through to arrive the receptor site is divided into an array of grid cells whose size is dependent on the geographical scale of the problem noting that the grid sizes must be sufficiently large for the assimilation of reasonable trajectory segments endpoint. Then PSCF is calculated by counting each 1 hr trajectory segment endpoint that ends up with that grid cell.

Suppose N represents the total number of trajectory segment endpoints for the whole study period, T. If the number of endpoints that fall in the ij-th cell is n_{ij}, the probability of an event, A_{ij} is given by;

$$P\left[A_{ij}\right] = \frac{n_{ij}}{N}$$

Suppose N represents the total number of trajectory segment endpoints for the whole study period, T. If the number of endpoints that fall in the ij-th cell is n_{ij}, the probability of an event, A_{ij} is given by;

$$P\left[A_{ij}\right] = \frac{n_{ij}}{N}$$

where $P[A_{ij}]$ is a measure of the residence time of a randomly selected air parcel in the ij-th cell relative to the entire study period, T.

If, for the same cell, there are a subset of m_{ij} endpoints for which corresponding air parcel arrive at the receptor site with pollutant concentrations higher than an arbitrarily defined value, the probability of this "matched" event, B_{ij} is given by;

$$P\left[B_{ij}\right] = \frac{m_{ij}}{N}$$

Then the PSCF for ij-th cell is given by the following relation

$$PSCF = \frac{P\left[B_{ij}\right]}{P\left[A_{ij}\right]} = \frac{m_{ij}}{n_{ij}}$$

PSCF is a conditional probability of an air parcel to bring polluted air to the receptor site when it comes over that particular grid. The value of PSCF ranges between 0 and 1. When the calculated PSCF value is

close to 0 then that particular cell is unlikely to be the source region. However, when it is close 1 then that cell indicates the “high potential” source area of the pollutant arrives at the receptor site.

2.5.3. Enrichment Factors

Enrichment factor is simple statistical approach used to separate anthropogenic pollutants from natural pollutants. It gives limited but valuable preliminary information on the sources of measured parameters at a receptor.

Enrichment factor can be calculated as follows;

$$EF_c = \frac{(C_X/C_R)_{air}}{(C_X/C_R)_{soil}}$$

where $(C_X/C_R)_{air}$ is the ratio of concentration of the measured parameter, C_X, to the concentration of reference element, C_R, in the air and $(C_X/C_R)_{soil}$ is the same ratio in the reference soil. Mason’s soil composition (Mason, 1966) is used in this study as the reference soil composition. The selection of reference element is very important in EF_c analysis to get correct results. The reference element to be used should be non-volatile lithophile element, which is abundant in crustal material, accurately measured with various analytical techniques, and to be measured at all samples. In EF_c calculations, generally Al is used as the reference element if measured as it is the only element which obeys all these criteria. When Al is not measured at the study area then other crustal elements like Fe, Co, Si, and Sc can be used as reference element, too.

Elements which have EF_c values equal to unity can be assigned as crustal element if local soil composition is used as the reference soil composition. However, in this study local soil composition is different from the reference soil composition. Therefore, the elements which

have EF_c values lower than 10 are judged as crustal elements and higher than 10 are judged as anthropogenic elements.

2.6. Back-trajectory Analysis

Back-trajectory analysis is a very useful method to study the origin and the history of an air parcel. The backward trajectory models keep track of the path of the air masses during their 10 day travel before they reach the receptor site.

In this study, a publicly available model (TL511L60) on the CRAY C90/UNICOS super computer at the European Center for Medium-Range Wheather Forecast Center (ECMWF, Reading, U.K.) were used to obtain three dimensional (3-D), five and a half day back-trajectories arriving at the receptor site at four barometric levels (900, 850, 700 and 500hPa).

The ECMWF general circulation model, TL511L60, consists of a dynamical component, a physical component and a coupled ocean wave component. The model calculates the position of the air mass at every 15 minutes. The atmosphere is divided into 60 layers up to 0.1 hPa (about 64 km). The model uses a regular latitude-longitute grid system with a resolution of 1.5x1.5 degrees to produce data at every 6 hours (00, 06, 12 and 18UTC) per day.

CHAPTER 3

MATERIALS AND METHODS

3.1. General

Çubuk II Air Sampling Station is located at a rural site in Central Anatolia region of Turkey at approximately 50 km away from the city of Ankara and 12 km away from Çubuk town (33.10 longitude east of Greenwich and 40.10 latitude north of Equator). The station has been operated by Ministry of Health Refik Saydam Hygiene Center since its establishment in 1992. Air and precipitation samples has been collected and analyzed by this center since 1993. In this study, aerosol and gaseous pollutant data generated between February 1993 and December 2000 are taken from the Center by means of a protocol between the Center and the Middle East Technical University.

In the following sections one can found the general information about the materials and methods used in the site selection, collection and analysis of the samples. Detailed information can be found in the Appendix part.

3.2. Sampling Site

Site selection is an important step in establishing sampling station. As Çubuk station is an EMEP station site selection is done according to the criteria developed in the EMEP program. Site selection for all of the approximately 100 stations in the EMEP program were based on the same criteria given in the Appendix part.

Sampling station is a rectangular cabin with a surface area of 12 m^2. It consists of an air intake, a high volume sampler, a precipitation meter and a stack filter unit which are placed on a gravel platform with a height of 2.50 m, 2.00 m, 1.60 m, and 2.00 m, respectively above the ground level. In the station, meteorological parameters are also measured for inter-comparison purposes.

3.3. Sampling Procedures

Gaseous pollutants, namely, HNO_3, NH_3, SO_2 and NO_2 were collected with stack filter unit using a filterpack. In this method samples were collected onto cellulose filters impregnated with solutions, which specifically adsorbs one of these gases. These impregnated filters are placed in series behind an inert Teflon filter which removes particles.

In this study, KOH impregnated filter was used to collect HNO_3 and SO_2 from atmosphere. Similarly filters impregnated with citric acid and NaI were used to collect NH_3 and NO_2, respectively.

NO_2 samples were collection with iodine absorption method. In this method nitrogen dioxide is absorbed in a glass filter impregnated with sodium iodide (NaI) and sodium hydroxide (NaOH). The iodide reduces NO_2 to nitrite (NO_2^-).

Atmospheric particle (aerosol) samples were collected using a Digitel, model DHA-80 Hi-Volume Sampler. PTFE (Teflon) filters having diameters 47mm and pore size 2 um were used for sampling.

Sampling period is 24 hr for all samples. Filters are placed every Monday and they are removed from the samplers every Monday, Wednesday, and Thursday by the technicians. Blank filters are placed to the samplers every Monday in order to record any contamination of filters during the transport to and from the site and during the days that filters waited at the site.

3.4. Analysis of Samples

Sulfur dioxide, sulfate, nitrate, ammonium and nitric acid samples are analyzed with Dionex/DX-100 model spectrophometer. Na_2CO_3 is used as the eluent and Merck standart solution is used in the analysis.

NO_2, NH_3 and NH_4^+ samples are analyzed with Unicam Philips Spectrophotometer. NO_2 samples has been anaylzed with spectrofotometric nitrite determination method. In this method, nitrite (NO_2^-) and sulphanilamide form a diazo compound in acid solution which by a coupling reaction with NEDA, N-(1-naphthyl)-ethylenediamine-dihydrochloride, gives a red azo dye which is measured spectrophotometrically at 540 nm.

NH_3 and NH_4^+ are determined by spectrophotometric indophenol blue method. In an alkaline solution (pH 10.4-11.5) ammonium ions react with hypochlorite to form monochloramine. In the presence of phenol and an excess of hypochlorite, the monochloramine will form a blue colored compound, indophenol, when nitroprusside is used as catalyst. The total concentration of ammonium and ammonia is determined by spectrophometrically at 630 nm by measuring indophenol.

Mg, Ca, K are determined by an atomic adsorption spectrophotometer. In order to determine Pb, Cd and V, atomic absorption spectrophotometer is coupled with a graphite atomization unit by locating a graphite tube in the sample compartment of the AAS.

In the analysis, Perkin Emler 1100 B Atomic Absorbtion Spectroscopy and HGA 700 Atomization Unit is used. Mg, Ca, K, Pb, Cd, and V elements are determined at 285.2 nm, 422.7 nm, 766.5 nm, 217.0 nm, 228.8 nm and 319.6, respectively.

3.5. Data Quality Assurance

An EMEP Quality Assurance manager at the Chemical Coordinating Center and a National Quality Assurance manager of Turkey are responsible for implementing harmonized quality assurance system, including documentation of standards and reference materials.

CHAPTER 4

RESULTS AND DISCUSSION

4.1. General Characteristics of the Data

The summary of the descriptive statistics of the aerosols and gaseous pollutants measured at Çubuk II Air Sampling Station from March 1993 to December 2000 is presented in Table 3.1. The values given include the number of samples, arithmetic mean, associated standard deviation, geometric mean and median values.

It is seen from the Table 3.1 that the standard deviations observed are comparable or higher than the arithmetic mean values of the concentrations measured. In atmospheric studies such high standard deviations are generally observed due to large variations in meteorological conditions, physical and chemical transformations in the atmosphere, changes during air mass transport patterns and the variations in the source strengths.

4.1.1. Distribution Characteristics of the Data

The distribution characteristics of atmospheric data depend on the meteorological conditions and source emission variables. While the emissions from sources may be approximately constant, the successive mixing and dilution of pollutants as they are transported from source to receptor site results in a log-normal distribution for the ambient concentrations (Güllü, 1996).

Table 4.1. Arithmetic mean, standard deviation, geometric mean and median values of measured parameters

Parameter	N	Average ($ng\ m^{-3}$)	STD ($ng\ m^{-3}$)	Geometric Mean ($ng\ m^{-3}$)	Median ($ng\ m^{-3}$)
SO_2	1519	2552.63	4571.55	841.28	960.00
NO_2	1518	2906.83	2367.09	2229.00	2455.00
HNO_3	1639	395.70	481.73	250.50	270.00
NH_3	1743	375.22	315.68	246.90	315.71
SO_4^{2-}	1656	1963.86	1769.66	1248.12	1640.00
NO_3^-	1264	524.41	643.57	288.80	317.00
NH_4^+	1346	540.51	497.40	338.30	440.00
Pb	872	17.03	32.57	7.03	8.00
Cd	897	232.97	448.83	105.00	118.00
V	870	2.26	3.59	1.34	1.50
Mg	220	190.10	212.08	99.53	113.50
Ca	203	631.67	586.02	367.09	408.00
K	218	355.99	501.14	174.46	170.00

As can be seen from Table 4.1, there are large differences between arithmetic and geometric mean values whereas median and geometric mean values are comparable. This is an indication that the data set is log-normal distributed.

Skewness is value used to measure the symmetry or shape of the data. In ideal Gaussian distribution the value of skewness is zero. Non—zero values of the skewness indicate deviation from Gaussian distribution. Skewness can be both positive or negative. Positive values of skewness indicates a tailing to the right of the maximum. In such positively skewed data sets arithmetic mean is larger than the median and geometric mean values. The negative values of skewness indicates

a tailing to the left of the maximum and in such data sets arithmetic mean values of the parameter is smaller than its median and geometric mean values.

Skewness values for the measured parameters are given in Table 4.2. The positive skewness values for all parameters in the table suggest deviation from symmetric Gaussian distribution.

In describing the positively skewed data, log-normal or Weibull distributions can be used. In this study, Statgraphics Software was used to apply the Kolmogrov-Smirnov goodness-of-fit test to the data set to test if the assumed log-normal distribution, which is the most frequently observed distribution in atmospheric data sets is statistically significant. In this test, Statgraphics performs Chi-square test which divides the range of the variable into non-overlapping intervals and compares the number of observations in each class to the number expected based on the fitted distribution. Then Kolmogrov-Smirnov test computes the maximum distance between the cumulative distribution of the variable and the cumulative distribution function of the fitted log-normal distribution. The computed maximum distance is referred to as Kolmogrov-Smirnov (K-S DN) statistic.

The observed significance level for the Kolmogrov-Smirnov (K-S DN) statistic is presented by a value of ALPHA. As a disproof of the null hypothesis that the distribution is log-normal, ALPHA-value can be approximately computed from the equation given below;

$$\text{ALPHA} = \left(0.12 + \sqrt{\text{N}} + \frac{0.11}{\sqrt{\text{N}}} \right) \times \text{DN}$$

The reliability of the K-S DN statistic increases with increasing number of samples (N). In this study, the sample sizes for all parameters measured have adequate degrees of freedom to use the DN statistics.

Table 4.2. Skewness and Kolmorogov-Smirnov (KS-DN) statistic results for measured parameters

Parameter	Skewness (ng m^{-3})	DN	ALPHA	p-value	Log-normal Distribution
SO_2	4902.10	0.142	5.565	0	No
NO_2	4171.11	0.204	7.997	0	No
HNO_3	6675.41	0.061	2.483	9.48E-06	No
NH_3	2530.66	0.101	4.238	0	No
SO_4^{2-}	2911.39	0.126	5.174	0	No
NO_3^-	2765.86	0.036	1.288	0.073	Yes
NH_4^+	2819.19	0.102	3.768	0	No
Pb	6835.51	0.078	2.315	4.79E-05	No
Cd	7383.31	0.049	1.480	0.025	No
V	8720.76	0.287	8.508	0	No
Mg	2377.99	0.057	0.867	0.458	Yes
Ca	1337.08	0.058	0.835	0.511	Yes
K	3284.04	0.024	0.364	0.999	Yes

The ALPHA value greater than 1.358 for a variable indicates that the cumulative distribution function a composition is significantly different from the null hypothesis (i.e. log-normal distribution) at a 95% confidence level. The results are also supported by the p-value in which the p-value below 0.05 means the null hypothesis is rejected at a 95% confidence level.

As can be seen in Table 4.2, for SO_2, NO_2, HNO_3, NH_3, SO_4^{2-}, NH_4^+, Pb, Cd and V ALPHA > 1.358 and $p<0.05$ indicating that their distribution do not fit to log-normal distribution with 95% confidence. For, NO_3^-, Mg, Ca and K the ALPHA < 1.35 and $p > 0.05$ suggesting that these parameters are log-normally distributed in the data. The K-S statistics demonstrated that majority of parameters measured in this study are not log-normally distributed within 95% confidence interval. This does not support the hyphotesis that most atmospheric data are log-normally

distributed. However, it should be noted that K-S statistics showed that the distributions are not log-normal, it did not, in any way, suggests that the distributions are Gaussian. The frequency distributions of Cd and SO_4^{2-} are depicted in Figure 4.1. As can be seen from the figure frequency distributions of Cd and SO_4^{2-} are right skewed and not Gaussian. Similar right skewed pattern are observed for all parameters, except NO_2 which showed a fairly symmetrical pattern.

4.1.2. Comparison with other data

In order to assess the state of pollution in an urban or an industrial area one may compare measured concentration levels with the regulatory standards. However, it is not meaningful to use regulatory standards for comparison in rural areas like Çubuk, where pollutant concentrations are very low. A better approach used to determine the state of pollution in rural atmosphere is to compare the measured concentrations with the corresponding data collected at comparable sites around the world. In this study, data obtained from Çubuk station is compared with the data from other EMEP (European Monitoring and Evaluation Programme) stations in Europe and data from other stations in Turkey.

4.1.2.1. Comparison with EMEP stations

Data from EMEP network, which consists of approximately 100 rural stations distributed all over Europe, was selected for comparison for a number of reasons. (1) The selection of sampling site is based on the same criteria in all EMEP stations. The stations in the network are all rural stations which are not under direct influence of any point or area sources. They are established at least 50 km away from the large pollution sources (towns, power plants, major motorways), 100 m away from the small scale domestic heating with coal, fuel oil or wood, 100 m away from minor roads, 500 m away from the main roads, 2 km away from the application of manure, stabling of animals, and 500 m away

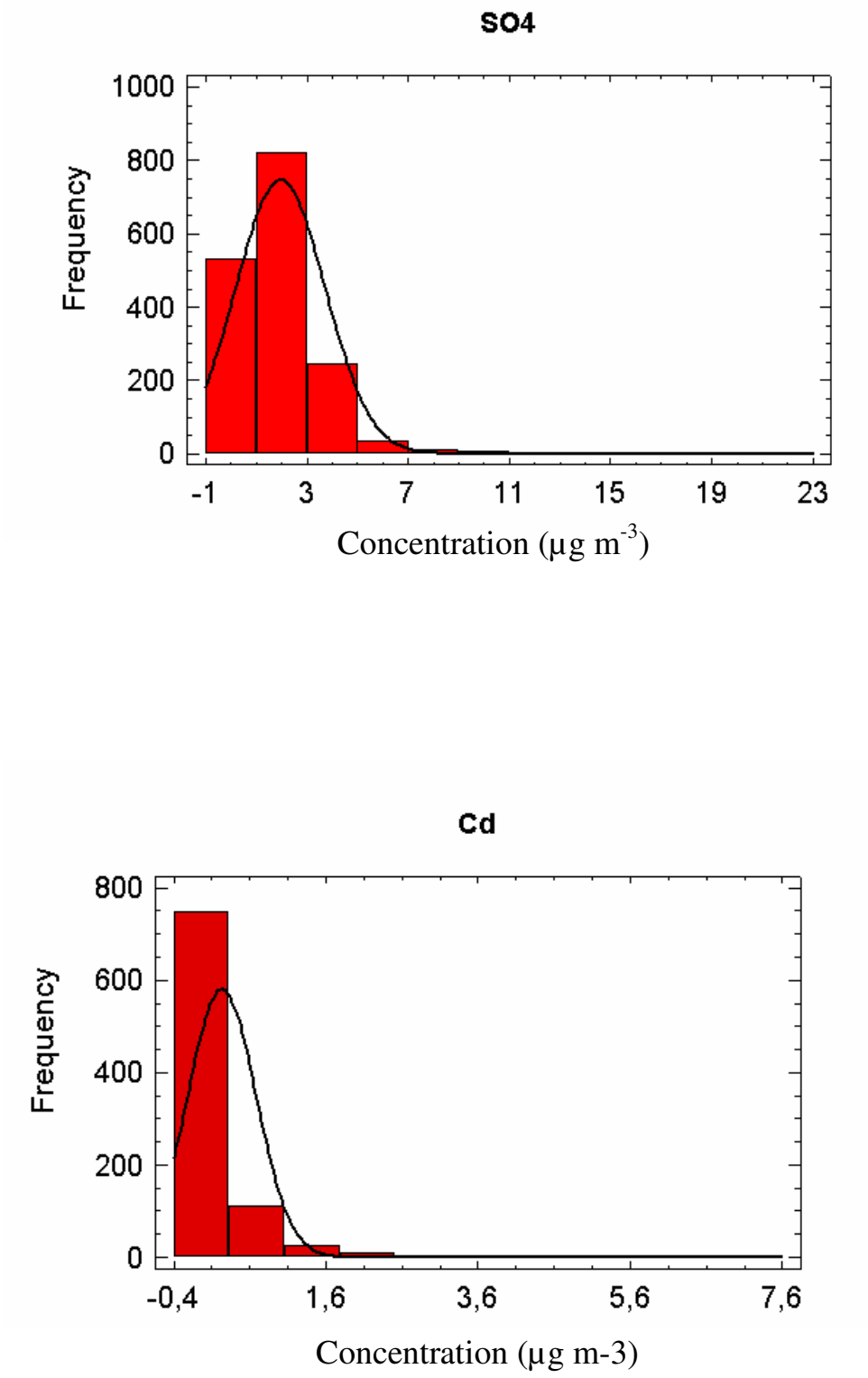

Figure 4.1. Frequency histograms of Cd and SO_4^{2-}

from the grazing by domestic animals on fertilized pasture with taking into consideration of the meteorological and topographic conditions, and quantity of emissions from the sources. (2) Sample collection and analysis methods are the same in all stations. (3) A similar strict data quality control is applied to generated data in all stations. (4) Although the distribution of stations is not exactly uniform (with higher density of stations in western Europe and smaller number of stations in eastern and southern parts of the continent), the network includes most of the polluted and relatively clean regions in Europe.

Comparison of the concentrations measured at Çubuk station with other EMEP stations is presented in Figure 4.2. The data for other EMEP stations are taken from the EMEP report (Hjellbrekke, 2001). EMEP stations used for this comparison are listed in Table 4.3.

As can be seen from the Figure 4.2, NO_2, NH_3, HNO_3, NO_3^- and NH_4^+ concentrations measured at Çubuk station are generally lower than concentrations of these parameters measured in most of the EMEP stations and SO_4^{2-} concentrations are comparable with values generated in EMEP network. Only SO_2 concentrations measured at Çubuk station are higher than the SO_2 concentrations measured in most of the stations located at European countries. SO_2 remains in the atmosphere for only a few days. Taken into account this short atmospheric life time it could be said that there are local sources influencing the Çubuk station, most probably the city of Ankara.

Another interesting point in this comparison exercise is the relatively low levels of SO_4^{2-} at the Central Anatolia. Median SO_4^{2-} concentration measured in this study is 1.6 µg m^{-3}. This observed concentration is significantly lower than SO_4^{2-} concentrations measured in the Mediterranean and Black Sea regions, which varies between 7 µg m^{-3} and 12 µg m^{-3} (Hacısalihoğlu et al., 1992; Güllü et al., 1998; Luria et al., 1996). Similar low SO_4^{2-} concentrations are also reported at another

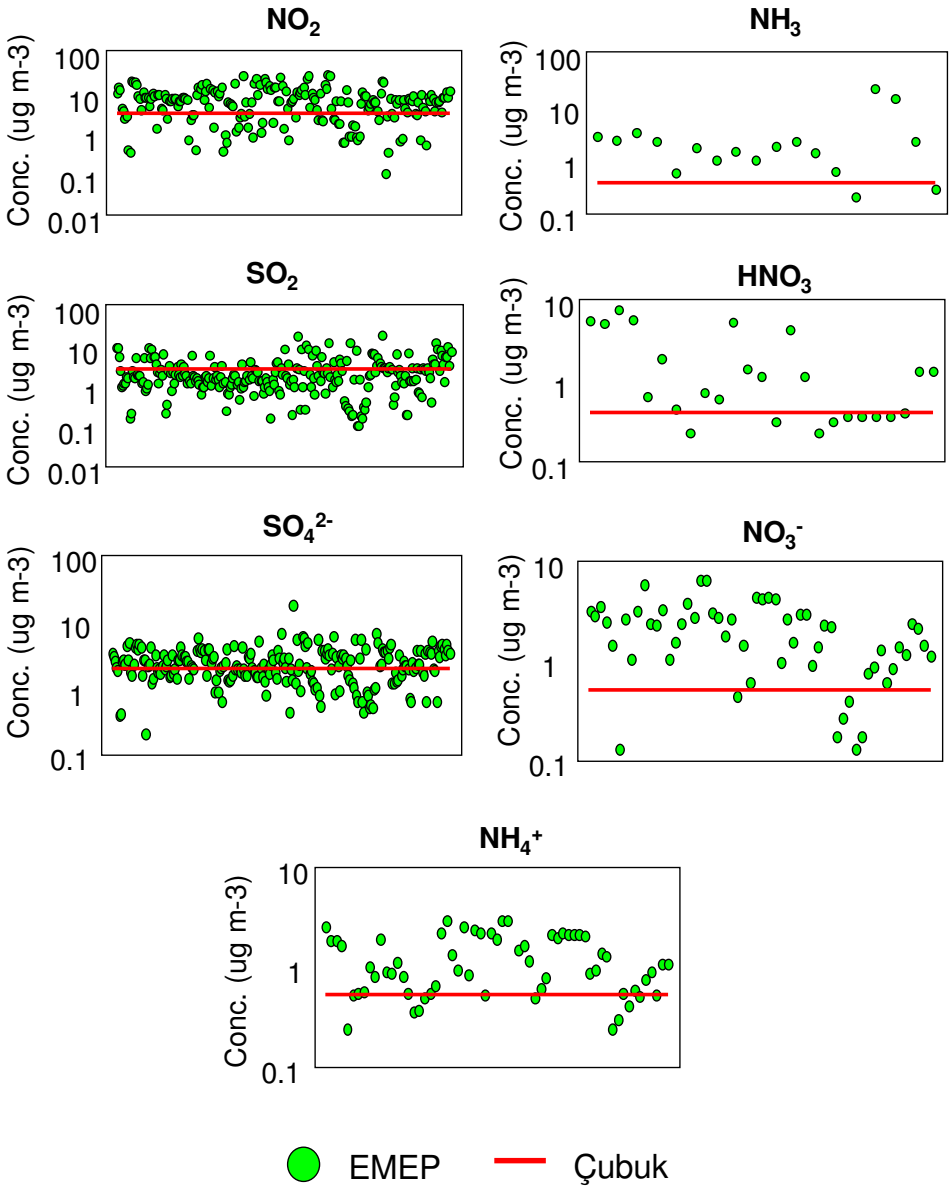

Figure 4.2. Comparison of concentrations measured at Çubuk station with other EMEP stations

Table 4.3. EMEP stations with locations and height above sea

Country	Station codes	Station name	Location		Height above sea
			Lat.	Long.	(m)
Norway	NO0001R	Birkenes	58°23'N	8°15'E	190
	NO0008R	Skreådalen	58°49'N	6°43'E	475
	NO0015R	Tustervatn	65°50'N	13°55'E	439
	NO0039R	Kårvatn	62°47'N	8°53'E	210
	NO0041R	Osen	61°15'N	11°47'E	440
	NO0042G	Spitsbergen, Zeppelinfjell	78°54'N	11°53'E	474
	NO0055R	Karasjok	69°28'N	25°13'E	333
Poland	PL0002R	Jarczew	51°49'N	21°59'E	180
	PL0003R	Sniezka	50°44'N	15°44'E	1604
	PL0004R	Leba	54°45'N	17°32'E	2
	PL0005R	Diabla Gora	54°09'N	22°04'E	157
Portugal	PT0001R	Braganca	41°49'N	6°46'W	691
	PT0003R	V. d. Castelo	41°42'N	8°48'W	16
	PT0004R	Monte Velho	38°05'N	8°48'W	43
Russian Federation	RU0001R	Janiskoski	68°56'N	28°51'E	118
	RU0013R	Pinega	64°42'N	43°24'E	28
	RU0016R	Shepeljovo	59°58'N	29°07'E	4
	RU0017R	Danki	54°54'N	37°48'E	150
Slovenia	SI0008R	Iskrba	45°34'N	14°52'E	520
Slovakia	SK0002R	Chopok	48°56'N	19°35'E	2008
	SK0004R	Stará Lesná	49°09'N	20°17'E	808
	SK0005R	Liesek	49°22'N	19°41'E	892
	SK0006R	Starina	49°03'N	22°16'E	345
Spain	ES0001R	San Pablo	39°33'N	4°21'W	917
	ES0003R	Roquetas	40°49'N	0°30'W	50
	ES0004R	Logrono	42°27'N	2°30'W	445
	ES0005R	Noya	42°44'N	8°55'W	685
	ES0006R	Mahon	39°52'N	4°19'E	78
	ES0007R	Viznar	37°14'N	3°32'W	1265
	ES0008R	Niembro	43°27'N	4°51'W	134
	ES0009R	Campisabolos	41°17'N	3°9'W	1360
	ES0010R	Cabo de Creus	42°19'N	3°19'E	23
	ES0011R	Barcarrola	38°29'N	6°55'W	393
	ES0012R	Zarra	39°5'N	1°6'W	885
Sweden	SE0002R	Rörvik	57°25'N	11°56'E	10
	SE0005R	Bredkälen	63°51'N	15°20'E	404

Table 4.3. EMEP stations with locations and height above sea (Cont'd)

Country	Station codes	Station name	Location		Height above sea
			Lat.	Long.	(m)
Sweden	SE0008R	Hoburg	56°55'N	18°09'E	58
	SE0012R	Aspvreten	58°48'N	17°23'E	20
Switzerland	CH0001G	Jungfraujoch	46°33'N	7°59'E	3573
	CH0002R	Payerne	46°48'N	6°57'E	510
	CH0003R	Tänikon	47°29'N	8°54'E	540
	CH0004R	Chaumont	47°03'N	6°59'E	1130
	CH0005R	Rigi	47°04'N	8°28'E	1030
Turkey	TR0001R	Cubuk II	40°30'N	33°00'E	1169
United Kingdom	GB0002R	Eskdalemuir	55°19'N	3°12'W	243
	GB0004R	Stoke Ferry	52°34'N	0°30'E	15
	GB0006R	Lough Navar	54°26'N	7°54'W	126
	GB0007R	Barcombe Mills	50°52'N	0°02'W	8
	GB0013R	Yarner Wood	50°36'N	3°43'W	119
	GB0014R	High Muffles	54°20'N	0°48'W	267
	GB0015R	Strath Vaich Dam	57°44'N	4°46'W	270
	GB0016R	Glen Dye	56°58'N	2°25'W	85

station located on the Anatolian Plateau (Uludağ station). The reason for observed low SO_4^{2-} concentrations at the Anatolian plateau is not known, but one suspects a totally different flow pattern at the Central Anatolia and coastal regions.

4.1.2.2. Comparison with Other Stations Located at Turkey

In order to assess the pollution level of Central Anatolia with regard to other regions of Turkey, the concentrations measured at Çubuk II Air Sampling Station is compared with data obtained from Antalya, Amasra and Uludağ stations which are all rural stations.

Antalya station is located at a coastal site at the Mediterranean coast of Turkey, at approximately 20 km east of the city of Antalya. The altitude of the station is 20 m. Two different data sets were generated at the station. About 40 element and major ions were collected with PM-10 High Volume Sampler between March 1992 and December 1993 in the first data set. Samples were analyzed by atomic absorption spectrometry, instrumental neuron activation analysis, ion chromatography and colorimetry. The geometric mean concentrations of SO_4^{2-}, NO_3, NH_4^+, V, Pb, Mg, Ca and K are used for comparison (Güllü, 1996).

Second data set is generated by collecting 33 elements with High Volume Impactor between August 1993 and May 1994. Samples were analyzed with graphite furnace atomic absorption spectrometry, instrumental neuron activation analysis, ion chromatography and colorimetry. The geometric mean concentration of Cd is used for comparison (Kuloğlu, 1997).

Amasra station is located 20 km east of Amasra town and 3.5 km far from the Black Sea. The altitude of the station is 150 m. About 46 element and major ions were collected with PM-10 High Volume Sampler between April 1995 and July 1997. Samples were analyzed by atomic absorption spectrometry, instrumental neuron activation analysis, ion chromatography and UV/VIS spectrometry. The geometric mean concentrations of SO_4^{2-}, NO_3, NH_4^+, V, Pb, Mg, Ca and K are used for comparison (Karakaş, 1999).

Uludağ station is located Sarıalan region of Uludağ mountain at approximately 20 km south of the city of Bursa. The altitude of the station is 1685 m. 8 elements and major ions were collected with TSP sampler between September 1993 and March 1994. The samples were analyzed by atomic absorption spectrometry, ion chromatography and

colorimetry. The geometric mean concentration of SO_4^{2-}, NO_3, NH_4^+, Mg, Ca and K are used for comparison (Karakaş, 1995).

Comparison of concentrations of elements and ions measured in this study with the concentrations reported in other coastal stations are depicted in Figure 4.3. Sulfate, NO_3, NH_4^+, V, Pb are known as anthropogenic elements as they originate from anthropogenic sources with negligible contribution from natural sources (Gordon, 1980). As can be seen from the figure, concentrations of the anthropogenic elements measured at Çubuk station are significantly smaller than the concentrations measured at Antalya and Amasra stations whereas comparable with concentrations measured at Uludağ station. It is worthy to point that the concentrations measured at Antalya and Amasra stations have comparable values within themselves.

The main reason for the observed difference between concentrations of pollutants at coastal areas and high altitude sites at the central Anatolia is the transport patterns affecting the region. Air masses originating from Europe enter the Mediterranean basin through two channels. One of these is the depression between Italy and Greece and the other one is the Aegean Sea. Since air masses go around the Anatolian plateau, rather than crossing it, sites at the central Anatolia do not receive polluted air masses as much as the receptor areas at the coasts. This flow pattern was observed through modeling studies (Kallos et al., 1998; Wanger et al., 2000) and low concentrations observed in this study are the first confirmation of the postulated flow pattern.

This already complicated flow pattern is further complicated by circulation cells that oscillate pollutants back and forth between the sea and the coast. Examples of such local systems are observed in Iberian Peninsula (Millan et al. 1991; Martin et al., 1991; Gangoiti et al., 2001) and on the coast of Israel (Ranmar et al., 2002; Tov et al., 1997). The existence of recirculation systems due to sea-land breeze flows is not

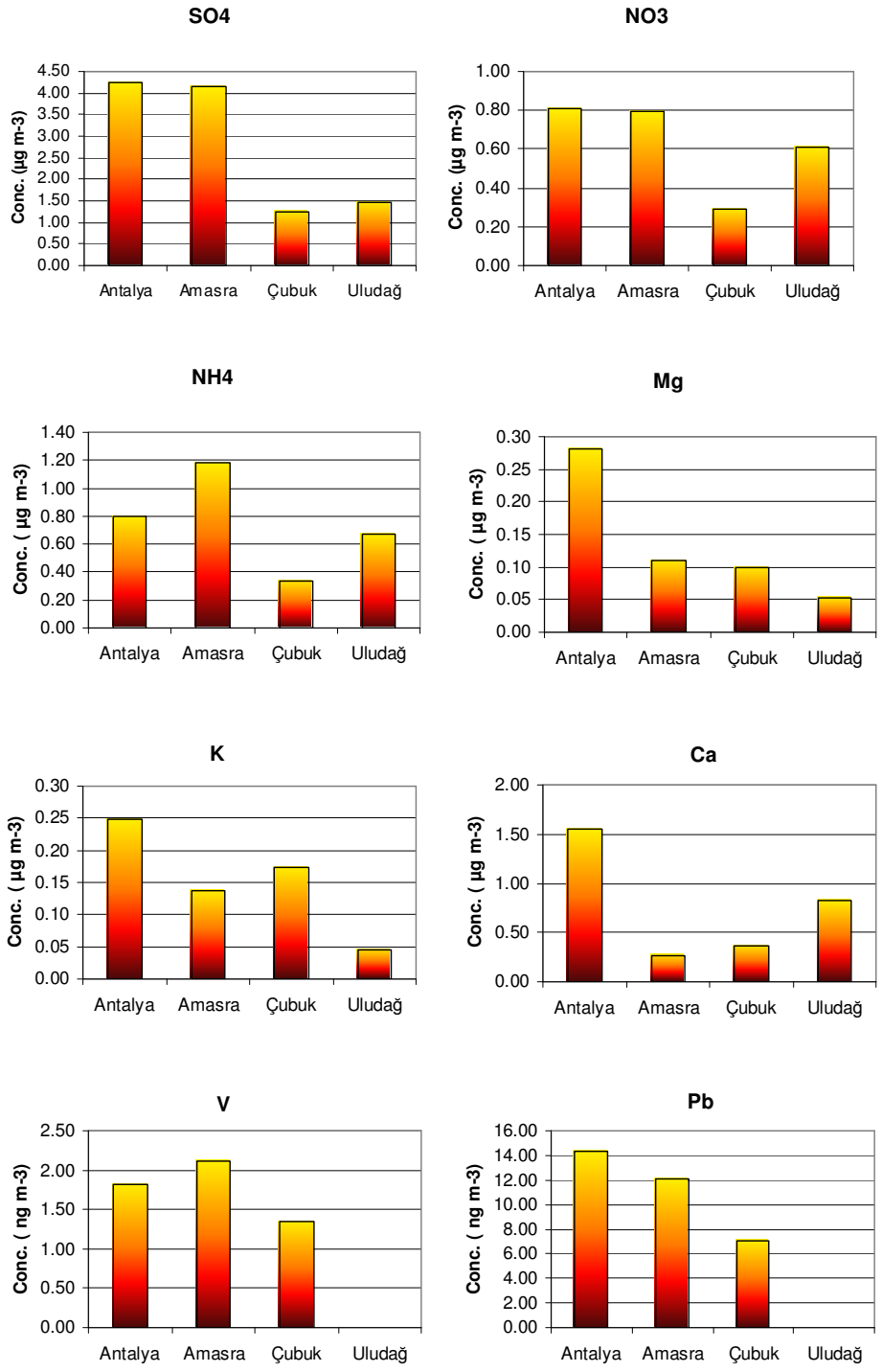

Figure 4.3. Comparison of concentrations measured at Çubuk station with other stations located at Turkey

known at the coastal regions of Turkey (not because they do not exist, but because studies to reveal them are lacking). If such recirculation patterns do exist, they would result in higher pollutant concentrations at the coastal sites.

Unlike other anthropogenic pollutants, Cd concentrations measured at Çubuk station followed different trend. Geometric mean of Cd concentration measured at Çubuk station is 105 ng m^{-3} which is a very high value when compared with the concentrations measured at Amasra and Antalya stations. Cadmium concentrations measured at Amasra and Antalya are 0.21 and 0.17 ng m^{-3}, respectively. Such high Cd concentrations are not likely to be due to strong influence of local sources, because in such a case one would expect to see similar high concentrations of most of the locally emitted pollutants, which is not the case. High Cd concentrations observed in this study probably an artifact due to sample contamination.

Sources of K, Mg and Ca is the crustal material in the Central Anatolia. Certain fraction of these elements may originate from sea salt in coastal areas, but at a location 400 km from the nearest coast their main source is expected to be soil. Concentrations of these natural components of atmospheric aerosol are comparable in Çubuk, Uludağ and Amasra stations and fairly high in the Antalya station. Observed pattern is not surprising, because at coastal sites there is an additional marine source for concentrations of these elements, which render their concentrations high at these sites relative to stations located at the Central Anatolia. The difference between the Amasra and Antalya stations are probably due to relative distances of these two stations to the coast.

4.2. Temporal Variations of Pollutants

4.2.1. Short-term (Episodic) Variations

Short-term variations of the measured parameters in Çubuk station are given in Figures 4.4–4.16. As can be seen from the figures, concentrations of all parameters show high episodic variations. Such high variability is the common feature in most atmospheric data and may have different reasons, such as variations in the source strengths, transport patterns or meteorological conditions in different data sets. During their long range transport, pollutants are removed from the atmosphere via rain. So, the variations in the amount and intensity of rain is also a factor that determine the variations of concentrations of pollutants on both daily and seasonal basis.

The parameters measured in Çubuk station have anthropogenic and natural sources. It is well established that at least some of the observed concentrations of anthropogenic species like SO_4^{2-} and HNO_3 originate from distant sources (Erduran and Tuncel, 2001; Karakaş, 1997). Consequently, the variations in the sources which are located

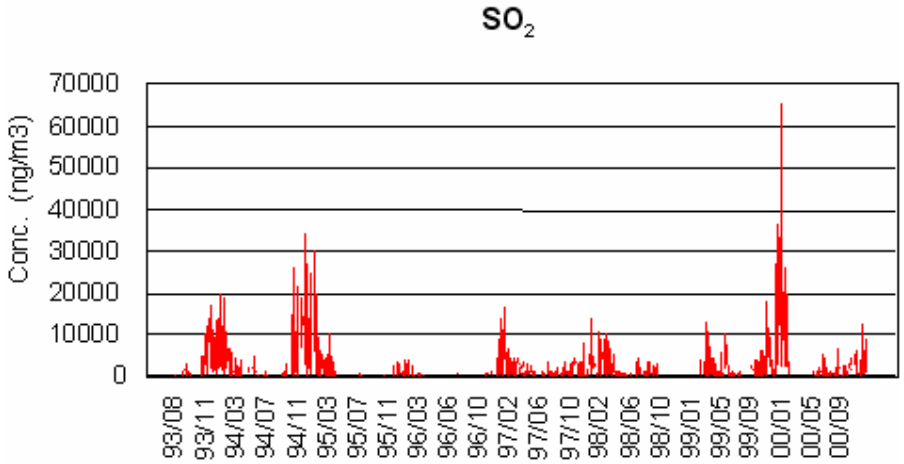

Figure 4.4. Temporal Variation of SO_2

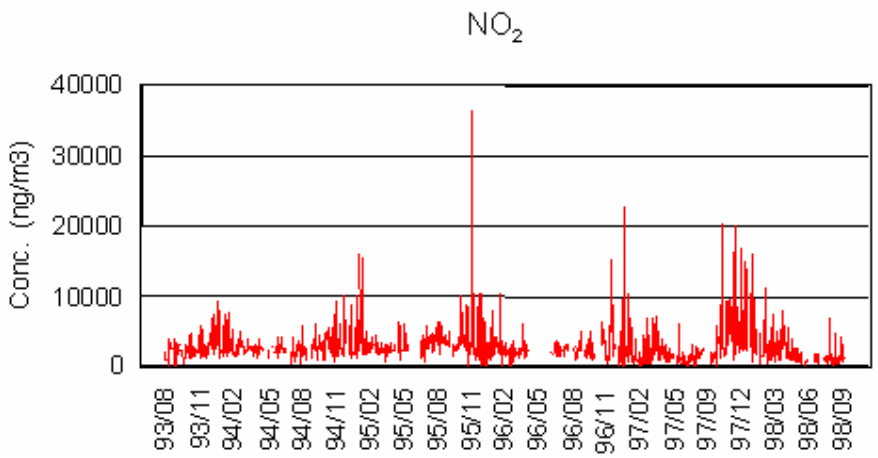

Figure 4.5. Temporal Variation of NO_2

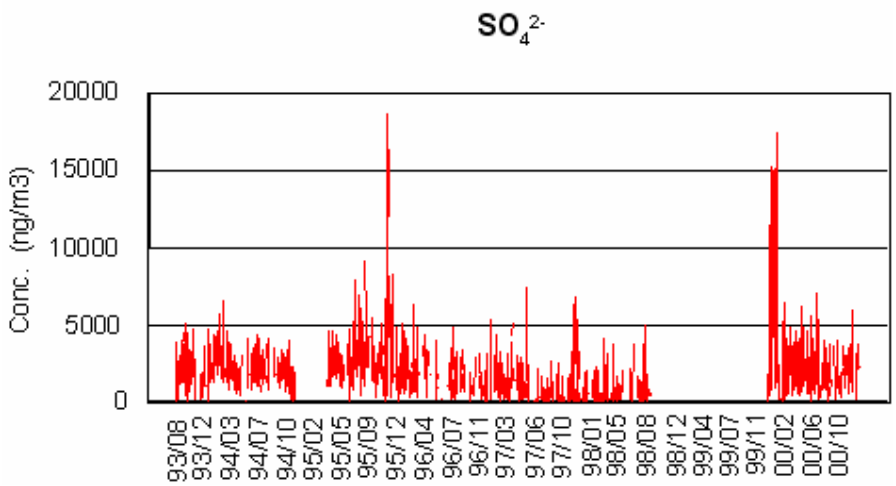

Figure 4.6. Temporal Variation of SO_4^{2-}

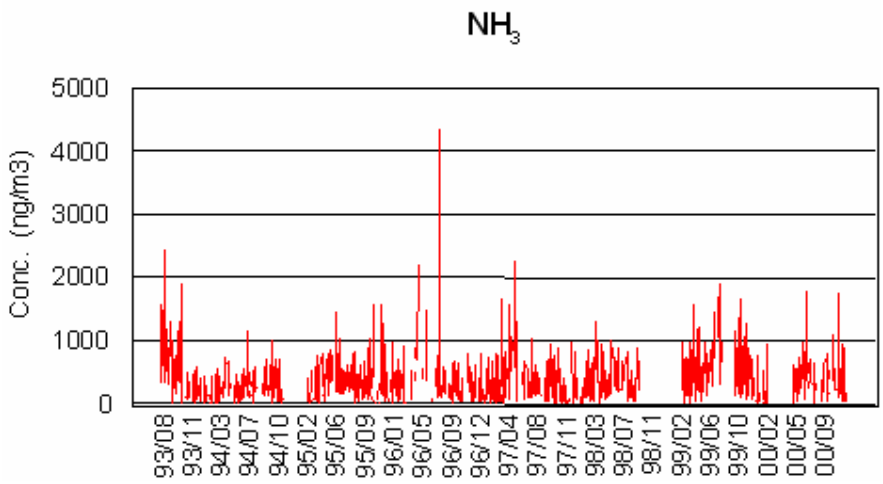

Figure 4.7. Temporal Variation of NH_3

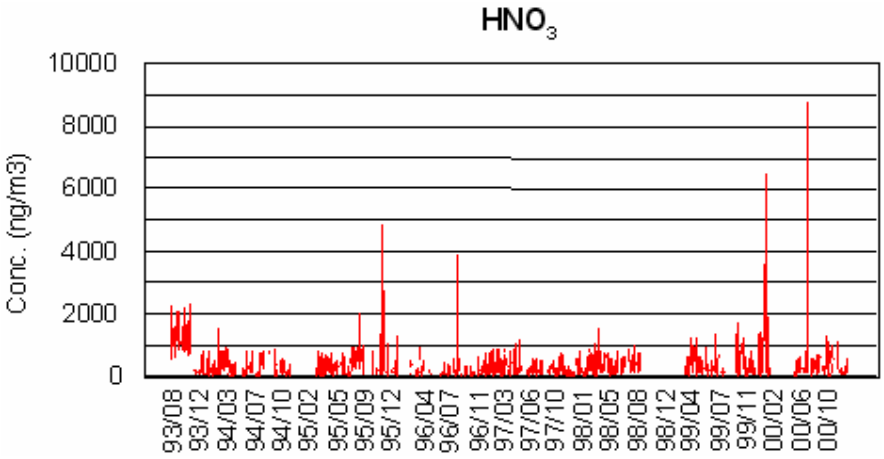

Figure 4.8. Temporal Variation of HNO_3

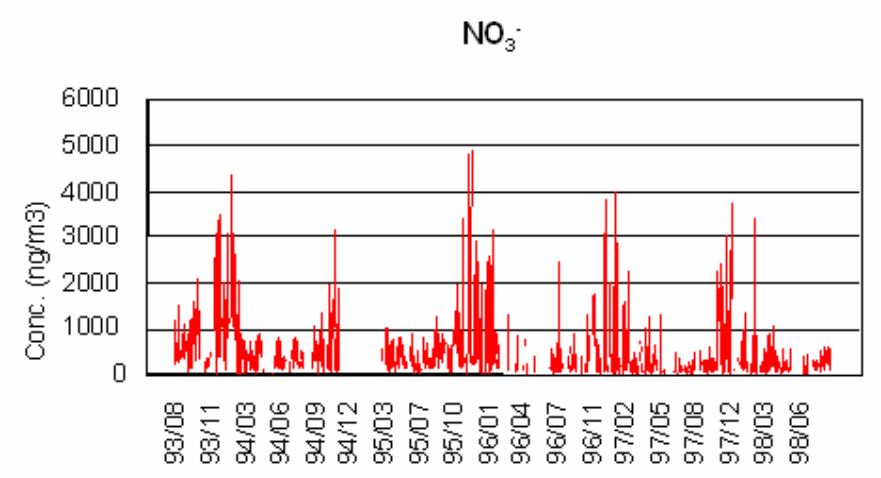

Figure 4.9. Temporal Variation of NO_3^-

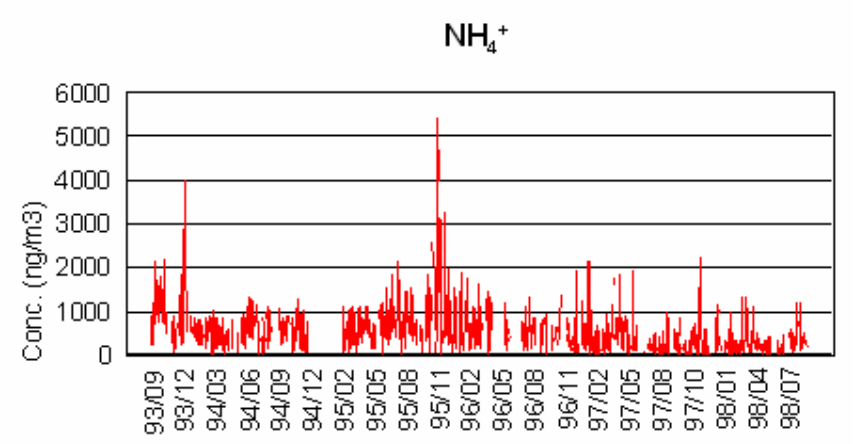

Figure 4.10. Temporal Variation of NH_4^+

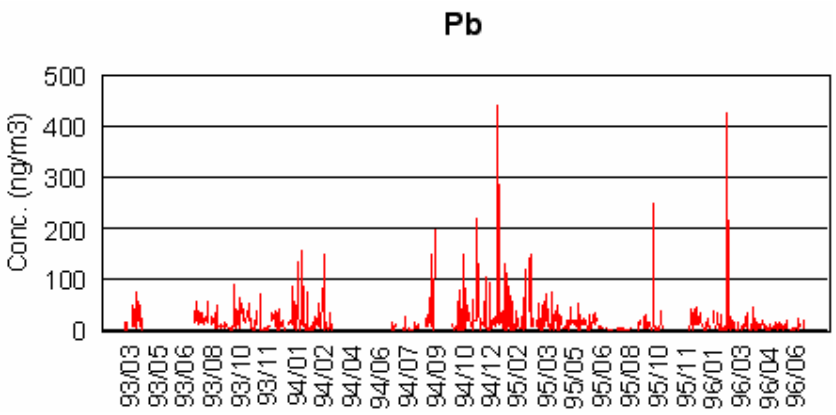

Figure 4.11. Temporal Variation of Pb

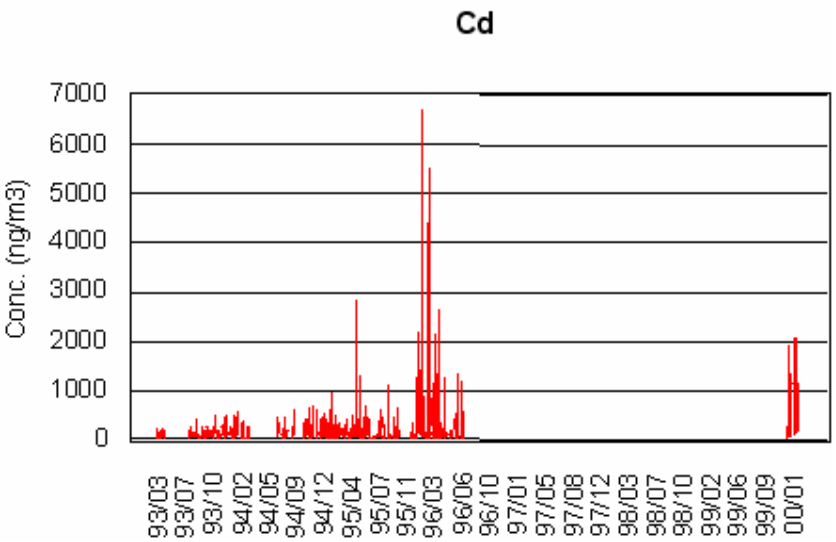

Figure 4.12. Temporal Variation of Cd

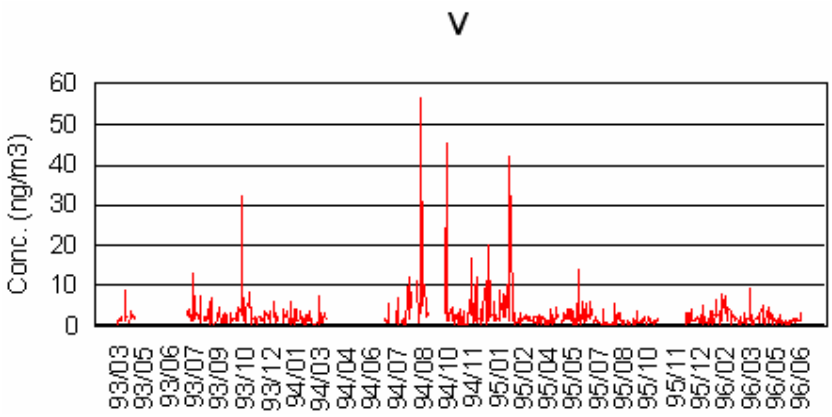

Figure 4.13. Temporal Variation of V

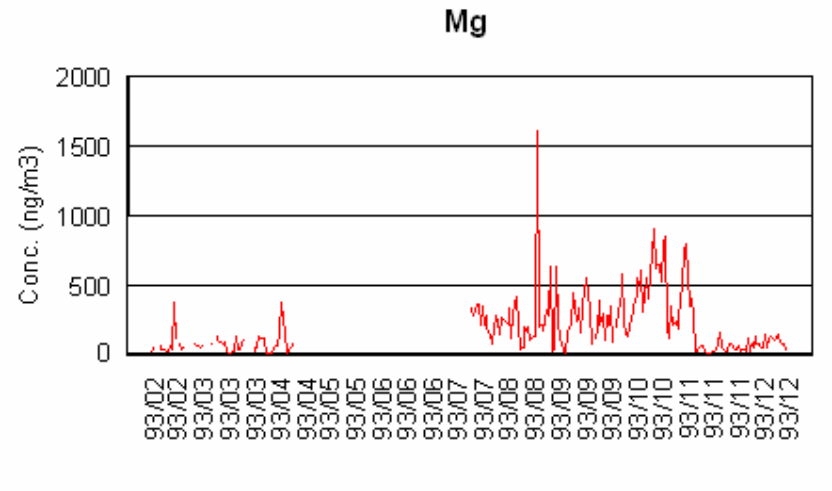

Figure 4.14. Temporal Variation of Mg

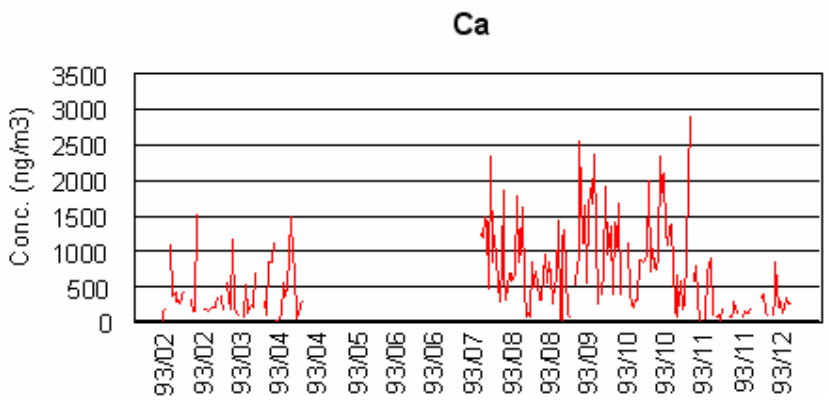

Figure 4.15. Temporal Variation of Ca

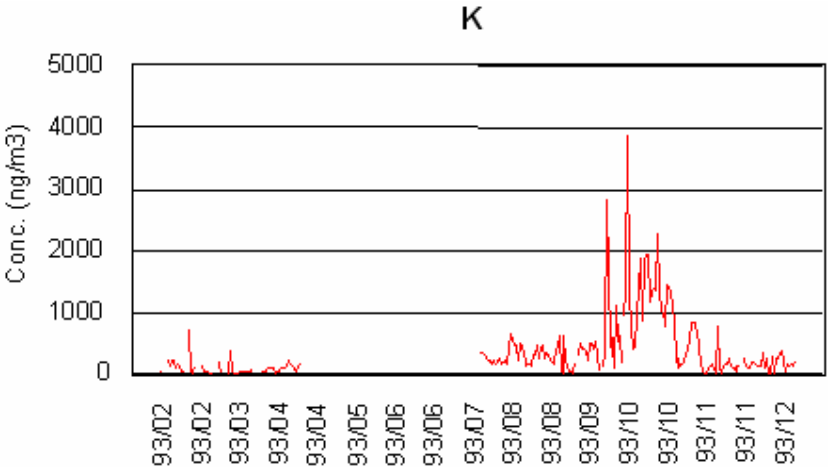

Figure 4.16. Temporal Variation of K

thousands of kilometers away can not have an impact on their concentrations measured at the Çubuk station.

Observed episodic high concentrations of pollution derived parameters are probably due to transport patterns and meteorological features, such as the mixing height.

Backtrajectories of selected SO_4^{2-} concentration episodes are depicted in Figure 4.17. During high episodes the concentration of SO_4^{2-} ion increases form its geometric mean value 0.84 μg m^{-3} to 18.7 μg m^{-3}. As can be seen from Figure 4.17, trajectories corresponding to high SO_4^{2-} episodes, with few exceptions, originate from NW and W sectors. These two sectors include majority of high anthropogenic emission areas in Eastern and Western Europe. A similar relation between sectors from which trajectories originate and episodes can be seen in the concentrations of most pollution derived species. Clear association of episodes in concentrations of SO_4^{2-} and other pollution-derived parameters indicates that episodes are at least partly due to change in transport direction. Such relation between episodes in concentrations of anthropogenic species and transport direction was observed in most of the studies performed in the region (Güllü et al., 1998; Karakaş, 1999).

Another mechanism that generates episodes is the washing of the atmosphere by local rain events at the sampling point. Rainfall at the sampling point clears the atmosphere and results in low concentrations of both natural and anthropogenic species; it can generate a “minimum” in concentrations. If this happens during a period of high concentration of a parameter an episode can be generated. The relation between minima in concentrations of parameters and rain events were observed in this study and will be discussed later in the manuscript. However, it should be noted that Central Anatolia receives very low rainfall. Annual average rainfall in the Çubuk meteorological station is 455 mm. On the average there were approximately 30 events each year. Considering

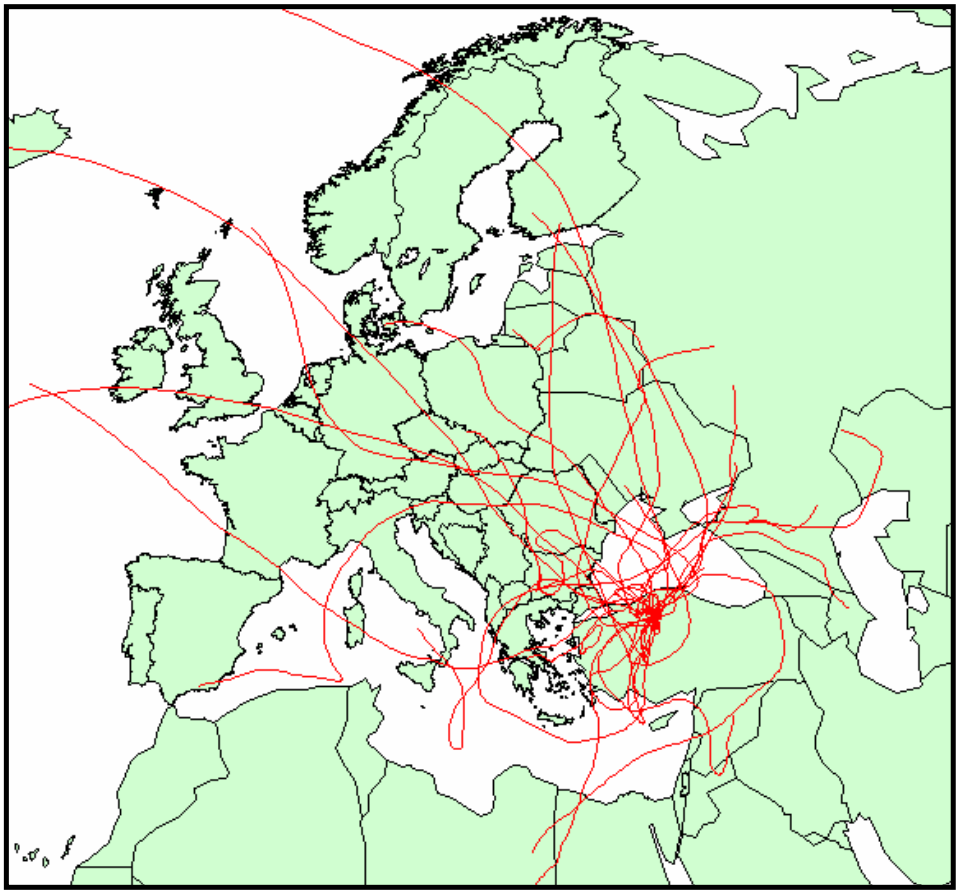

Figure 4.17. Back trajectories corresponding to high SO_4^{2-} concentration days

that some of those events were too small to cause substantial change in the atmosphere and some occurred during low concentration periods and hence did not cause an identifiable episode, one can conclude that variations in transport pattern is more important in determining short-term variations in concentrations of species than local rainfall.

For crustal elements like Mg, Ca and K, the situation is somehow different. The resuspension of soil into the atmosphere are high in summer months when the surface of the soil is dry. The formation of

crustal aerosols is highly dependent on the local wind speed. The weathering of soil is enhanced by strong winds when the soil surface is dry. So, the short-term variations of concentrations of crustal elements measured at the station are dependent on the variations in the source strength. The effect of rain in generating episodes are the same in both crustal and anthropogenic elements.

Consequently, short-term variations in concentrations of pollution derived elements in this study were generated by variations in transport patterns and those observed in crustal elements are due to variations in source strengths. The local rain are expected to generate some episodes in concentrations of both anthropogenic and crustal elements, but this effect is not expected to be significant.

4.2.2. Effect of Local Rains on Concentrations of Measured Parameters

Rain scavenges gases and particles from atmosphere and thus concentrations of parameters measured. Since the local rain events can affect temporal behavior of parameters, the magnitude of this mechanism was investigated. Both the local and distant rain events that coincide with the upper atmospheric movement of air masses that carries pollutants to our sampling point do affect concentrations of pollutants at the receptor. This section deals with the effect of local rain events. It would be good if the effect of distant rain could also be studied, but such an assessment not requires rain data from all over Europe and Asia, but also data on cloud height, rain intensity etc. Unfortunately such data do not exist in any organization, national or international.

When it rains, falling hydrometeors washes out all the pollutants between the cloud base and the surface. As a result of this process,

which is called below cloud process or washout, concentrations of pollutants in rain water increase in atmosphere decrease.

The effect of rain scavenging on observed concentrations of all parameters measured in this study are depicted in Figures 4.18–4.26. These figures show time series plots of ions and elements in log scale. Rain events are indicated by bars on the same figure. Rainfall data is obtained from a recording raingouge at the station.

For most of the parameters measured in this study, rain events correspond to a dip or minimum in the concentration plot. This indicate that rain do cause a decrease in the concentrations of measured parameters. However, there are few cases in each plot where this observation is not valid, i.e. concentrations are high in the day it rained. These few disagreements with general trend are probably due to difficulty of matching rain and concentration data. Both rain data and concentration data are in 24 hr averages. But they do not necessarily start and end at the same time. For example rain may start at 3:00 at night and the sample is changed at 10:30 in the morning. If the rain stops at 2:00 in the afternoon, although they are both recorded for the same day, the rain effects the previous sample not the sample started in that particular day. Consequently, effect of rain can be seen one day before or one day after the particular day for which it is recorded. This naturally causes the deviations from the general trend shown in the figure.

When it rains, most of the pollutants are washed out from atmosphere and, as a result of this atmospheric concentrations are low. After the rain stops, atmosphere starts to filled with the pollutants transported from distant sources. The time period between rain event and return of the atmosphere to pre-rain levels can be defined as “reloading time”.

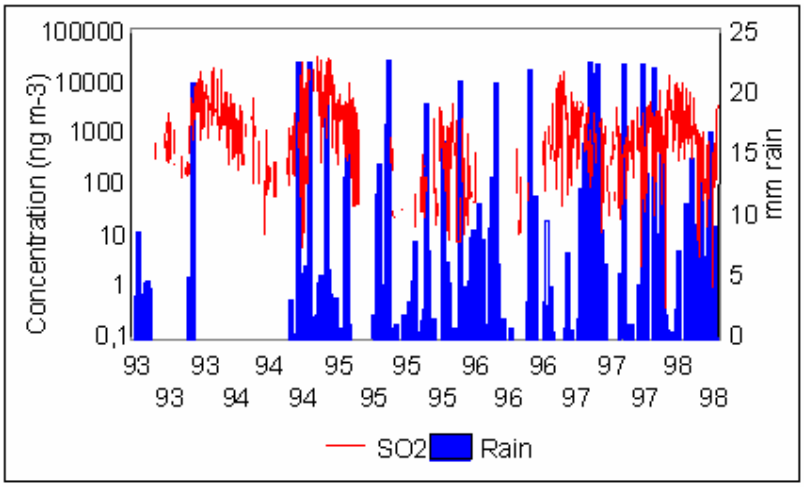

Figure 4.18. Effect of Local Rains on Concentrations of SO_2

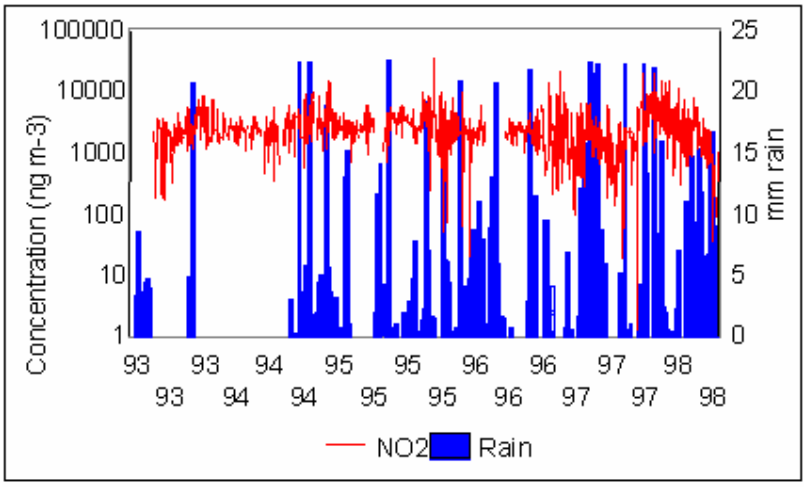

Figure 4.19. Effect of Local Rains on Concentrations of NO_2

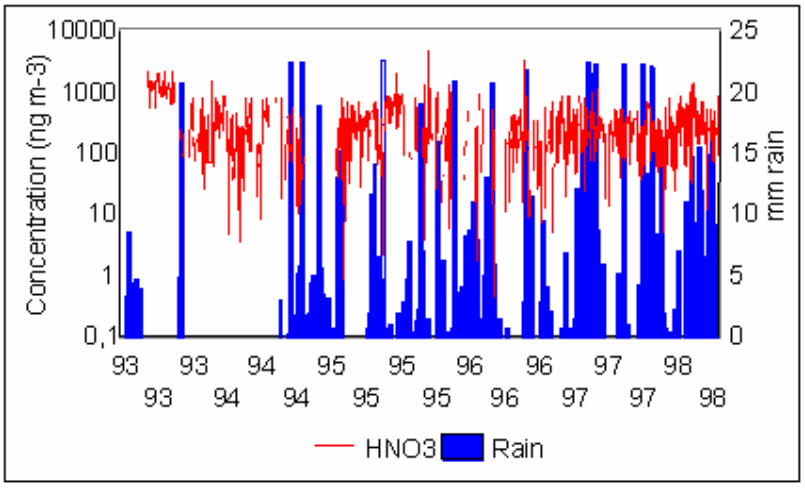

Figure 4.20. Effect of Local Rains on Concentrations of HNO_3

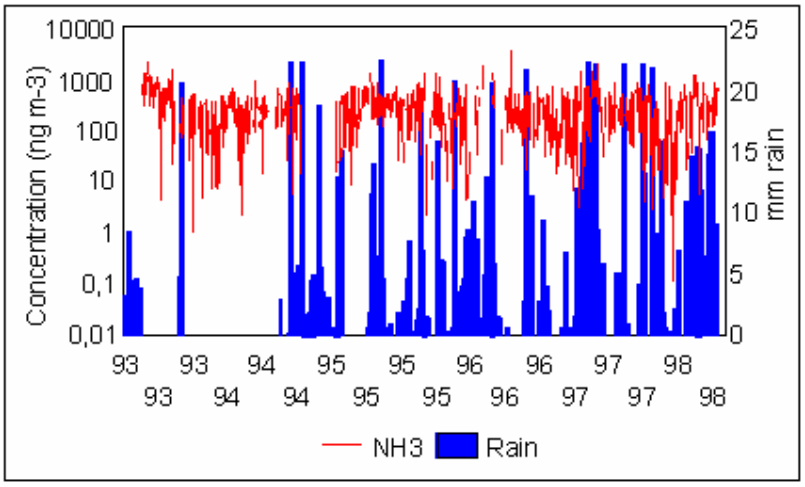

Figure 4.21. Effect of Local Rains on Concentrations of NH_3

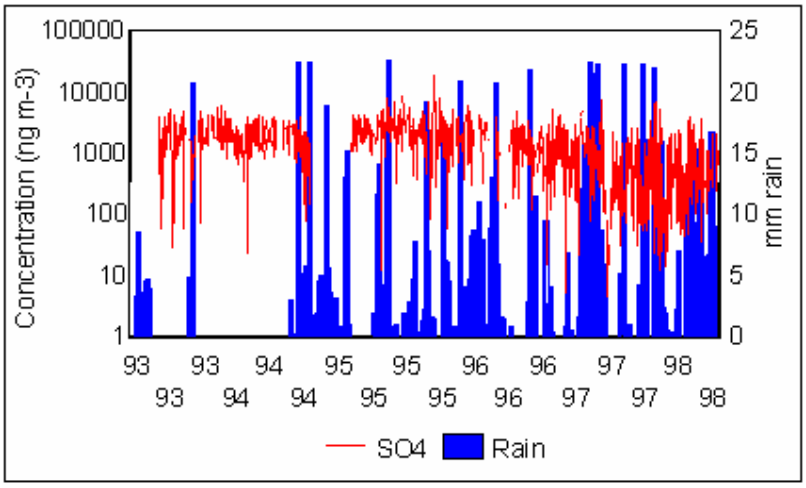

Figure 4.22. Effect of Local Rains on Concentrations of SO_4^{2-}

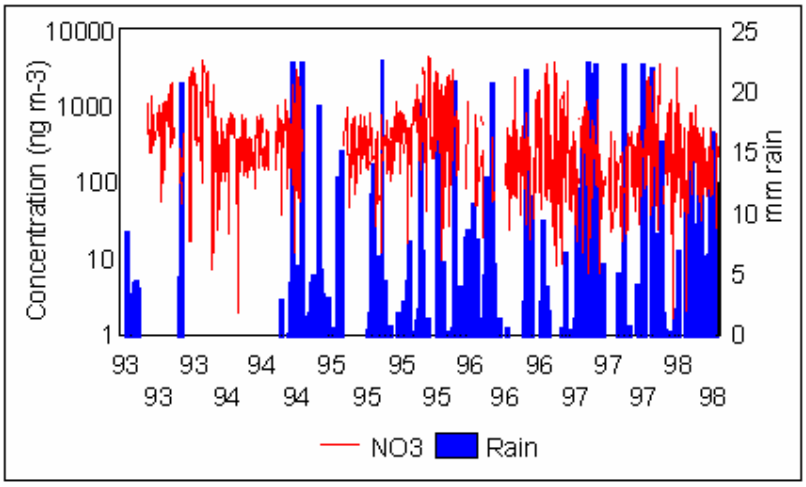

Figure 4.23. Effect of Local Rains on Concentrations of NO_3^-

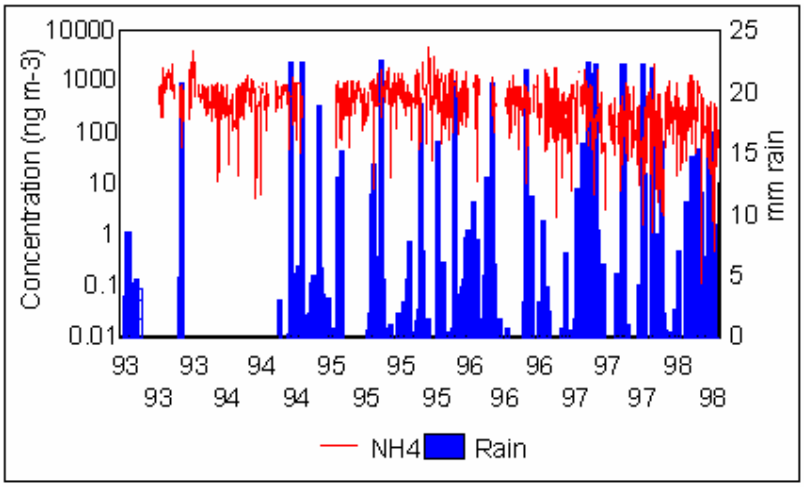

Figure 4.24. Effect of Local Rains on Concentrations of NH_4^+

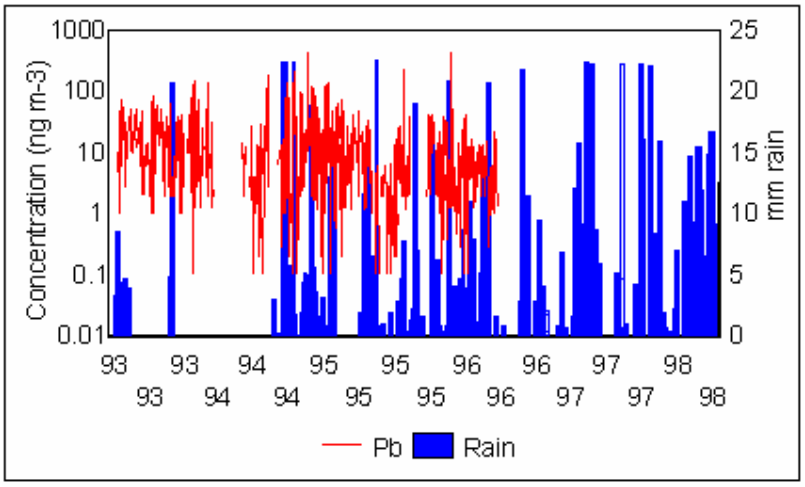

Figure 4.25. Effect of Local Rains on Concentrations of Pb

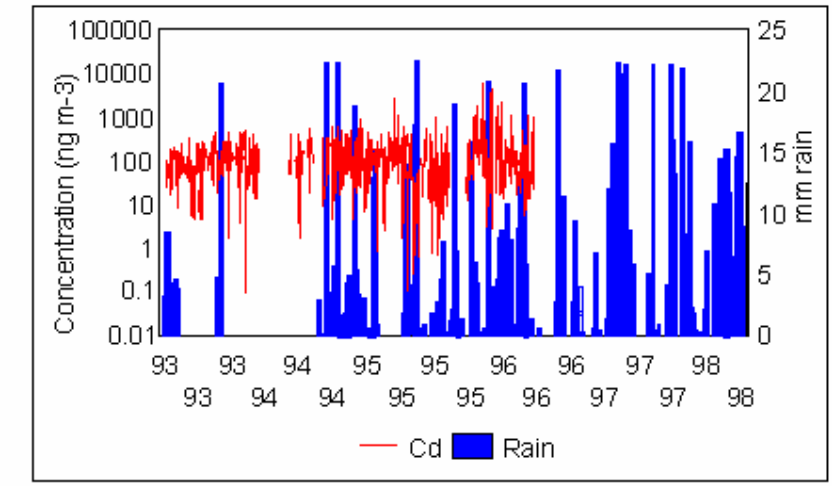

Figure 4.26. Effect of Local Rains on Concentrations of Cd

Median concentrations of elements and ions after 0 – 12 days after the rain event are depicted in Figure 4.27. As can be seen from the figure, for most of the parameters there is a clear increasing trend with increasing number of days from the rain.

The reloading time of the atmosphere seems to be different for different species. For HNO_3, SO_4^{2-}, NH_4^+, Pb, Cd, Mg, Ca and K the steady increase in their concentrations continues 5-7 days. The variation after 7 days does not seem to be related with the rain. Consequently for these elements reloading time of the atmosphere is approximately 7 days. For SO_2 the consistent increase is longer. The reloading time of atmosphere for SO_2 seem to be 9 days.

There is no clear difference observed between anthropogenic elements like SO_4^{2-}, Cd and parameters with natural sources such as Ca, Mg and K. Similarly, there is no significant difference observed between gases and particle-bound elements and ions according to their reloading time to atmosphere.

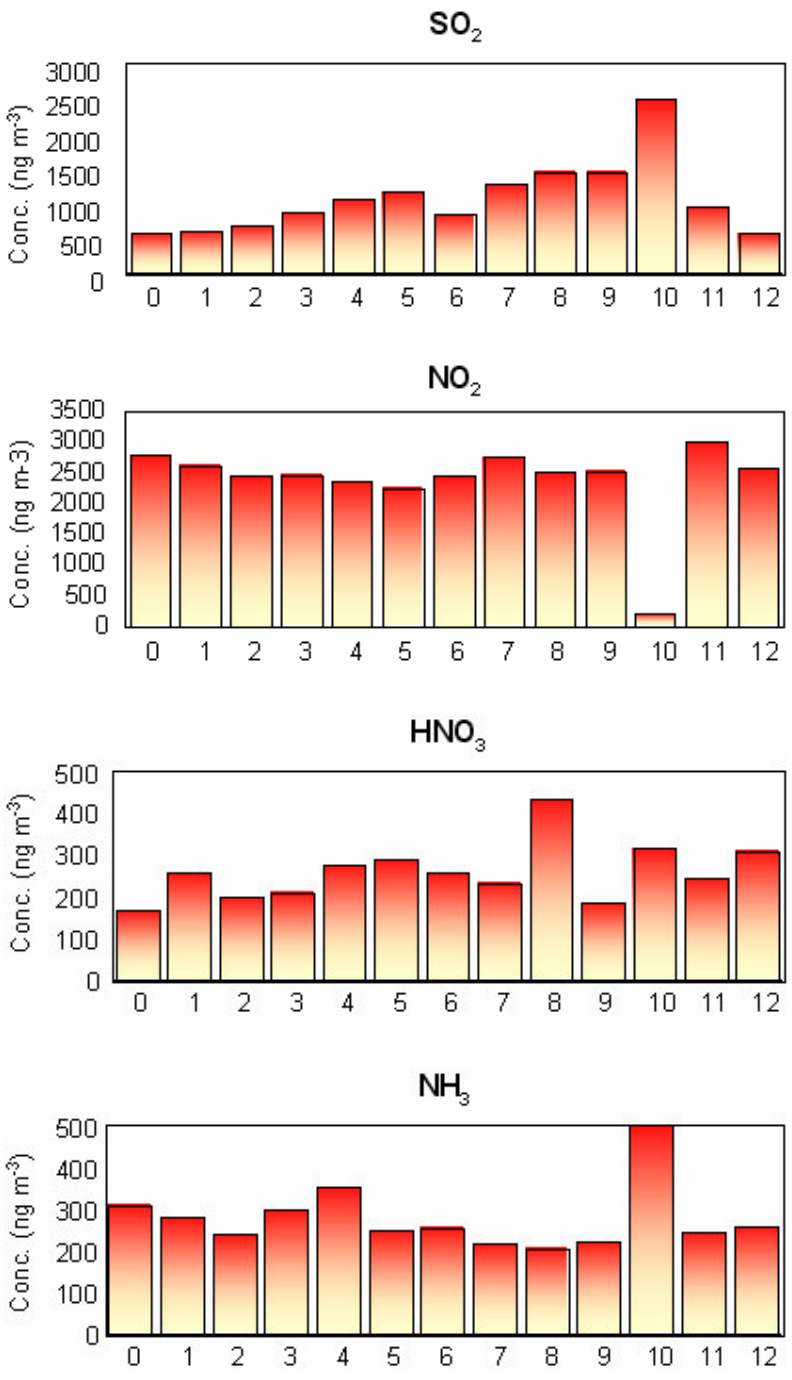

Figure 4.27. Average Concentrations of Elements Measured Between 0 and 12 days After Rain Event

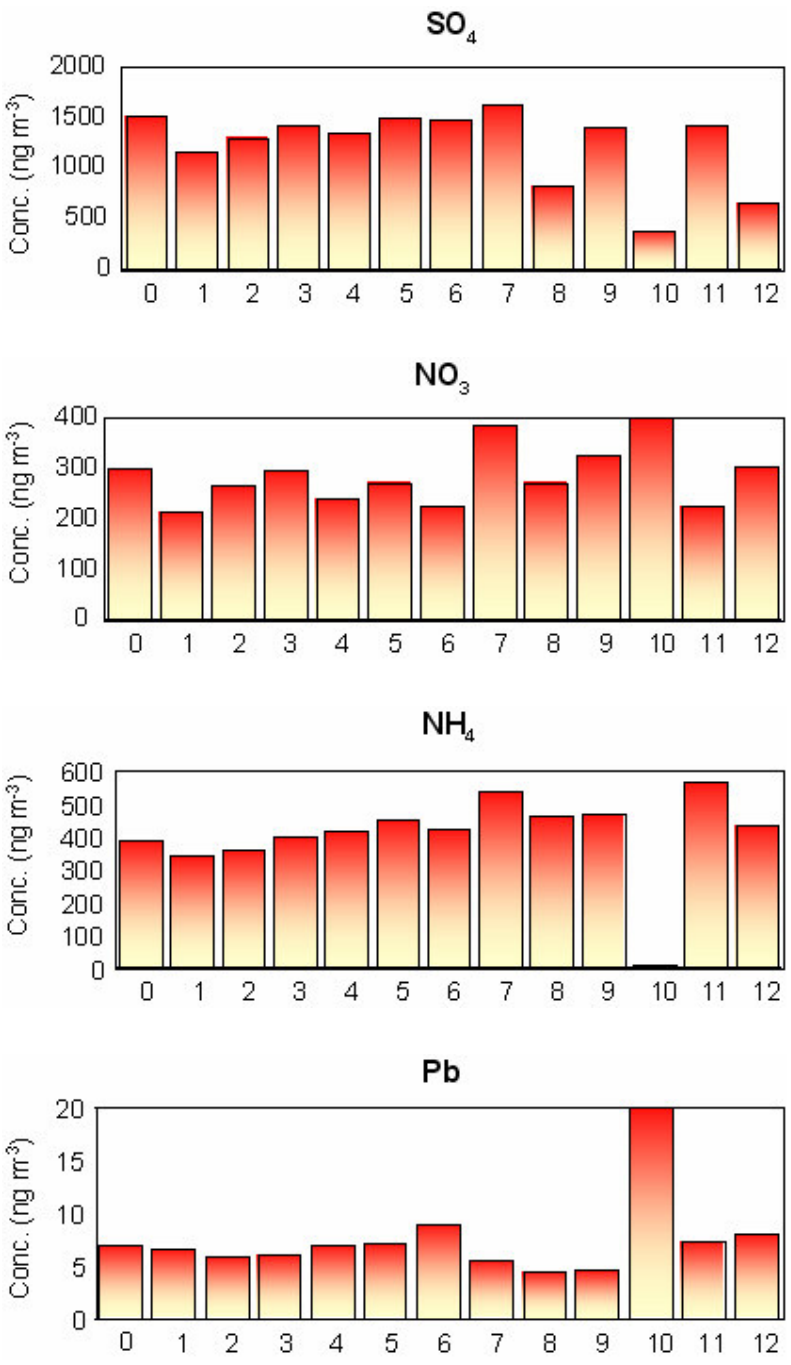

Figure 4.27. Average Concentrations of Elements Measured Between 0 and 12 days After Rain Event (Cont'd)

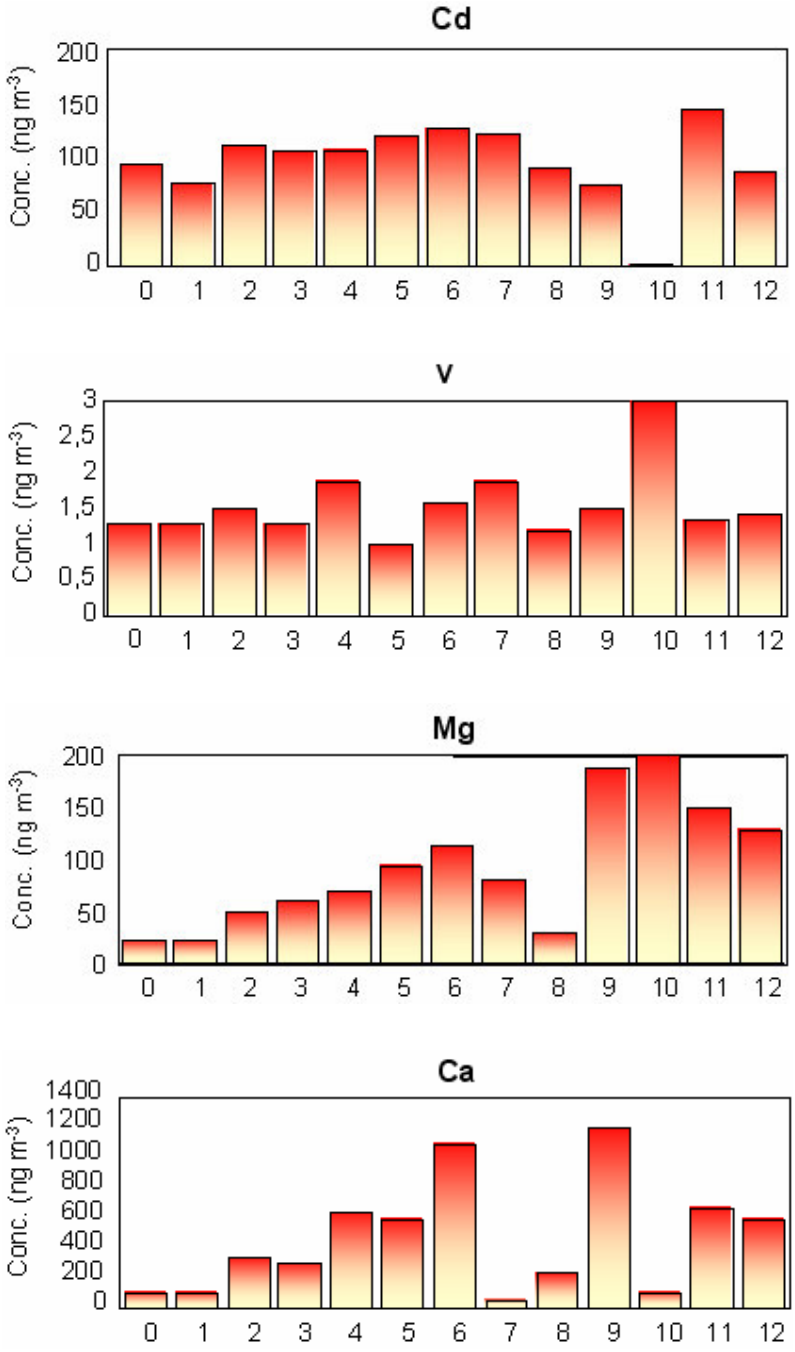

Figure 4.27. Average Concentrations of Elements Measured Between 0 and 12 days After Rain Event (Cont'd)

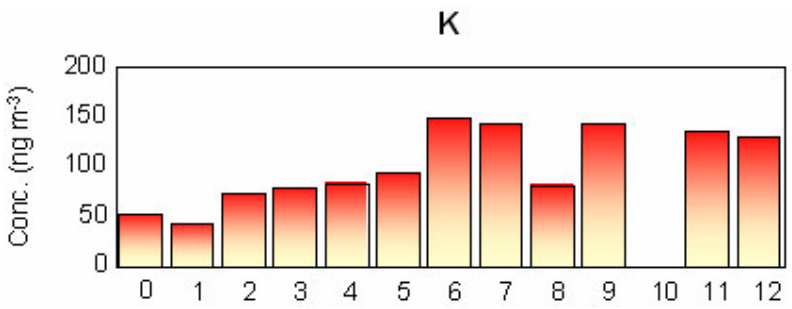

Figure 4.27. Average Concentrations of Elements Measured Between 0 and 12 days After Rain Event (Cont'd)

For NO_2, NH_3 and V there is no consistent increase observed as in other species. The reason is not clear. Normally the increasing trend after rain events, which is observed in other parameters are expected for all species. If there is no significant change after rain event it may mean (1) that gas or particle is not scavenged efficiently with rain and (2) atmosphere is reloaded with that specie as soon as rain stops.

NO_2 is not highly soluble in water. For example it is 100 times less soluble than SO_2 (Henry's law constants for SO_2 and NO_2 are 1.2 and $3.4x10^{-2}$ K(mol/atm) at 298 K, respectively). Consequently removal of NO_2 from atmosphere via rain may not be an efficient mechanism and it may explain lack of variation in NO_2 concentration with time from rain event.

However, NH_3 is highly soluble in rain and is expected to be scavenged much better than SO_2. Rapid reloading of atmosphere with NH_3 is also not expected. It is worthy to note that NH_3 concentration measured at Çubuk station is smaller than NH_3 concentrations measured in other Turkish stations and in EMEP stations and it is suggested that there is no significant NH_3 emissions in the vicinity of the station. The reason for

such behavior of NH_3 is not clear. The reason for similar lack of variation in V concentrations after rain event is also not clear, because most of the particle bound parameters showed a steady increase after rain events. V is the only exception and there is no explanation for such lack of variation.

The median concentrations of measured parameters in all samples and excluding samples corresponding to first five days after every rain and fractional difference between the two are given in Table 4.4. In this table, since in the five days after rain event concentrations of parameters increase gradually, the influence of rain on average concentrations of measured parameters are eliminated by excluding the data corresponding to these five days.

Table 4.4. Contribution of Local Rain on Average Concentrations

	Overall Average		Average without first 5 days after rain		Percent Difference
	AVG ($ng\ m^{-3}$)	Median ($ng\ m^{-3}$)	AVG ($ng\ m^{-3}$)	Median ($ng\ m^{-3}$)	
SO_2	2387	863	2650	1191	28
NO_2	2995	2504	2786	2469	-1
HNO_3	371	254	426	291	13
NH_3	348	281	346	275	-2
SO_4^{2-}	1866	1613	1998	1852	13
NO_3^-	543	329	589	374	12
NH_4^+	553	449	607	515	13
Pb	16.8	8.0	17.5	9.0	11
Cd	198	107	167	111	3.6
V	2.25	1.50	2.48	1.50	0
Mg	191	121	235	184	34
Ca	633	460	723	581	21
K	367	173	461	237	27

The results indicate that the contribution of washout or below-cloud processes on SO_2 concentration at the sampling site is 28%. In other words, if there were no rain observed SO_2 concentration would be 28% higher. When the data in table viewed with this perspective it can be seen that the reduction in median concentrations of most of the measured parameters due to local rain scavenging varies between 11% for Pb and 34% Mg.

The median concentrations of parameters that did not show an increasing concentration trend after rain events, namely NO_2, NH_3 and V are not affected by the local rain processing as indicated by 0 or negative percent differences. Cd concentrations are also not affected substantially by the rain processing in the atmosphere.

4.2.3. Long-term (Seasonal) Variations

Seasonal variations of parameters measured in Çubuk station are given in Table 4.5 and visually shown in Figure 4.28. As can be seen from both the table and the figure, parameters measured can be divided into three groups according to their seasonal variations. First group consists of SO_2, NO_2, NO_3, Pb and Cd. Winter concentrations of these parameters are significantly higher than their concentrations in summer season. Second group includes SO_4^{2-}, HNO_3, NH_4^+ and V. The winter and summer concentrations of these parameters do not show any significant difference. NH_3, Mg and Ca are included in the third group. Summer concentrations of these parameters are significantly higher than the winter concentrations. Although there is not enough data for K to assess its seasonal variations, summer season concentrations are generally higher and it must be included in the third group.

There are two factors that affect the seasonal variations of parameters measured. The first one is the scavenging of pollutants from atmosphere during their long-range transport. Removal of the pollutants

Table 4.5. Winter and Summer Average Concentrations and Median Values of Parameters Measured

Parameters	Winter*		Summer**	
	Avg. Conc. ($\mu g\ m^{-3}$)	Median ($\mu g\ m^{-3}$)	Avg. Conc. ($\mu g\ m^{-3}$)	Median ($\mu g\ m^{-3}$)
SO_2	3.716 ± 5.602	1.8	0.930 ± 1.324	0.48
NO_2	3.462 ± 2.893	2.72	2.268 ± 1.292	2.23
HNO_3	0.381 ± 0.515	0.24	0.408 ± 0.449	0.31
NH_3	0.303 ± 0.275	0.23	0.440 ± 0.335	0.37
SO_4^{2-}	2.097 ± 2.086	1.66	1.835 ± 1.389	1.59
NO_3^-	0.738 ± 0.841	0.42	0.329 ± 0.263	0.27
NH_4^+	0.596 ± 0.596	0.47	0.484 ± 0.365	0.42
Pb	0.021 ± 0.041	0.01	0.011 ± 0.017	0.01
Cd	0.297 ± 0.555	0.15	0.149 ± 0.226	0.09
V	0.002 ± 0.003	0.002	0.002 ± 0.003	0.001
Mg	0.177± 0.218	0.08	0.207 ± 0.203	0.18
Ca	0.482 ± 0.541	0.27	0.814 ± 0.589	0.72
K	0.403 ± 0.591	0.13	0.291 ± 0.332	0.21

* Winter season includes months between October and March
** Summer season includes months between April and September

from atmosphere via rain is an important factor that affects their seasonal variations (Güllü et al, 1998; Bergametti et al., 1989). Pollutants which have distant sources are washed out from the atmosphere as the air mass which carries them passes through rain events. As the frequency of rain is higher in winter months, the pollutants which have source regions far away from the receptor site can hardly reach to the receptor site in winter. So, for the pollutants which are long-range transported to Central Anatolia, winter concentrations are expected to be lower than summer concentrations. The species, which have local sources, on the other hand, have less chance to be removed from the atmosphere via rain, because the distance, which they travel before they are intercepted at the station, is

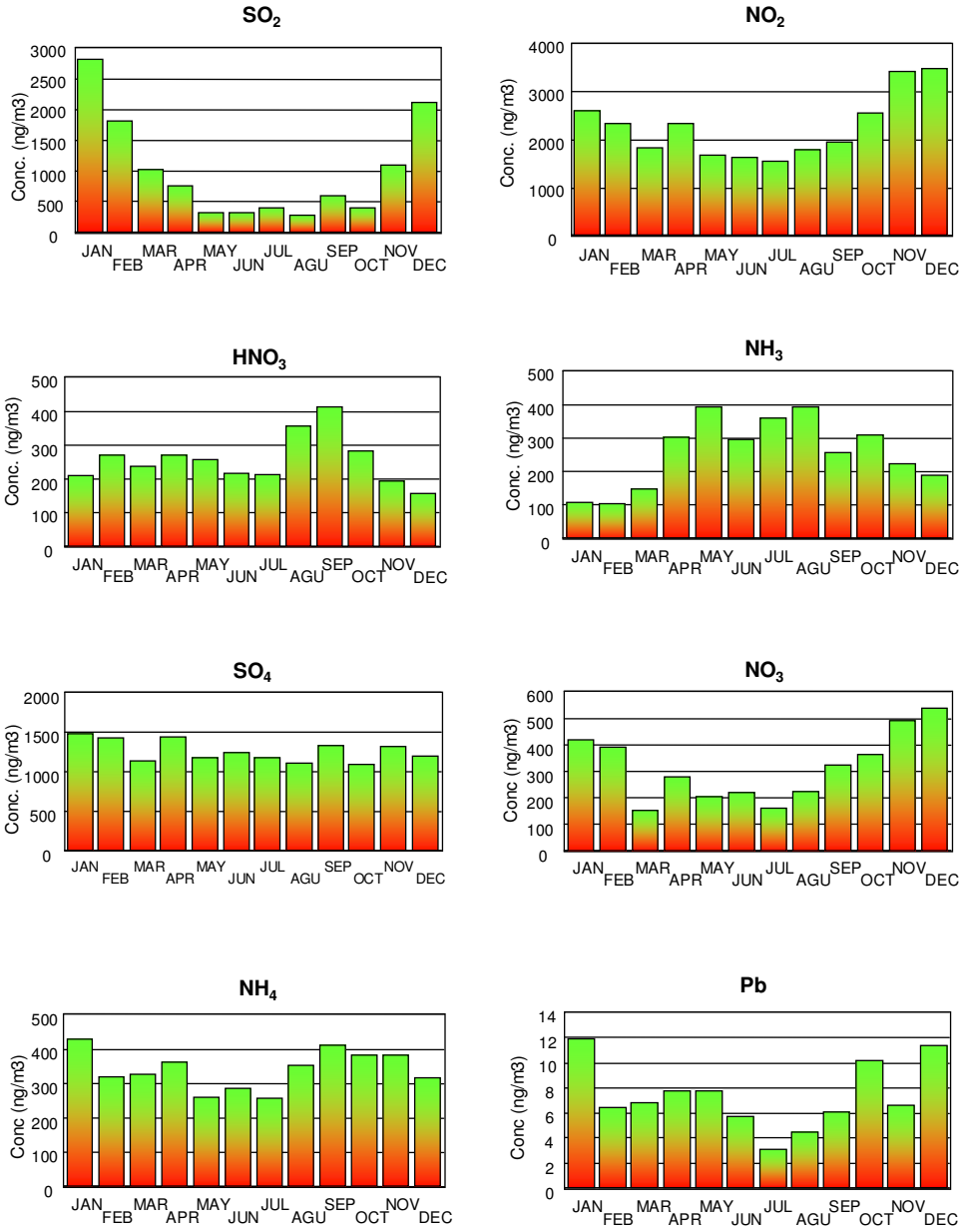

Figure 4.28. Monthly Average Concentrations of Measured Parameters

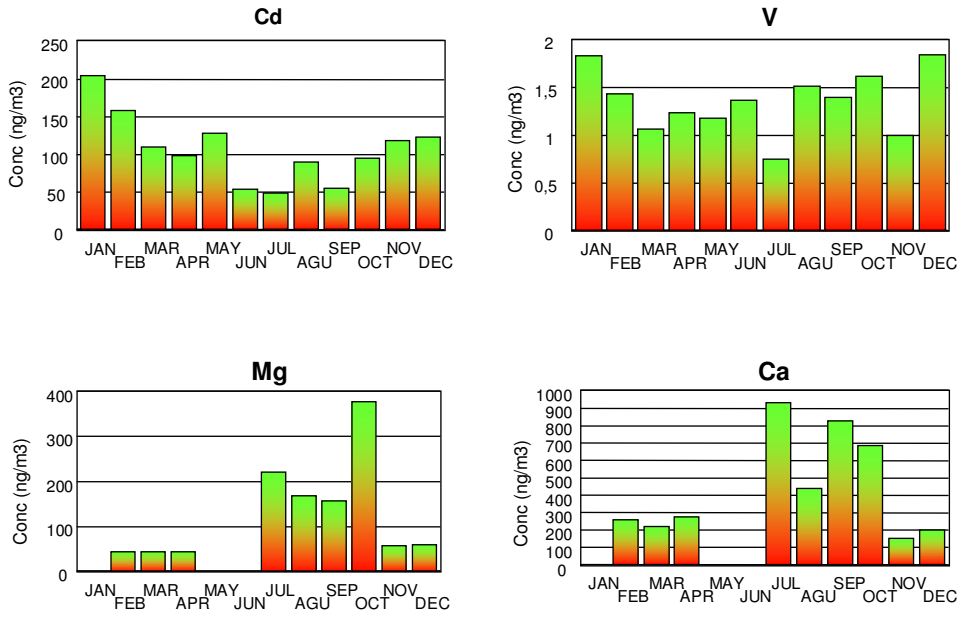

Figure 4.28. Monthly Average Concentrations of Measured Parameters (Cont'd)

shorter. Consequently, winter concentrations of locally produced species is expected to be higher than their summer concentrations. This mechanism suggests that SO_2, NO_2, NO_3, Pb and Cd which have higher concentrations in winter months may have local sources. Among these SO_2 and NO_2 have fairly short lifetime in the atmosphere. Presence of these two parameters in this group confirms that SO_2, NO_2, NO_3, Pb and Cd is likely to be emitted from local sources. The term "local" does not necessarily mean areas in the immediate vicinity of the station. The region within central and western Turkey are all within one-day trajectory distance to the station. Emissions in this region can reach the station without significant scavenging. Consequently, local refers roughly the area within Turkey.

The photochemical reactions can be another reason for observing high concentrations of NO_2 and SO_2 in winter. SO_2 and NO_2 are transformed to SO_4^{2-} and NO_3^- via photochemical reactions in the atmosphere. As

the rate of photochemical reactions is higher in summer months (due to higher solar radiation) both SO_2 and NO_2 are oxidized to SO_4^{2-} and NO_3^- at a faster rate in summer months. Consequently, if the photochemical reaction rate is the determining factor in seasonal variations in the concentrations of reactive species, then concentrations of SO_2 and NO_2 are expected to decrease and those of SO_4^{2-} and NO_3^- are expected to increase in the summer season. Although, SO_2 and NO_2 concentrations are higher in winter, concentrations of SO_4^{2-} and NO_3^- are not significantly higher in summer, suggesting that photochemical conversion is not the determining factor in seasonal variability in their concentrations.

As indicated before, the concentrations of the second group of parameters including SO_4^{2-}, HNO_3, NH_4^+ and V do not show any significant seasonal variations. Nitric acid, SO_4^{2-} and NH_4^+ have man made sources. They can be generated locally or they can be transported from distant sources. Temporal behaviors of these four parameters are not the same with their seasonal variations in other studies at the eastern Mediterranean region. In most of the studies performed in the region all four of these parameters are found to have higher concentrations in summer season, which is explained by both more extensive rain scavenging in winter and faster photochemical formation rate during summer months (Güllü et al., 1998; Mihalopoulos et al., 1997; Kouvarakis et al., 2002; Luria et al., 1996; Danalatos et al., 1995). Unlike those observed in indicated studies, SO_4^{2-}, HNO_3, NH_4^+ and V do not have higher concentrations in summer period, but they do not also have higher concentrations in winter, like the parameters that are strongly affected from local sources. If the rain scavenging is the main mechanism that determine seasonal patterns of measured species in this region, as suggested by most of the studies (Güllü et al., 1998; Kubilay and Saydam 1995; Luria et al., 1996; Bergametti et al., 1989; Remoudaki et al., 1991), then observed similarity between summer and

winter concentrations of SO_4^{2-}, HNO_3, NH_4^+ and V in this study indicates a higher contribution of local sources to Central Anatolia atmosphere than those observed at coastal Mediterranean stations. When this is coupled with fairly low concentrations of anthropogenic parameters, such as SO_4^{2-}, NH_4^+, NO_3^-, Pb etc. at the Çubuk station, than those observed at the coastal sites, it can be concluded that sources affecting observed concentrations of pollution-derived parameters at the Central Anatolia are different from source regions affecting coastal areas in the Eastern Mediterranean region.

Concentrations of species in the third group, namely NH_3, Mg, Ca and K are higher in summer than in winter. For Mg, Ca and K this is due to high resuspension of crustal element in summer. In winter months, Anatolian Plateau is covered by mud and ice. So, the weathering of soil into atmosphere would be at a minimum level. Whereas, dry soil surface in summer months favors the formation of crustal aerosols. It should be noted that Ca, Mg and K were measured for a short period in 1993 and seasonal variability bases on such short data can have significant uncertainties. However, crustal source for these elements are well known and they showed summer high concentrations in all studies in the region. Consequently their higher concentrations in summer at Çubuk station, gives the impression that their temporal behavior is more or less the same with that observed in all other stations in the region.

The reason for observed high concentrations of NH_3 in summer months is different from the others. The main source of NH_3 is the ammonium containing fertilizers or animal grazing. In the Mediterranean region, fertilizer is shown to be the dominating source for NH_3 emissions (Al Momani et al., 1998; Güllü et al., 1998; 2000). Fertilizers are generally applied to soil in Spring months; furthermore the increase of temperature during summer season enhances both the volatilization of NH_3 from fertilizer containing soil and its conversion to NH_4^+ ion.

4.3. Dry Deposition

Dry deposition is the transfer of atmospheric constituents, in the form of either gases or particles, to any surface without first being dissolved in atmospheric water droplets. In this regard, dry deposition is an important mechanism for removing pollutants from the atmosphere in the absence of precipitation. Atmospheric deposition occurs either as wet deposition or dry deposition. In most parts of the world wet deposition is the main form of deposition. However, in regions with low annual rainfall dry deposition can be comparable or even higher than wet deposition. Mediterranean region is characterized with low rainfall (<1000 mm in most parts, particularly in the eastern parts of the basin). Annual rainfall In the Çubuk area is approximately 400 mm), which is very low even compared to other regions in the eastern Mediterranean. (excluding desert areas). Consequently, dry deposition fluxes of measured species are expected to be unusually high in the region.

Dry deposition is usually characterized by a deposition velocity, V_d, which is defined as the dry deposition flux, F_d, to the surface divided by the concentration, [S], of the species.

$$V_d = \frac{F_d}{[S]}$$

Then dry deposition flux, which is the amount of the species deposited per unit area per time in a geographical location, can be calculated if the deposition velocity and the pollutant concentration are known.

Dry deposition velocity is related with resistance, r:

$$V_d = \frac{1}{r}$$

where r has two components:

$$r = r_{gas} + r_{surf}$$

where r_{gas} is the gas phase resistance and r_{surf} is the surface resistance.

The gas phase resistance (r_{gas}) is determined by the vertical eddy diffusivity which depends on the evenness of the surface and the meteorology, for example, wind speed, solar surface heating, and so on. The surface resistance (r_{surf}) depends on the characteristics of the surface, like type, plants, wetness, etc.) as well as the nature of the pollutant deposited. As a result, dry deposition velocity show a wide range depending on the conditions during the measurements.

If the dry deposition velocities of parameters can be found, dry deposition fluxes can be calculated, simply by multiplying v_d value for each specie with its concentration. In this study v_d values for each parameter was found from literature and multiplied with the measured concentrations of that parameter to derive the fluxes. Results are presented in Table 4.6, together with the vd used for each parameter. Dry deposition velocities of SO_2, NO_2, HNO_3, were obtained from the model study by Singles et al. (1998). These values are in consistent with values determined by other measurements and model studies in the literature (Tohno et al, 2001; Takahashi et al, 2001; Luria et al, 1996; Duyzer, 1994). Dry deposition velocities of elements that are known to be associated with submicron particles, namely SO_4^{2-}, NO_3^-, NH_4^+, Pb and Cd, are assigned as 0.1 cm s^{-1} and those of elements which are known to be associated with coarse particles, namely, Mg, Ca and K are assigned as 2 cm s^{-1} (Herut et al, 2001; Duce et al., 1991). However we modified the v_d for NO_3^-. Nitrate is formed by gas to particle formation in the atmosphere and hence is expected to be in the form of submicron particles (gas-to-particle conversion, as mechanism is known to produce very small particles). However, in most of the size distribution studies NO_3^- is found to be associated with coarse particles (Havranek et al., 1996; Holsen et al., 1993; Pakkanen, 1996; Zhuang et

Table 4.6. Dry Deposition Velocity and Dry Deposition Fluxes of Parameters Measured

Parameters	Dry Deposition Velocity ($cm\ s^{-1}$)	Dry Deposition Flux ($\mu g\ m^{-2}\ day^{-1}$)
SO_2	0.8	1,800 ± 3,200
NO_2	0.1	251 ± 204
HNO_3	2.2	752 ± 915
NH_3	0.8	259 ± 218
SO_4^{2-}	0.1	169 ± 152 (1600)
NO_3^-	2	900 ± 1100 (1500)
NH_4^+	0.1	46 ± 43 (465)
Pb	0.1	1.5 ±2.8 (11)
Cd	0.1	20 ± 38 (0.15)
V	1	1.9 ± 3.1 (2.0)
Mg	2	328 ± 366 (1500)
Ca	2	1,100 ± 1,000 (3800)
K	2	615 ± 866 (440)

Numbers in parenthesis are the corresponding dry deposition fluxes of elements measured at a rural station at Antalya (Kuloğlu, 1997)

al., 1999; Spokes et al., 2000; Yeatman et al., 2001). This is attributed to reaction of HNO_3 on sea salt and soil aerosol surfaces (Zhuang et a., 1999; Spokes et al., 2000; Yeatman et al., 2001). These literature suggests that the v_d value of 0.1 cm s^{-1} for NO_3^- suggested by Herut et al. (2001) and Duce et al., (1991) would severly underestimate the NO_3^- dry deposition flux at our site. Consequently, v_d value of 2.0 (the value suggested to be used for coarse particles) was used to calculate NO_3^- dry deposition flux. Finally, dry deposition velocity of NH_3 is assigned as 0.8 cm/s (Tohno et al, 2001; Duyzer et al, 1994).

Dry deposition fluxes calculated can be put into descending order as SO_2, Ca, NO_3^-, HNO_3, K, Mg, NH_3, NO_2, SO_4^{2-}, NH_4^+, Cd, V and Pb. As can be seen from the table, SO_2 has the highest dry deposition flux with its high dry deposition velocity and concentration. As crust originated Ca, Mg and K are found in big fractional particles it is expected that they have high dry deposition fluxes. High dry deposition flux of HNO_3 can be also explained by its high dry deposition velocity. At the end of the order, there are small particles and gases which have low concentrations and dry deposition velocities. Dry deposition fluxes of particulate species are also shown in Table 4.6. Comparison of Antalya fluxes with the ones calculated in this study shows that dry deposition fluxes are generally lower at Çubuk station except Cd due to unexpected high concentration of Cd measured at Çubuk station. The difference is reasonable for K, Ca, Mg, V and NO_3^-, but about an order of magnitude for SO_4^{2-}, NH_4^+, Cd and Pb. Part of the observed low deposition flux in this study is real and stems from lower concentrations of elements at Central Anatolia, but some of the difference is inherent to the method used in dry deposition flux calculations in this study.

In this study all of the SO_4^{2-}, NH_4^+, Pb and Cd was assumed to be in the fine aerosol fraction and a fairly low v_d value was used to calculate their deposition flux. However, a small fractions of these species can occur in the coarse fraction, either due to sticking of fine particles onto coarse aerosol or contribution of coarse sea salt (Rojas et al., 1993; Dulac et al., 1989; Holsen et al., 1993). Small and large particles do not contribute to dry deposition flux equally. Coarse fractions of elements are much more influential on the total dry deposition flux. Please note that v_d values used for coarse and fine elements to calculate their deposition fluxes in this study (also in literature) are 2 and 0.1, respectively. This difference in the v_d values is a good indication of the dominating influence of coarse particles on the dry deposition fluxes of elements. In this study elements were assumed to be all in the coarse

fraction or all in the fine fraction. There was no problem for Ca, Mg and K which are associated with coarse particles. Even if small fraction of their mass is in the fine fraction this would not cause a significant difference in their dry deposition fluxes, because contribution of fine mass on dry deposition flux is not much. That is why deposition fluxes of these elements are in reasonable agreement with deposition fluxes measured in Antalya. However, the approach used in this study can severely underestimates dry deposition fluxes of elements that are associated with fine particles, if even a small fraction of that element occurs in the coarse fraction, because, as pointed our before, the contribution of that small fraction in the coarse mode can have substantial effect on dry deposition flux (Dulac et al., 1989; Arimoto et al., 1985; Kuloğlu et al., 2001). Large differences in dry deposition fluxes of Cd, Pb, SO_4^{2-} and NH_4^+ are at least partly due to inappropriate handling of their size distribution by the method used in this study. However, it should also be noted that dry deposition fluxes of elements and ions are expected to be lower in Çubuk, even if the same methods were used in calculations, due to lower concentrations at the central Anatolia, but probably not this much.

The discussions in this section suggests that single dry deposition velocity approach used to calculate dry deposition fluxes in this study can give reasonable approximation of fluxes for coarse fraction elements, but it can underestimate dry deposition fluxes of fine elements depending on their size distributions. Consequently dry deposition fluxes of elements found in this study should be considered as lower limit values rather than actual deposition.

Wet deposition fluxes of some of the elements and ions were also calculated at Çubuk station (Tuncer et al., 2001). Dry deposition fluxes calculated in this study are compared with wet deposition fluxes reported by Tuncer et al., 2001 in Table 4.7.

Table 4.7. Dry and Wet Deposition Fluxes of Parameters Measured

Parameters	Dry Deposition Flux (mg m^{-2} yr^{-1})	Wet Deposition Flux (mg m^{-2} yr^{-1})
SO_4^{2-}	61.68	806.56
NO_3^-	900	526.94
NH_4^+	16.79	337.25
Mg	119.72	38.77
Ca	401.50	448.74
K	224.47	99.58

Dry deposition fluxes of K, Mg, Ca and NO_3 are comparable with their wet deposition fluxes. However, wet deposition fluxes of SO_4^{2-} and NH_4^+ are about an order of magnitude higher then their corresponding dry deposition fluxes. In the previous discussion it was demonstrated that the method used in this study can severely underestimates the dry deposition fluxes of these two ions. Observed large difference between dry and wet deposition fluxes of SO_4^{2-} and NH_4^+ is probably an artifact due to method. In general it can be stated, with a certain margin of caution, that dry and wet deposition fluxes at the Central Anatolia are comparable for most of the elements measured in this study. This is consistent with the extremely low annual rainfall in the region.

4.4. Sources of Pollutants

So far, general characteristics of the data, the temporal variations and dry deposition fluxes of the measured species were investigated. Although, temporal variations, to a certain extent, give information about the sources, there is a need to perform statistical techniques that are more pointed to source identification. In the following sections application of statistical methods that are commonly used in source apportionment studies are discussed. The methods applied varied from simple ones, such as correlation analysis and calculation of enrichment

factors to more sophisticated techniques, such as application of positive matrix factorization (PMF) and potential source contribution function (PSCF).

4.4.1. Correlations between Parameters

Binary correlations between parameters are one of the simplest statistical methods used to determine the sources of pollutants, or the chemical processes that participate, measured at the receptor site. Although simple, this method gives fair amount of information on how the species co-vary in the data set. It should also be noted that correlation analysis is generally a preliminary study in source apportionment and should be supplemented by other statistical studies.

In urban areas strong correlations between the concentrations of measured parameters indicate that they have similar sources as the samples are collected in a short time after they are emitted from the source. However, the concentrations measured in rural areas are not directly affected by the sources, so for rural areas, correlations between parameters provide information on the chemical and physical process as well as sources.

The correlations and correlation coefficients (r) between the concentrations of measured parameters in Çubuk station are given in Figure 4.29. It can be seen from the figure that there are two groups of parameters that are strongly correlated among them. Conventional correlation coefficients can not be a good indicator of relation between parameters by itself, because relation also depends on number of data points included in the statistical test. In this section the term “correlation” is used only if the probability of chance correlation between parameters is less than 5% ([P(r, n)]< 0.05).

The first group includes Ca, Mg and K for which the main source is the resuspended soil particles. As they are all emitted from the same source, observed correlations between them is expected.

The second group of parameters which show strong correlation includes SO_4^{2-}, NO_3^-, NH_4^+, SO_2, NO_2 and HNO_3, Among these, SO_4^{2-}, NO_3^- and NH_4^+ have particularly strong correlations with each other. Both SO_4^{2-} and NO_3^- are formed in the atmosphere through photochemical reactions. Since the parameters affecting the rate of photochemical reactions, such as temperature and radiation, are the same for these two ions observed high correlation is not surprising. Strong correlation between SO_4^{2-} and NO_3^- were observed in most of the atmospheric studies (Sanz et. al. 2002; Charron et. al. 2000) As could be seen from the figure NH_4^+ ion shows strong correlation with SO_4^{2-} and NO_3. This is due to the fact that acidic species H_2SO_4 and HNO_3 formed in the atmosphere are neutralized by NH_3 to form NH_4NO_3 and $(NH_4)_2SO_4$. So as the parts NO_3 and SO_4^{2-} ions in the atmosphere are found as NH_4NO_3 and $(NH_4)_2SO_4$, NH_4^+ ion show a strong correlation with NO_3 and SO_4^{2-} ions.

In the Figure 4.29, it is seen that SO_2 correlates well with SO_4^{2-} and NO_2 correlates with NO_3^-. The SO_2 and NO_2 are the precursor gases for SO_4^{2-} and NO_3^- ions, respectively. Concentrations of SO_4^{2-} and NO_3^- in the atmosphere depends on (1) concentrations of SO_2 and NO_2, from which they form and (2) meteorological conditions, particularly the solar flux, which enhances or suppresses conversion of SO_2 to SO_4^{2-} and NO_2 to NO_3^-. Partial dependence of SO_4^{2-} concentrations on SO_2 and NO_3^- concentrations on NO_2 levels can explain observed correlations between these ions and their precursor gases.

The correlations have indicated that relations between anthropogenic parameters are due to atmospheric processes, such as formation rate, neutraliztion etc rather than source similarities. This is supported by

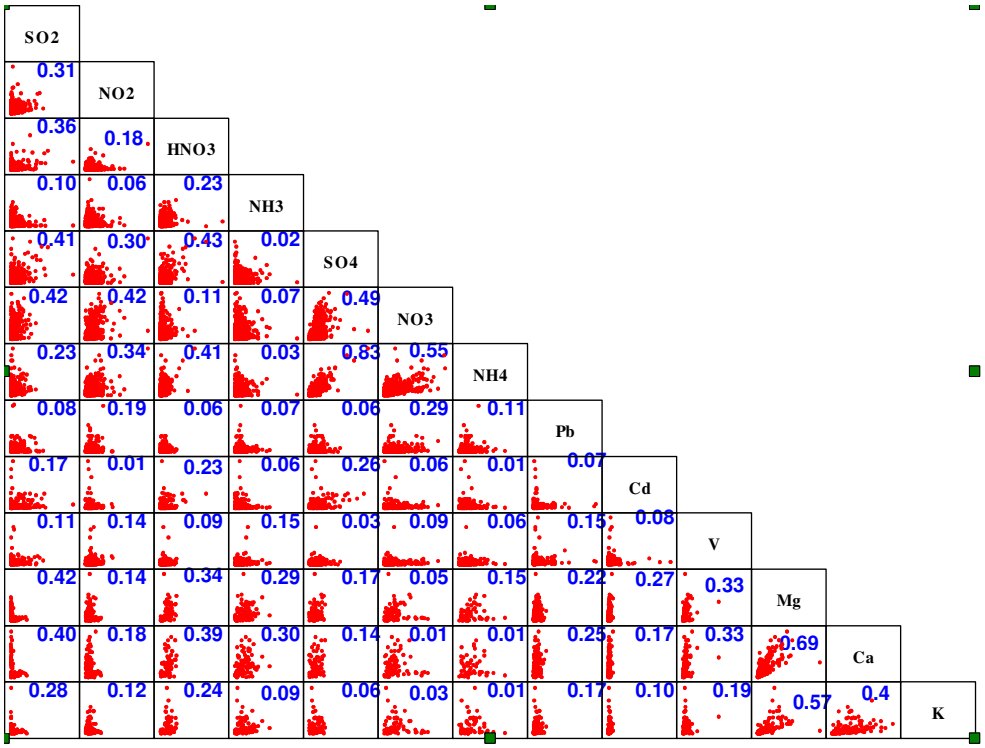

Figure 4.29. Correlations between the measured parameters at Çubuk Station

the fact that Pb and Cd, which originate from anthropogenic sources, but do not participate in atmospheric chemistry (they are emitted on particles, they remain on particles through atmospheric transport and eventually they deposit on particles), are not correlated significantly with any of the parameters measured.

4.4.2. Enrichment Factors

Aerosols and gaseous pollutants are emitted from various natural and anthropogenic sources and mixed in the atmosphere. Enrichment factors is a convenient tool to show how much of the measured

parameters originate from natural sources, such as soil and sea salt and how much have anthropogenic origins.

Crustal enrichment factor (EF_c) of an element is given by the following relation:

$$EF_c = (C_x/C_{ref})_{sample}/(C_x/C_{ref})_{soil}$$

Where, $(C_x/C_{ref})_{sample}$ is the ratio of the concentration of test element X (the element for which the enrichment factor is to be calculated) to the concentration of the crustal reference element and $(C_x/C_{ref})_{soil}$ is the corresponding ratio in soil. The use of the later ratio necessitates the availability of soil composition data. Since all aerosol studies are not accompanied by soil measurements, global compilation of soil composition are commonly employed in EF_c calculations. Few such large compilations are available (Taylor, 1972; Wedephol, 1969; Vinagradov, 1996; Mason, 1966). In this study Mason (1966) compilation was used to calculate EF_c's of measured parameters.

The selection of reference element is important in EF_c analysis. The reference element to be used should be non-volatile lithophile element, which is abundant in crustal material, accurately measured with various analytical techniques, to be measured in all samples and should not have any known anthropogenic source. In EF_c calculations, generally Al is used as the reference element if measured as it is the only element which obeys all these criteria. When Al is not measured at the study area then other crustal elements like Fe, Co, Si, and Sc can be used as reference element.

Crustal enrichment factors are the most common enrichment factor used in the literature, because soil is an ubiquous component of aerosol everywhere and contributes to the concentrations of all elements and ions, even the anthropogenic ones. However, marine enrichment factors (EF_m) can also be calculated using a sea salt reference element

(universally Na) instead of crustal reference element. Calculations of EF_m can be useful if the sampling point is located on a coastal region where sea salt is an important component of aerosol, but is not very meaningful in receptors that are far from the coast, such as Çubuk station.

If the only source of an element is crustal material than the EF_c for that element should be unity. However, due to the differences between Mason's soil composition and the local soil composition, EF_c values lower than 10 indicates that the parameter measured is crustal material and higher than 10 indicates that the parameter is anthropogenic compound.

In this study, none of the elements that are commonly used as reference (Al, Si, Fe, Sc, Co etc) were measured. Among the parameters measured the soil is expected to be the only source for Mg, Ca and K. In this regard, one of these elements could be used as reference element in this study. However, it is fairly well known that concentrations of these elements show differences from place to place depending on the mineralogy of the soil. Besides, these elements are measured only in the year 1993, so if one of these elements are used as reference element the enrichment factor calculations would be limited to one year. For this reason, it is investigated that V could be used as reference element, which is measured longer time between years 1993 to 1996.

Although V primarily originates from soil, it is also emitted to the atmosphere, in significant quantities as a result of fuel-oil combustion, indicating some part of the V in the atmosphere has an anthropogenic source. Because of this reason, V is not commonly used as a reference element in EF_c calculations. However, most of the studies performed in rural areas in Turkey have clearly demonstrated that soil is the dominating source of V and contribution of oil combustion on measured

V concentrations is small (Güllü et al., 1998; Karakaş, 1999) and can only be seen in the fine aerosol fraction in size separated aerosol samples (Kuloğlu, 1997). This means that maybe V can be used as reference element in this study where no other proper crustal markers were measured.

The correlations between the EF_c values calculated for SO_4^{2-} ion by using V, Mg, Ca and K as reference element are given in Figure 4.30. As can be seen from the figure, the enrichment factors calculated using Mg and K as reference element correlates well with each other and falls to a narrow strip around the line with slope 1. However, linear regression between Mg – Ca and K – Ca, although also correlated, show a larger scatter in the data and consistently lie on the high Ca side of the line with slope 1, indicating EF_c's calculated using Ca as reference element are consistently higher than EF_c's calculated using both Mg and K as crustal reference element.

Enrichment factors using V as reference element correlates strongly with EF_c's calculated using Mg and K as reference, but is significantly different from those calculated with Ca as reference, particularly at high EF_c values.

This simple correlation analysis suggests that elements K, Mg and V can be used as crustal reference in EF_c calculations in this study. However, anomalously low EF_c values will be obtained when Ca is used as reference element. This indicates that soil aerosol intercepted at Çubuk station has higher Ca concentration than Ca concentration in Mason's (1966) global average soil. This is reasonable, because the soil in the Mediterranean region is known to be alkaline, which means it contains high concentrations of $CaCO_3$. However, it also indicates that Ca, which is the most commonly used crustal element when only major ions are measured in aerosols (or precipitation), should not be used as reference element in the Mediterranean region.

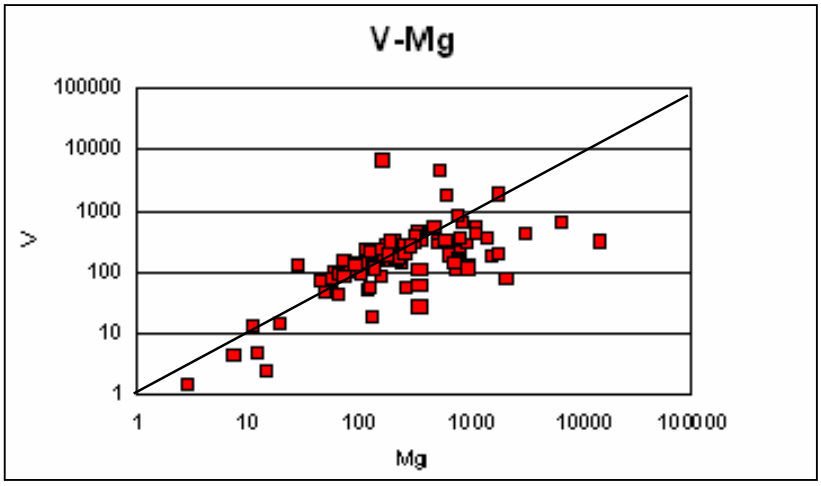

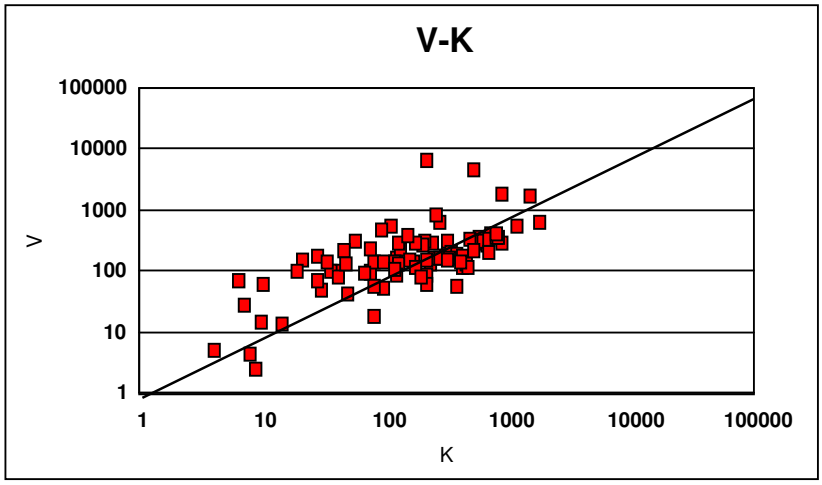

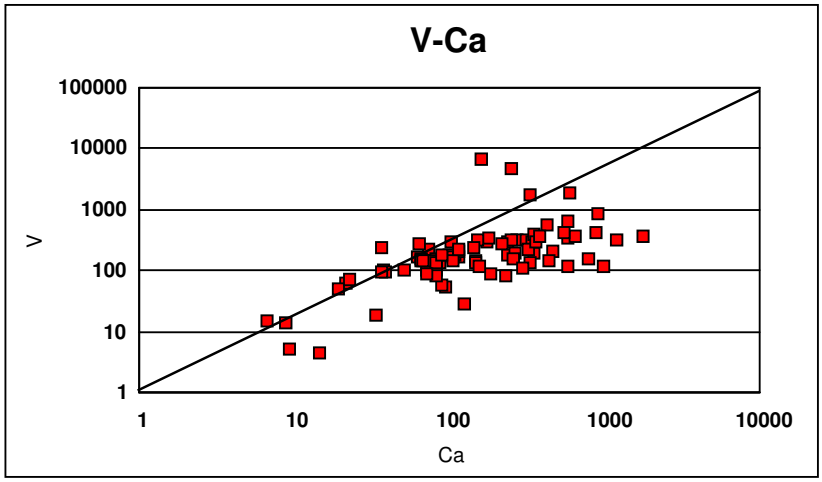

Figure 4.30. Correlations between the EF_c Values Calculated for SO_4^{2-} Ion by using V, Mg, Ca and K as Reference Element

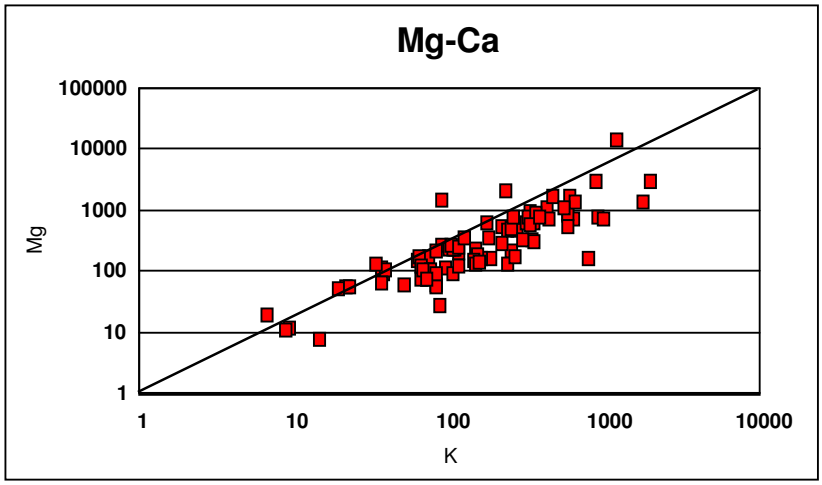

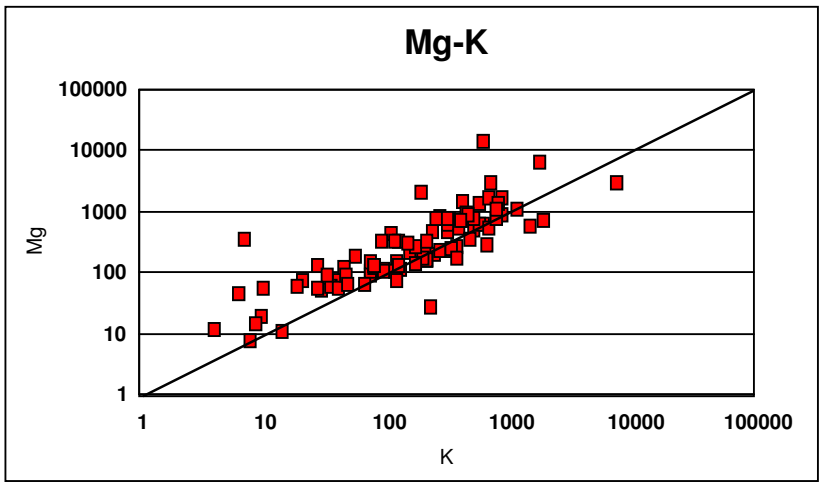

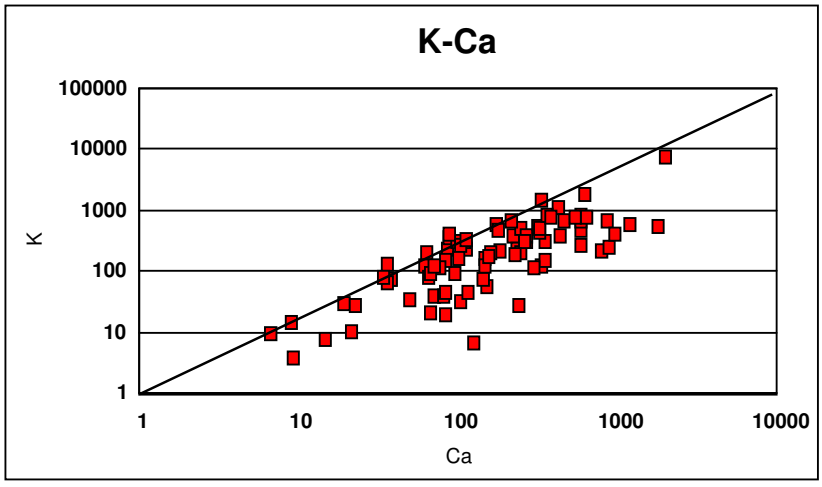

Figure 4.30. Correlations between the EF_c Values Calculated for SO_4^{2-} Ion by using V, Mg, Ca and K as Reference Element (Cont'd)

As another test for the suitability of V, K and Mg as reference crustal element in this study, EF_c's of parameters calculated using both V and K as reference element were compared with the corresponding EF_c's calculated at Antalya and Amasra stations using Al as crustal reference element. If there are substantial differences in EF_c's calculated with V or K as reference element, then there should be very significant differences between the enrichment factors calculated at Çubuk and the other two stations. Enrichment factors of parameters measured are given in Figure 4.31. As can be seen from the figure, the EF_c's of parameters between stations are not large enough to change conclusions in the discussion of enrichment factors of elements. The only exception to this conclusion are higher EF_c's of Ca and Mg at the Antalya station. These higher values at Antalya are not due to different reference elements used (note that EF_c of Ca and Mg at Antalya are also higher than corresponding EF_c's at Amasra where Al was used as reference element), but due to higher Ca and Mg measured in Antalya station. Calcium concentration measured at Antalya station is the highest measured in Turkey due to both higher $CaCO_3$ content of soil and more frequent incursions of Saharan Dust, which is known to be very highly enriched in $CaCO_3$. The Mg concentrations at Antalya station is high, because the station is located at the coast and sea salt is a well known source of Mg.

With these comparisons it is concluded that, although they are not ideal markers for crustal material (due to high variability in their concentrations in soil from one place to another), V and K can be used as crustal reference element when there is no other proper crustal marker available. However, the use of Ca should be avoided in the Mediterranean region. Mg performed equally well in this study, but strong sea salt contribution can render it unsuitable at coastal sites.

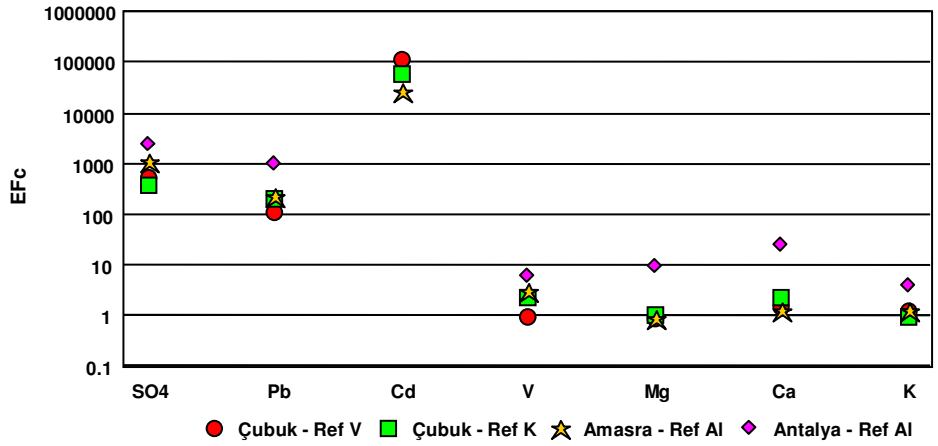

Figure 4.31. Enrichment Factors of Parameters Measured at Çubuk, Antalya and Amasra Stations

4.4.2.1. Enrichments of elements in the Central Anatolia

Sulfate, Pb and Cd are highly enriched in the aerosol (with EF_c's ranging between 100 for Pb and 10 000 for Cd) in Çubuk indicating that, contribution of soil on their measured concentrations is not significant. Enrichment factors of V, Mg, Ca and K, on the other hand, are all less than 10, suggesting dominating contribution of soil component in aerosols on their observed concentrations. This pattern is not unusual and commonly observed in most of the studies performed in the Mediterranean region.

Seasonal variations of enrichment factors of measured parameters are given in Figure 4.32. Enrichment factors of SO_4^{2-}, Ca, Mg and K are higher in summer months compared to their EF_c's in winter season. Calcium, Mg and K are all crustal material and their concentrations in atmosphere are higher in summer months than winter months. In winter months, the formation of aerosols by wind from ice covered soil surface is at a minimum level. In contrast, dry soil surface in summer months

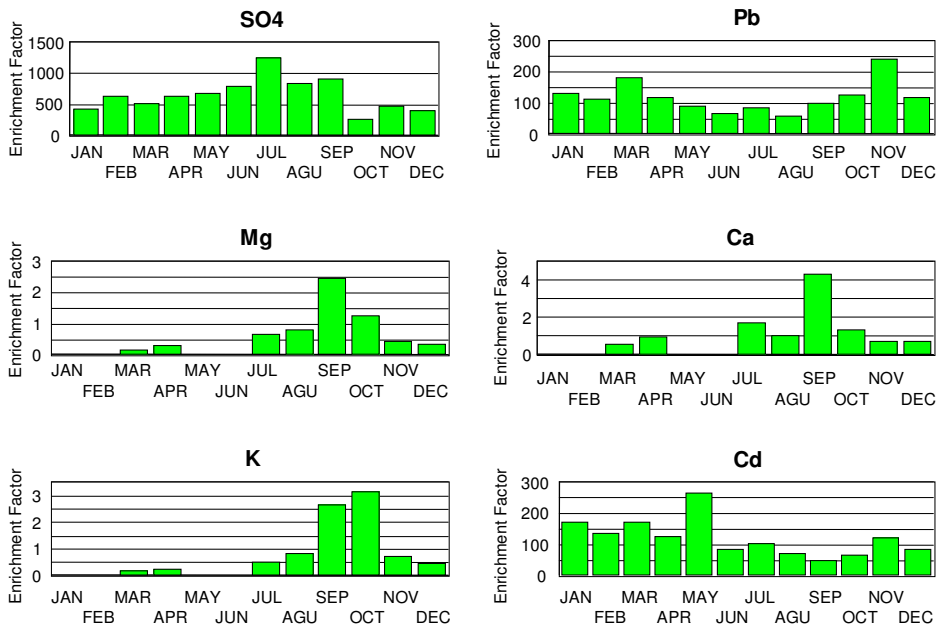

Figure 4.32. Seasonal Variations of Enrichment Factors of Parameters Measured at Çubuk Station

favors the formation of aerosols. Consequently, observed higher enrichments of soil-related elements is due to seasonal variation in their source strengths.

The higher EF_c values of SO_4^{2-} in summer months is due to different reasons. As SO_4^{2-} is an anthropogenic element, the high EF_c values observed in summer months can be due to higher transportation and low values observed in winter can be due to lower transportation of this ion to Central Anatolia. During winter months air parcels transported from source regions to Turkey are washed out by rain and SO_4^{2-} ion is washed out from the atmosphere with other elements and ions. So, the levels of pollutants that transported long range to the region are low in winter months.

The seasonal variations of enrichment factors of Pb and Cd are different from others. As can be seen from the figure, the EF_c values of these

elements which are known as anthropogenic originated are high in winter months. There can be two reasons for that: (1) as crustal aerosols are low in winter months the elements whose concentrations do not decrease like crustal aerosols would have high EF_c values in winter months, (2) if Pb and Cd have local sources as they would have no chance to washed out from the atmosphere like elements long range transported, they would have high EF_c values in winter. As can be seen from Section 4.2.4, the temporal variations of concentrations of parameters measured, the concentrations of Pb and Cd are high in winter season. Then, the reason of high EF_c values in winter months is the increase of their concentrations in winter months and decrease in the concentrations of soil related parameters in winter can further enhances the summer-winter difference in the EF_c's of Pb and Cd.

4.4.3. $SO_4^{2-}/(SO_2 + SO_4^{2-})$ Ratio

Particulate sulfate has received increasing attention during recent decades due to the effects of acid deposition and climate change. Sulfate aerosols directly affect the radiative budget of the Earth by scattering the light (Gebhart and Malm, 1994; White, 1990). To act as a cloud condensation sulfate is also responsible for forming clouds which affects the solar radiation (Latha et.al., 2004). They also cause visibility degradation and affect the human health (Waldman et. al. 1993).

Sulfate is formed in the atmosphere by photooxidation reaction of SO_2 to SO_4^{2-}. The major path of this reaction is via HO radical which is given below;

$$SO_2 + HO + (H_2O + O_2) \longrightarrow H_2SO_4 + HO_2$$

Daily average conversion rate of SO_2 to SO_4^{2-} is only 0.02 h^{-1} in summer when the highest conversion occurs (Matvev et al., 2002). Due to this slow conversion rate and the slow dry deposition velocity of particulate sulfate, atmospheric life of SO_4^{2-} can be as long as 10 days

in the absence of precipitation. Consequently, $SO_4^{2-}/(SO_2+SO_4^{2-})$ ratio can be used as an indicator which shows the chemical age of an air mass (Luria et al., 1996). Since SO_2 gradually converts to SO_4^{2-} during its transport in the atmosphere, low values of SO_4^{2-}-to-total S (SO_2 + SO_4^{2-}) ratio indicates that SO_2 is released to the atmosphere near the receptor site and high values of the ratio SO_2 is released to the atmosphere far away from the receptor site. Values close to 0.02 were found in power plant plumes (close to source) and higher values were reported for 4 – 6 hr travel time (Meagher et al., 1978).

In this study, $SO_4^{2-}/(SO_2+SO_4^{2-})$ ratio was calculated for each sample and the average value is 0.54±0.29, which indicates that approximately half of the SO_2 is oxidized to SO_4^{2-} by the time air masses are intercepted at our station. Luria et al. (1996) have found SO_4^{2-}-to-total S ratios as 0.4 at Israel.

The relation between SO_4^{2-}-to-total S and distance of the source to receptor is shown in Figure 4.33, where trajectories those correspond to highest and lowest 50 SO_4^{2-}-to-total S ratio values are plotted. Although there is not a one-to-one correspondence, the general appearance of the picture clearly demonstrate that low values of the ratio are generally associated with short and high value of the ratio is generally associated with long trajectories. One should not expect one-to-one correspondence between the trajectory length and SO_4^{2-}-to-total S ratio, because some trajectories move unusually fast some corresponds to higher than expected conversion rates.

If the average conversion rate of SO_2 to SO_4^{2-} is taken as 0.02 hr^{-1} this corresponds to atmospheric SO_2 residence time of 10 days (99% of SO_2 is oxidized within 10 days) (Matvev et al., 2002). The average value for the SO_4^{2-}-to-total S at our sampling point (0.54) corresponds to atmospheric residence time of 35 hours and 24 hours when a faster oxidation rate of 0.03 hr^{-1} is used in calculations, to account for faster

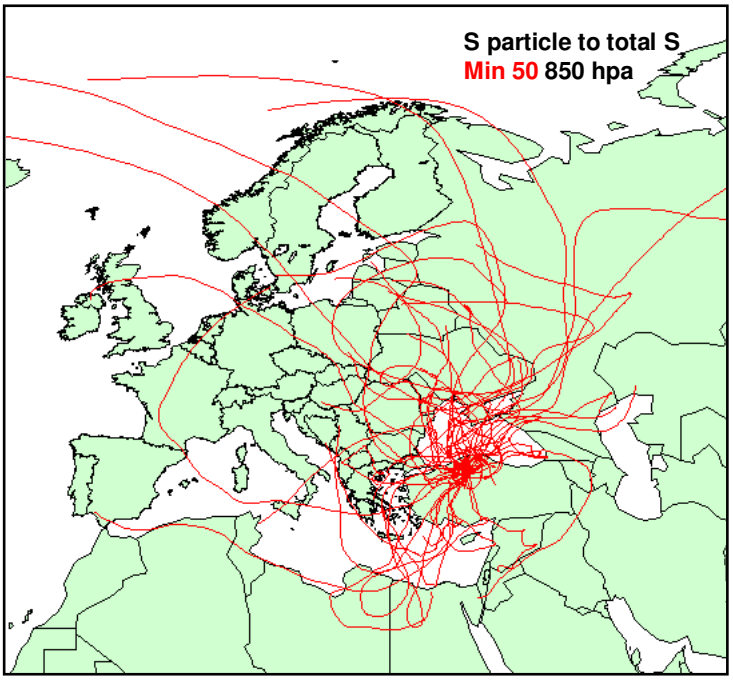

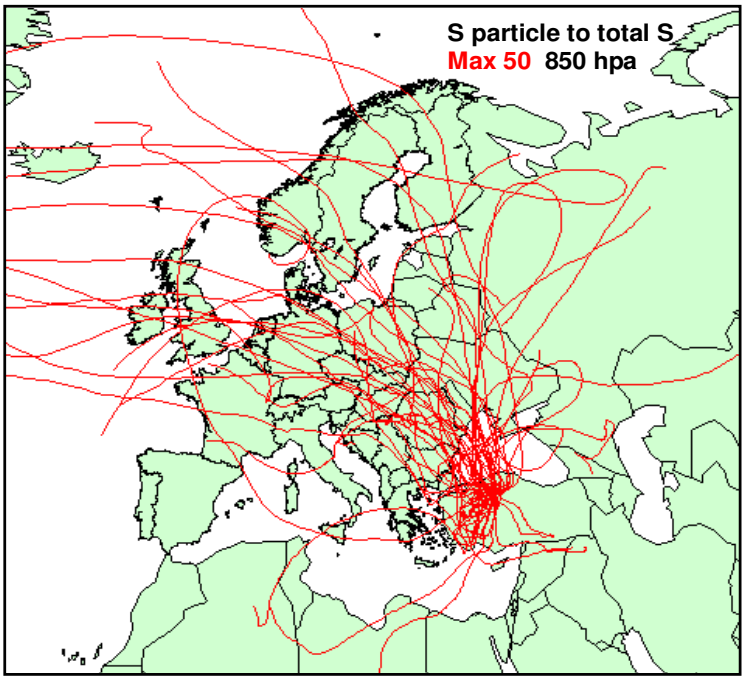

Figure 4.33. Trajectories correspond to highest and lowest 50 SO_4^{2-}-to-total S ratio values

oxidation in rain. Consequently, it can be concluded that, on the average, the sources of SO_4^{2-} observed at our receptor lies between 1-2 day trajectory distance away.

The trajectory distances that corresponds to 24-h and 48-hr transport time from the station were found and depicted in Figure 4.34. To prepare the figure, the end points of 24-h and 48-h long backtrajectories were plotted and circles that includes 90% of these end points are shown in the figure. For each case there were few trajectories corresponding unusual fast transport. In these cases trajectories were extending well beyond the circles shown in the figure. These cases were excluded when the circles are prepared, because they were not representative for an average transport distance.

One to two day transport distance extends to part of the Balkan countries, but not beyond them, suggesting that Central Anatolia are affecting primarily from source within Turkey and Balkan Countries and not affected as much from distant sources. This conclusion is supported by potential source contribution calculations, which is discussed later in the manuscript and modeling studies performed for the Mediterranean region (Erdman et al., 1994).

It should also be pointed out that, the estimation of location of sources based on SO_4^{2-}-to-total S ratio is a very crude approximation, as it bases on conversion rate, which changes significantly depending on the solar flux and pollution level in the air mass, but it at least provides information if the station is affected from very local sources or the SO_4^{2-} observed is transported from sources that are not in the immediate vicinity of the station. The ratio observed in this study indicates that contribution of distant sources is more important than the contribution of local sources on observed SO_4^{2-} levels. Seasonal variation of $SO_4^{2-}/(SO_2+SO_4^{2-})$ ratio is given in Figure 4.35. There is a very clear

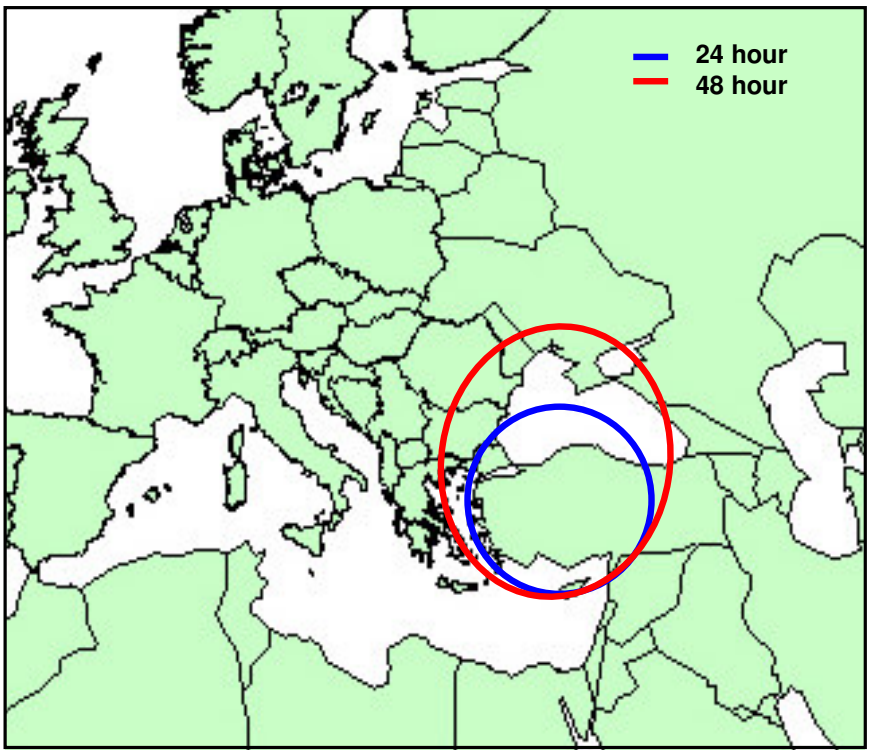

Figure 4.34. The trajectory distances that corresponds to 24-hr and 48-hr transport time from the Çubuk station

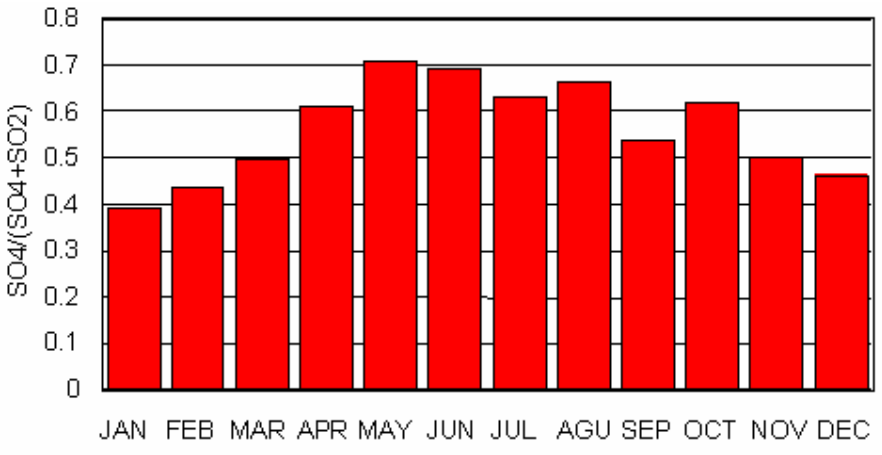

Figure 4.35. Seasonal Variation of $SO_4^{2-}/(SO_2+SO_4^{2-})$ Ratio

seasonal trend in SO_4^{2-}-to-total S ratio with higher ratios in summer months. The ratio changes from approximately 0.7 in summer to 0.4 in January and December. There are two factors causing this seasonal variation.

One of them is the slower conversion rate in winter. It is well known that oxidation rate is slower in winter due to reduced solar flux. Slower oxidation results in lower $SO_4^{2-}/(SO_2+SO_4^{2-})$ ratio. For example the increase in the conversion rate from 0.01 in winter to 0.03 in summer can increase the calculated $SO_4^{2-}/(SO_2+SO_4^{2-})$ ratio from 0.3 in winter to 0.7 in summer, after 35 hr transport in the atmosphere.

Another factor that can result in higher $SO_4^{2-}/(SO_2+SO_4^{2-})$ ratio in summer is the increased SO_2 emissions at local sources in winter. In most of the Europe coal is burned in power plants for energy generation and SO_2 emissions are slightly higher in summer due to higher load of power stations owing to air conditioning in summer. However SO_2 emissions at local sources in Turkey, such as Ankara, Istanbul etc are significantly higher in winter, because coal combustion for space heating is still an important source. Enhanced SO_2 emissions at local sources in winter can result in lower $SO_4^{2-}/(SO_2+SO_4^{2-})$ ratio in this period. It is not possible to determine which one of these factors are more influential on observed seasonality of the $SO_4^{2-}/(SO_2+SO_4^{2-})$ ratio.

In the data set, $SO_4^{2-}/(SO_2+SO_4^{2-})$ ratio varies between 0.001 (which means almost all of the S in sample is in the form of SO_2, with literally no SO_4^{2-} in it) and 1.0 (where all of the S is in the form of SO_4^{2-} with no SO_2). Obviously, samples with ratios <0.1 are strongly influenced from local sources within Turkey, because even with the slowest reported conversion rate of 1% hr^{-1} $SO_4^{2-}/(SO_2+SO_4^{2-}) = 0.1$ corresponds to 10 hr stay in the atmosphere. Samples with ratio > 0.9, on the other hand, are not influenced from local sources, because even with unrealistically high conversion rate of 10% hr^{-1} for such conversion to occur the air

mass should stay in the atmosphere for about 1 day. With more realistic conversion rate of 2% hr^{-1}, the air mass should remain in the atmosphere for 5 days to have $SO_4^{2-}/(SO_2+SO_4^{2-}) = 0.9$. Consequently, comparison of concentrations of parameters in these two data subsets (samples having $SO_4^{2-}/(SO_2+SO_4^{2-}) >0.1$ and those having $SO_4^{2-}/(SO_2+SO_4^{2-}) >0.9$) can provide information on the distances of the sources of these species to our station.

The average and median concentrations of parameters measured in this study in samples with high and low ratios are given in Tables 4.8 and 4.9.

Concentrations of SO_2, NO_2, Pb and Cd are higher at low $SO_4^{2-}/(SO_2+SO_4^{2-})$ ratio data set, indicating that these parameters are impacted by local sources. Note that these species had lower concentrations in summer, which was attributed to their local sources in previous sections. Consequently, the same conclusion reached based on their $SO_4^{2-}/(SO_2+SO_4^{2-})$ ratios is a confirmation of previous finding.

Sulfate, NO_3^- and NH_4^+ have significantly higher concentrations in the samples with $SO_4^{2-}/(SO_2+SO_4^{2-}) > 0.9$ These are the ions with distant sources. Although for SO_4^{2-} and NH_4^+ this conclusion confirms the attribution of distant sources based on their temporal behavior, it contradicts with the earlier conclusions reached for NO_3^-. Nitrate concentrations were distinctly higher in winter suggesting that local sources of NO_x is the main contributor to observed NO_3^- levels at Çubuk. However, higher concentrations of this ion in samples with very high $SO_4^{2-}/(SO_2+SO_4^{2-})$ ratio suggests that sources of NO_3^- can not be local. The reason for such contradicting behavior of NO_3^- is not clear.

Concentrations of V, HNO_3 and NH_3 are comparable in both subsets of data, suggesting that these species are contributed equally by both local and distant sources. Ca, Mg and K were not included in the

Table 4.8. Concentrations of Parameters Measured for minimum 20% of $SO_4^{2-}/(SO_4^{2-} + SO_2)$ Ratio

Parameters	AVG ($ng\ m^{-3}$)	STD ($ng\ m^{-3}$)	Median ($ng\ m^{-3}$)	N
SO_2	6600	9600	3100	218
NO_2	4000	3400	3300	71
HNO_3	360	280	280	77
NH_3	350	331	290	75
SO_4^{2-}	400	670	140	78
NO_3^-	250	350	150	67
NH_4^+	190	220	100	66
Pb	42	48	16	7
Cd	340	324	190	12
V	2.1	1.8	1.9	12

Table 4.9. Concentrations of Parameters Measured for maximum 20% of $SO_4^{2-}/(SO_4^{2-} + SO_2)$ Ratio

Parameters	AVG ($ng\ m^{-3}$)	STD ($ng\ m^{-3}$)	Median ($ng\ m^{-3}$)	N
SO_2	120	170	72	182
NO_2	2800	2200	2500	529
HNO_3	420	600	260	505
NH_3	370	330	310	584
SO_4^{2-}	2200	1600	1900	745
NO_3^-	470	543	330	570
NH_4^+	640	530	540	582
Pb	11	21	6	336
Cd	170	240	90	325
V	2.3	2.1	1.9	334

analysis, because they were measured in only two samples in the low-ratio data subset.

4.4.4. SO_4^{2-}/NO_3^- ratio

In Europe SO_2 emission reduction, which are effective since mid 80's, resulted significant reductions in SO_4^{2-} levels in the Western Europe (Bailey et al., 1996). However, the protocol to reduce NO_x emissions in whole Europe became effective in late 90's and because of this similar decrease in NO_3^- levels is not observed. Based on this scenario, the SO_4^{2-}/NO_3^- ratio decreased to low levels in the Western European countries. Due to economic reasons, neither SO_2 nor NO_x emission control was effective in Eastern European countries until very recently. Consequently one would expect higher SO_4^{2-}/NO_3^- ratios in Eastern European countries and lower ratios in Western European countries. If this difference can be shown, then SO_4^{2-}/NO_3^- measured in the receptor can be used as tracer for air masses originating from Eastern and Western parts of the Europe.

In order to calculate SO_4^{2-}/NO_3^- ratios in Eastern and Western parts of the Europe, $SO_4^{2-}$and NO_3^- data for EMEP stations between 1977 and 2000 were used. Most of the stations in Western Europe do not measure aerosol NO_3^- concentrations probably due to measurement artifacts. Consequently, there are few NO_3^- data in Western European countries but abundant in Eastern European countries. But the difference in SO_4^{2-}/NO_3^- ratio measured in Western and Eastern European countries are so large that it can be seen even with few data.

As control of NO_3^- emissions are started at late 90's, SO_4^{2-}/NO_3^- ratio was calculated (i) for all years between 1977 and 2000, (ii) for the years before 1995 and (iii) for the years after 1995. There is a clear difference between SO_4^{2-}/NO_3^- ratio calculated for Western and Eastern European countries. SO_4^{2-}/NO_3^- ratio in Western European countries are close to

1 (average of all years in all western European countries is 1.3) whereas the ratio in Eastern European countries is significantly higher (the average of all data from all stations in Eastern European countries between 1977 and 2000 is 3.4).

There is not considerable difference in the SO_4^{2-}/NO_3^- ratios before and after 1995 in the Western Europe (average ratio before and after 1995 is 1.2 and 1.3, respectively) but there are significant differences in the Eastern Europe. The ratio is 3.8 before 1995 and 2.7 after 1995. This indicates that the reductions in Western Europe were completed before 1995, but in the Eastern Europe SO_4^{2-} reductions started later and SO_4^{2-} levels are still decreasing.

The average SO_4^{2-}/NO_3^- ratio in Çubuk are compared with the values reported for the Western and Eastern Europe in Figure 4.36. Since the ratio changes in time, both in Eastern European countries and at our site, comparison was conducted both for the whole period for which data is available, and for different time periods (1993 – 1995 and 1995 – 1998). The average ratio measured in Çubuk station is 3.7. This indicates that Çubuk station resembles Eastern European countries or receives emissions from those countries.

The SO_4^{2-}/NO_3^- ratio in Çubuk is 4.2 before 1995 and 3.2 after 1995. This confirms that atmospheric transport of pollutants to Çubuk station is primarily from Eastern European countries and not much from Western Europe.

Histograms of SO_4^{2-}/NO_3^- ratio at Çubuk, Eastern and Western Europe are given in Figure 4.37. It can be seen from the figure that there is a clear difference in the histograms of Eastern and Western EMEP countries. Most of the ratios in EMEP West are accumulated below 1.5. Whereas for EMEP East, SO_4^{2-}/NO_3^- ratios are mostly accumulated between 1 and 3.5. The median value for EMEP East and West whole

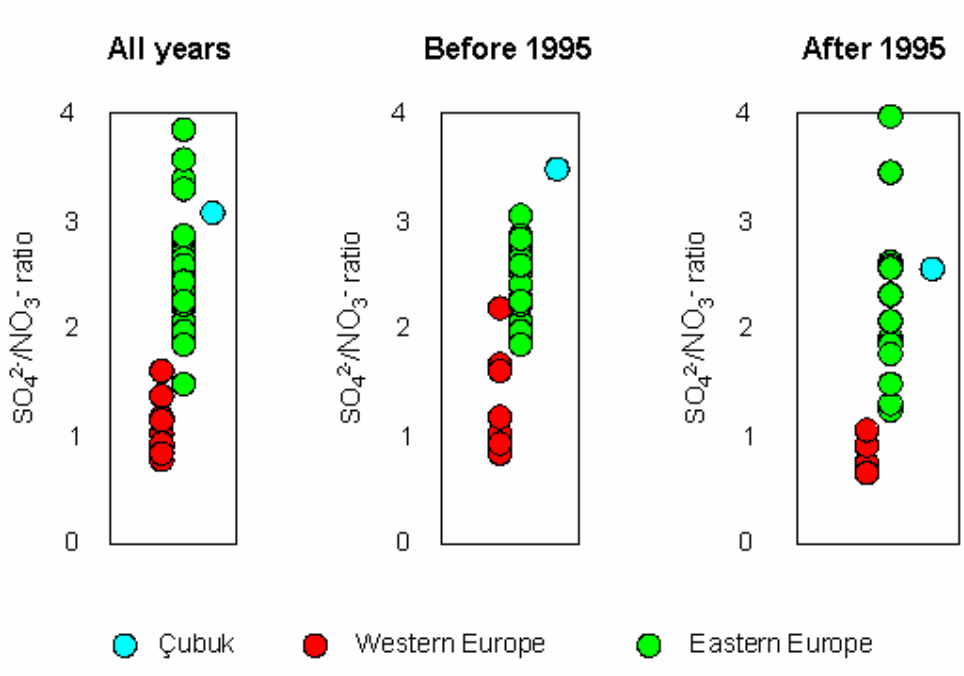

Figure 4.36. SO_4^{2-}/NO_3^- ratio at Çubuk and EMEP stations

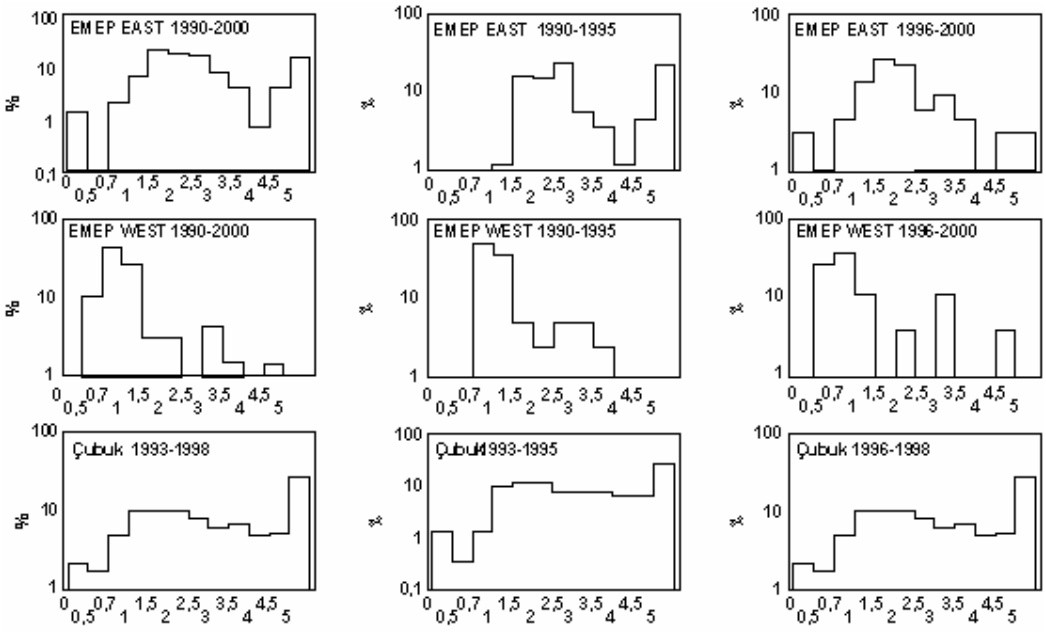

Figure 4.37 Frequency histograms of sulfate-to-nitrate ratio in Eastern, Western Europe and Central Anatolia

data are 0.96 and 2.47, respectively. The distribution for the Çubuk station is between East and West EMEP. Most of the data are in the high ratio range as in East EMEP, but there are some ratios below 1.5. Since ratios below 1.5 are very rare in EMEP East, these small ratios must correspond to transport from West EMEP. However, in the overall Çubuk station resembles East EMEP more than West EMEP.

There are significant differences between the histograms prepared for periods before and after 1995 in all data sets. The difference is small in the West EMEP, because the ratios were also low before 1995. The median values are 0.99 and 0.81 for before and after 1995 in the West EMEP.

In the East EMEP SO_4^{2-}/NO_3^- ratios shifted to smaller values in the after 1995 histogram. The median ratios for before and after 1995 are 2.74 and 2.08, respectively. Similar shift are also observed in the Çubuk data. There is less high ratios (>2.5) and more small ratios (<1.5). The median for before and after 1995 are 3.34 and 2.57, respectively. But bulk of the data is still in the high ratio region.

Discussions presented above demonstrated that SO_4^{2-}/NO_3^- ratio can be used as a tracer to discriminate air masses that originate from Western and Eastern Europe. However it should be noted that emissions in Balkan countries and Turkey have the same ratio with those in the eastern countries. Consequently high ratios can not be used to differentiate between the former eastern block countries, such as Poland, Belarus, and Ukraine etc. and nearby countries such as Bulgaria, Romania and Turkey. However, the ratio is a good tracer to differentiate the western European countries.

Since it is now established that samples with low SO_4^{2-}/NO_3^- ratio are likely to correspond to transport from Western Europe, concentrations of elements in samples with low ratio should represent, at least

qualitatively, the concentrations coming from Western Europe. The data set was divided into two parts, one having SO_4^{2-}/NO_3^- ratios <1.5 and the other >1.5. Concentrations of elements and ions were measured in these two data subsets and results are presented in Table 4.10.

Table 4.10. Median concentrations of elements and ions in samples with high and low SO_4^{2-}/NO_3^- ratios

	SO_4^{2-}/NO_3^- ratio	
	<1.5	>1.5
SO_2	1499	715
NO_2	3337	2437
HNO_3	251	281
NH3	370	272
SO_4	532	1739
NO3	550	295
NH_4	273	488
Pb	16	7
Cd	202	97
V	2,1	1,4
Mg	121	193
Ca	332	670
K	260	328

Concentrations of SO_2, NO_2, NH_3, Pb, Cd and V are approximately a factor of two higher in samples with SO_4^{2-}/NO_3^- ratio <1.5. These are elements and ions with man made sources. Since samples with low SO_4^{2-}/NO_3^- ratio are expected to originate from Western Europe, average concentrations of pollution derived elements are high in samples originating from Western Europe. But this does not mean that Central Anatolia is more impacted from western Europe, because there is only 190 samples with SO_4^{2-}/NO_3^- ratio <1.5, where as there is 650 samples with SO_4^{2-}/NO_3^- ratio > 1.5.

Concentration of only NH_4^+, Ca, K and Mg are higher in samples with SO_4^{2-}/NO_3^- ratio >1.5. The sources of Ca and Mg are soil and local winds are influential on concentrations of these elements, rather than transport direction.

In the atmosphere NH_4^+ forms by oxidation of NO_x. Since it is anthropogenic in nature, it is also expected to have higher concentrations in data subset with SO_4^{2-}/NO_3^- ratio < 1.5. The reason for higher NH_4^+ concentrations in samples with high SO_4^{2-}/NO_3^- ratio is not clear.

Long-term trend of SO_4^{2-}/NO_3^- ratio at Çubuk station is given in Figure 4.38. SO_4^{2-}/NO_3^- ratio do not illustrate a significant change until 1995; however, it starts to decrease after 1995. This pattern is similar to what is observed in Eastern European countries supporting that Central Anatolia is impacted more from Eastern Europe than Western Europe.

4.4.5. Potential Source Contribution Function

One of the main targets in rural aerosol studies is to identify source regions affecting observed chemical composition. As can be easily understood, identification and, if possible, quantification of source area have direct implications to develop national and international strategies for pollution abatement. Source region apportionment can be done either through numerical modeling or through experimental measurements. Each one of these techniques has their own advantages and disadvantages. For example, numerical modeling is cheap, fast and does not require highly skilled personnel. However, the results obtained are prone to fairly high uncertainties owing to various assumptions involved in the modeling itself and in calculating spatially distributed emissions, which is the key input parameter for the model.

Receptor oriented methods (collectively called as receptor modeling) require reliable large data sets, which is difficult and expensive to

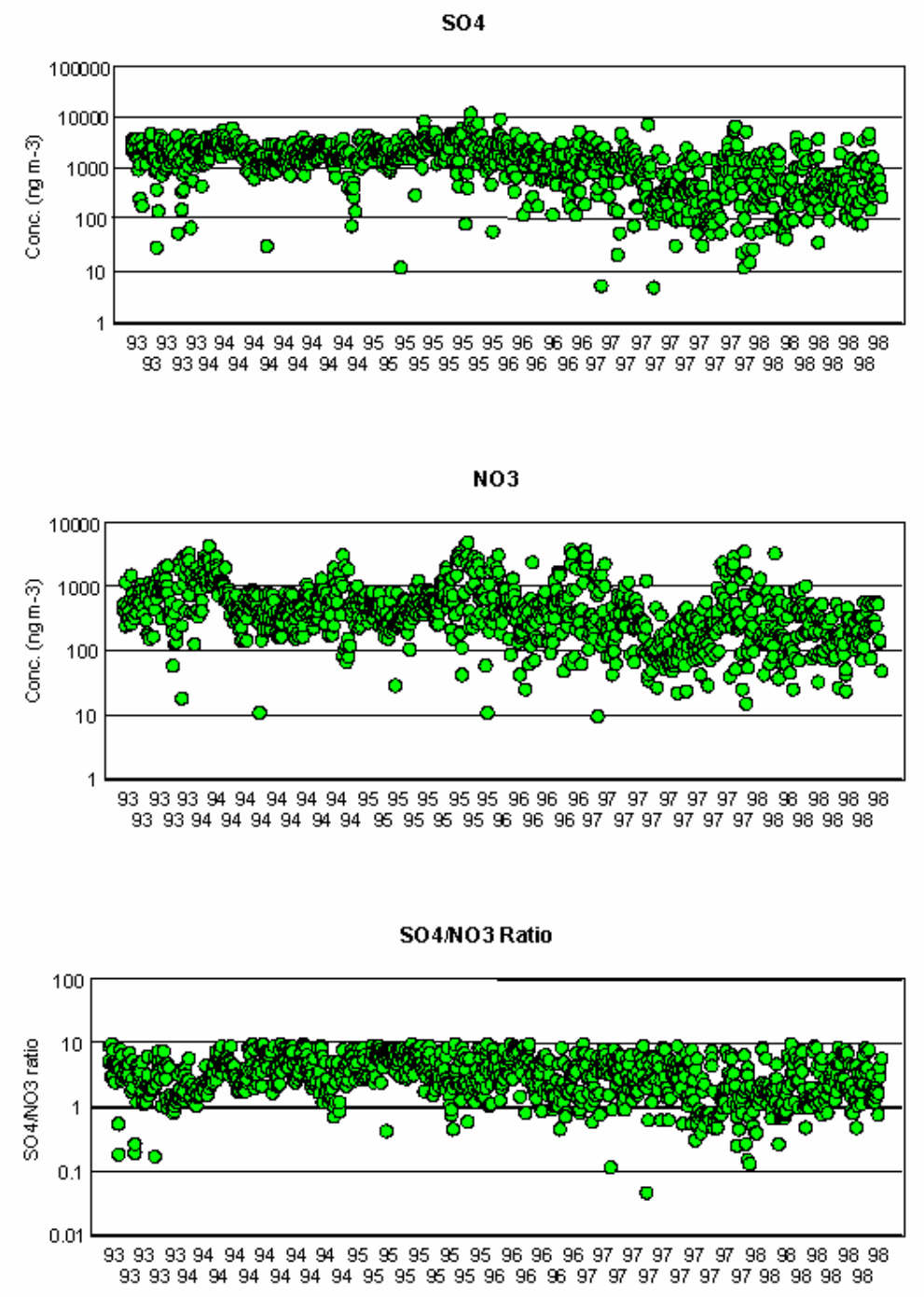

Figure 4.38. Long term trends in SO_4^{2-}/NO_3^- ratio

generate. However, if such data sets are available results much more accurate compared to numerical modeling, because such techniques involves statistical treatment of measured data and do not include any assumptions.

The data set generated at the Çubuk station is excellent in terms of temporal coverage and statistical significance, as important parameters were measured in very large number of samples covering a long period. However, it lacks some important marker species, such as Al and other litophiles for characterization of crustal material and Na to distinguish sea salt contribution. Some important anthropogenic source markers such as As and Se for thermal power plants are also not measured. This means that identification of source types can not be done with high resolution, but source region apportionment will have high statistical significance.

The approach used in this study for identification of potential source regions of measured parameters is called “potential source contribution function” (PSCF). The techniques that combine concentration information that bases on measurements and geographical information provided by backtrajectory calculations, to determine the source areas are in general called “trajectory statistics”. The PSCF is one of the techniques in this general category. It is fairly widely used to determine source areas around receptors (Liu et. al., 2003; Polissar et. al., 2001; Cheng and Lin, 2001; Lucey et. al., 2001; Lin et. al., 2001; Plaisance et. al., 1996; 1997; Hernandez et. al. 1996; Cheng et. al., 1993; 1996; Gao et. al. 1993; 1996; Hopke et. al., 1993; 1995; Stohl and Wotawa, 1995; Cheng et al., 1991; Zeng and Hopke, 1989; 1994).

The primary requirement in the PSCF is the presence of a data set, which includes concentrations of parameters for which the source areas will be calculated, measured in atmospheric aerosol samples collected at the same location for reasonably long period of time and one or two

backtrajectory calculated for each sample. The second requirement is the presence of backtrajectories calculated for each sample.

In this study isentropic backtrajectories were calculated at three pressure level (900 mb, 850 mb and 700 mb) for 5 days backward in time, using the ECMWF 3D, isentropic trajectory model. One trajectory was calculated starting at the mid point of every sample. Each trajectory consisted of hourly segments and model output included time, altitude, latitude and longitude of the air parcel at that particular hour. Combining these hourly segments it was possible to construct the history of the air parcel from which the sample was collected at the station.

To calculate the PSCF the study area which extends from west of UK to the Middle of Asia and from Siberia on the north to the equator was divided into 1° x 1° grids. Each grid element is called a "subregion". Then PSCF is calculated by counting each 1 hr trajectory segment endpoint that ends up with that grid cell both for 850 mb and 700 mb pressure level.

Suppose N represents the total number of trajectory segment endpoints for the whole study period, T. If the number of endpoints that fall in the ij-th cell is n_{ij}, the probability of an event, A_{ij} is given by;

$$P\left[A_{ij}\right] = \frac{n_{ij}}{N}$$

where $P[A_{ij}]$ is a measure of the residence time of a randomly selected air parcel in the ij-th cell relative to the entire study period, T.

If, for the same cell, there are a subset of m_{ij} endpoints for which corresponding air parcel arrive at the receptor site with pollutant concentrations high than an arbitrarily defined value, the probability of this "matched" event, B_{ij} is given by;

$$P\left[B_{ij}\right] = \frac{m_{ij}}{N}$$

Then the PSCF for ij-th cell is given by the following relation

$$PSCF = \frac{P\left[B_{ij}\right]}{P\left[A_{ij}\right]} = \frac{m_{ij}}{n_{ij}}$$

The potential source contribution function was calculated for SO_4^{2-}, NO_3^-, NH_4^+, NH_3, Pb and Cd. The PSCF calculations were not performed for SO_2 and NO_2 because they have fairly fast chemistry in the atmosphere and distribution of PSCF values depend on the rate with which they are depleted in the air mass. PSCF values were also not calculated for Ca, Mg, K and V because their atmospheric concentrations are dominated by the re-suspension of soil in the immediate vicinity of the station, which does not depend on the trajectory path.

The distribution of PSCF values for SO_4^{2-} is depicted in Figure 4.39. There are few regions with PSCF values higher than 0.7. This means that >70% of the trajectories that passes through these grids corresponds to high SO_4^{2-} concentrations at our receptor (this can be also interpreted as with >0.7 probability the grids contain source regions of SO_4^{2-}). These type of source regions are located at the central Russian Federation, a region to the east of the Caspian Sea, Northeast corner of Turkey and a region at southeast of Turkey.

The regions that are indicated with pink color on the map are the regions which can be considered as source regions with 40 - 70% probability. Such secondary potential source regions are more widely distributed in Figure 4.39. West of Turkey (the region extending from İstanbul to İzmir), all of the Balkan countries (Bulgaria, Romania, Albenia, most of Greece, Croatia, Serbia, south of Italy, north of Italy)

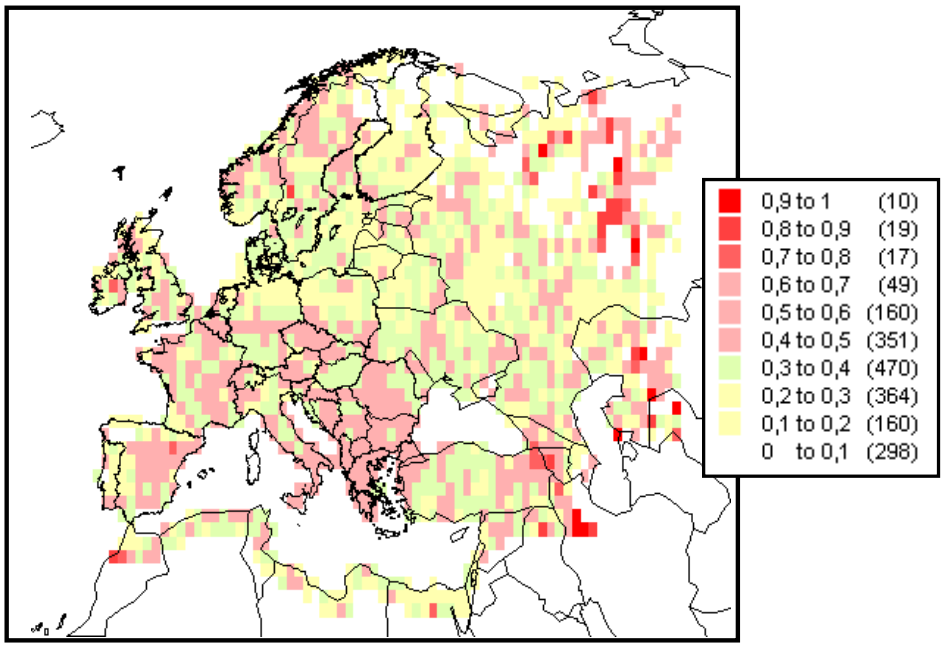

Figure 4.39. Distribution of PSCF values for SO_4^{2-} ion

regions in Spain, most of France, Slovakia, Czech Republic, parts of Germany and south of Poland and east of Turkey are potential source regions in this category.

Source regions with probability <40% are not considered significant, because highest 30% of the measured concentrations were selected as "high concentration" in PSCF calculations and even if there were no sources anywhere in the study area one would expect approximately 30% of the trajectories at each grid corresponds to this 30% of the data.

It can be interesting to compare source regions determined with the PSCF calculations for SO_4^{2-} with distribution of SO_2 emissions in Europe. The distribution of SO_2 emissions in Europe are given in Figure 4.40. The primary source region that is located to the north of the Caspian Sea (part of it is shown as light green and yellow in Figure

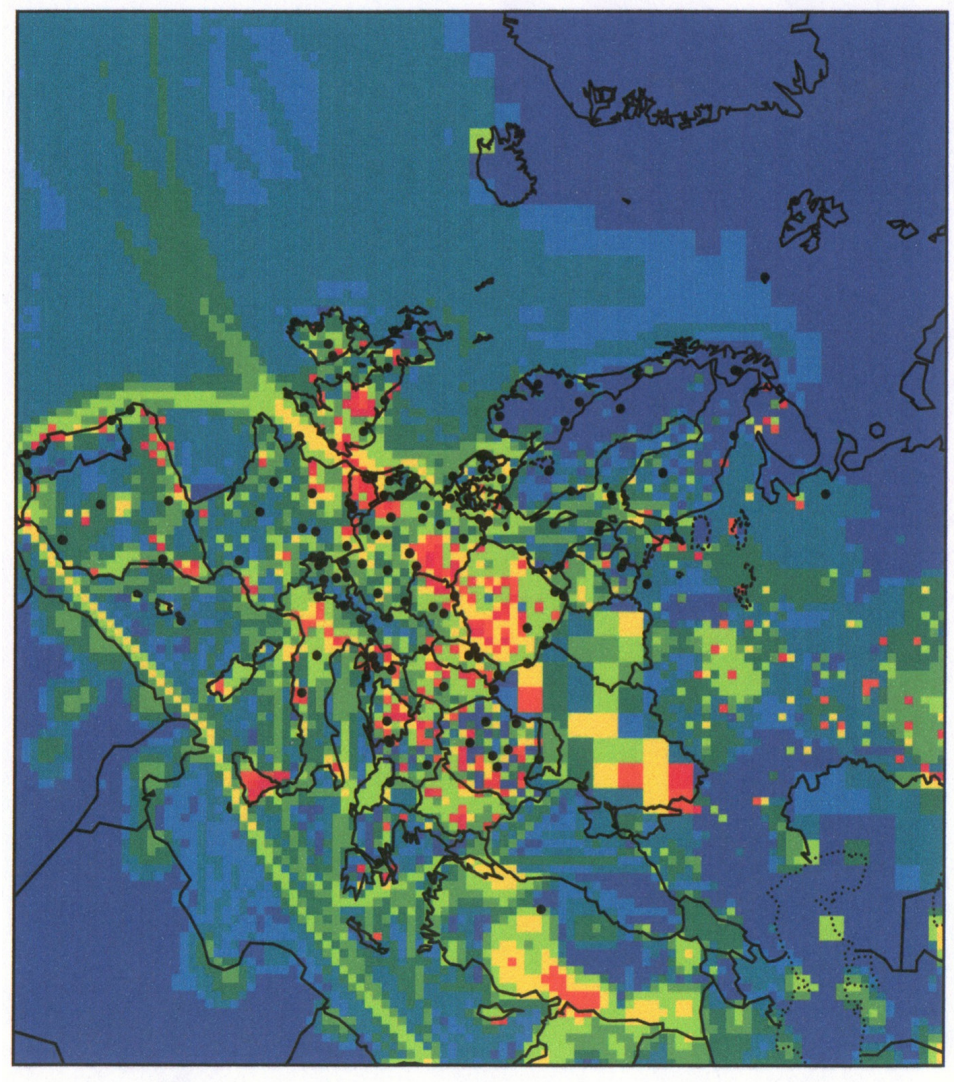

(*red = highest emission densities, dark blue = lowest emission densities*)

Figure 4.40. SO_2 emissions in Europe (Barrett et al., 2000)

4.40) is nicely determined as source region with higher than 70% probability by the PSCF distribution. The high emission area on the northeast coast of Turkey (probably due to Cu smelter at Artvin) is picked up as potential source area with probability >70% by the PSCF map. Also the high emission area at the south east corner of Turkey is approximated as an important potential source area in the PSCF map.

High emitting areas at the Turkmenistan, Uzbekistan and Iran, which are barely visible at the top of Figure 4.40 are nicely identified as strong potential source region.

The emission map shows that Balkan countries, particularly Bulgaria, Romania, Serbia and Croatia are among high SO_2 emitting regions in Europe. These regions are identified by PSCF as potential source areas for Central Anatolia. The corner between Czech Republic, Poland and Germany is one of the highest emitting areas in Europe and this region is identified as potential source area with 40 – 70% probability. High emission area in Belgium is also identified.

Besides these agreements between emission and PSCF pattern, there are some differences as well. Very strong SO_2 emissions at the Iskenderun and Urfa region in Turkey, due to emissions from Afşin-Elbistan power plant is not identified by the PSCF approach. Large parts of Spain and France are identified as potential source region in the PSCF approach used, but neither country are as strong SO_2 emitters. Ukraine is one of the strongest SO_2 emitter in Europe with the strongest emissions immediately to the north of the Azov Sea. Although PSCF identified the region on the north of the Azov Sea as a potential source area with 40 to 70% probability, Ukraine in general did not appear as a very significant source area. The same statements are also true for Poland and Belarus. These two countries are the highest SO_2 emitting countries in Europe. But they are not identified as very strong source regions in PSCF calculations. Strong emission area around Moscow is largely missed by the source apportionment.

There are several reasons for the mentioned disagreement between emissions and PSCF calculations. Actually one should not expect complete agreement between the two figures. High emissions at a given source area does not necessarily transported to the Central Anatolia. If no trajectory passes over the source area before it is

intercepted at our station, then that particular source region will not be identified as a source area affecting Central Anatolia. More important than this is the influence of rain on transport of species from source to receptor. Rain events on the path of air masses that carries pollutants to the Central Anatolia are completely washes out the pollutants from the air mass. Consequently, important emission areas far from Central Anatolia have less contribution to observed SO_4^{2-} levels than emission areas in nearby countries. This is the main reason why the high emission areas in the northern Europe are not as important source areas for the Central Anatolia whereas emission areas in France, Spain other Mediterranean countries are identified as potential source regions affecting chemical composition of particles at the Central Anatolia.

Another reason of some of the disagreement between emission and PSCF patterns is the different grid systems used in emission and PSCF calculations. 1º x 1º grid system is used. However, emissions are calculated 50 km x 50 km standard EMEP grid system. This shifted identified potential source areas from their emission points.

Inaccuracies in the emission estimates may generate some artifical high emission areas. In most of the European countries emissions are based on emission inventories reported by countries and hence they can be assumed to be correct. However, countries like Turkey, Ukraine etc do not report their emissions to EMEP (because there is no emission inventory). In such cases EMEP applies so called “expert estimates”, where they calculate emissions with best available information on population and industries. Such estimates are not as accurate as officially reported emissions. For example the emission map indicates a very strong SO_2 source area at the south of Turkey. There is Afşin Elbistan thermal power plant, which is a very important source of SO_2 emissions, but it is a point source and can not cause intense emissions at a 300 km strip.

It can be concluded that distribution of PSCF values over Europe replicates general features of emission patterns. The agreement is better at distances not too far from Central Anatolia and deviations increase at source regions at the Northwestern part of Europe due to stronger influence of rain scavenging on transport of pollutants from longer distances.

Based on the distribution of PSCF values, main sources of SO_4^{2-} observed in the western parts of Turkey, Balkan countries, France, Spain, Italy and parts of Germany, Poland, Czech Republic, Hungary, Slovakia. There are some point sources and industrial areas that are significant source areas as well. These are the industrial area located at the center of the Russian Republic, industrial activities at Uzbekistan and Turkmenistan and Cu smelter at the northeast corner of Turkey. The potential source regions in the first group appear as an area and probably consist of several sources in each of those countries. However, the later group includes specific industrial area in a country or a particular plant as in the case of a smelter.

As pointed out before, the countries located at the south of Europe are more important source regions compared to the countries at the northern Europe. This is not necessarily due to stronger SO_2 emissions at the South Europe, but owing to less effective rain scavenging of air masses that carries pollutants from this region to the Central Anatolia, due to both closer proximity of South Europe to Anatolia and significantly lower annual rainfall in this part of the continent.

One interesting source area is identified in the southern part of Italy at Sicily. Italy in general is a source region for measured SO_4^{2-} concentrations at the central Anatolia, because it is an industrialized county and close enough not to be affected from rain scavenging. Source regions at the north of Italy (on the Swiss border) and at Rome area are identified as potential source regions in this study. These

regions are highly industrialized regions in Italy and their identification is not surprising. However, a fairly large area at the south of Italy, including Sicily is also identified as potential source region. South of Italy is the least developed part of the country and one would not expect such strong anthropogenic SO_2 emissions there. However, the emission map given in Figure 4.40 also indicates a strong SO_2 emission at Sicily. A Strong SO_2 emission in that particular region is not due to anthropogenic sources, but owing to Mt Etna volcano. Consequently, identification of a potential source area at the south of Italy indicates that volcanic emissions from Etna are also a component in the aerosols that are collected at the central Anatolia and shows that the PSCF approach is a reliable technique at least for the sources within 2000 km from the receptor.

The distribution of PSCF for NH_4^+ ion is depicted in Figure 4.41. The distribution is very similar to the PSCF values calculated for SO_4^{2-} ion. This is not surprising, because NH_4^+ ion in the atmosphere is largely in the form of $(NH_4)_2SO_4$. Consequently, whenever a high SO_4^{2-} is measured a high concentration of NH_4^+ is also measured (that is why these parameters are so strongly correlated as discussed in Section 4.4.1). Since the potential source areas of SO_4^{2-} are determined by high SO_4^{2-} concentrations and associated trajectories and since the same trajectories are also associated with high NH_4^+ concentrations, then very similar distribution of PSCF values should be expected (and observed) for SO_4^{2-} and NH_4^+.

The distribution of PSCF values for NO_3^- are given in Figure 3.61. Potential source areas for NO_3^- are much more local than those for SO_4^{2-} (and NH_4^+). Most of the important source areas are located around the Mediterranean Sea. These include western part of Turkey, some regions in Eastern Turkey, Most of the Greece, Southern Italy (which may again be due to NO_x emissions from Mt Etna) Rome

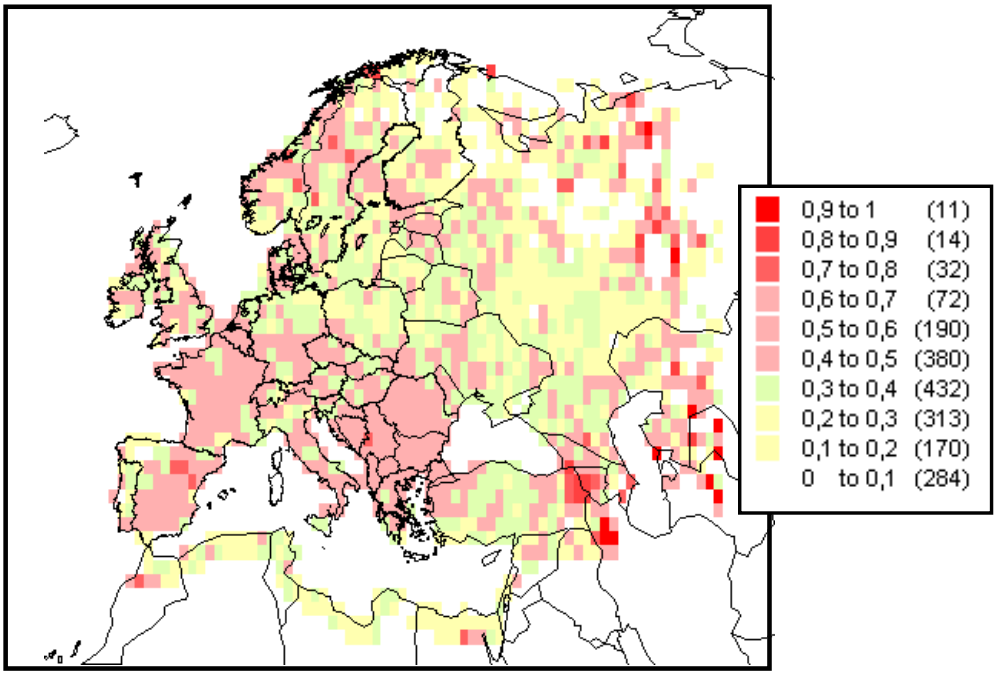

Figure 4.41 Distribution of PSCF values for NH_4^+ ion

area, southern France and Spain. Unlike SO_4^{2-}, countries in central and western Europe, such as Hungary, Czech Republic, Slovakia, Poland and Germany and Balkan countries are not important potential source areas for NO_3^- at the Central Anatolia. Again, unlike as in the case of SO_4^{2-}, area along the North African coast is a potential NO_3^- source area with 40 – 70% probability.

The observed local pattern for NO_3^- confirms our earlier conclusions based on seasonal variations of NO_3^- concentrations. Erdman et al. (1994) performed a numerical modeling study for the deposition of nutrients and heavy metals to the Mediterranean Sea. Authors concluded that the main source of NO_3^- deposited to the Mediterranean Sea is the emissions at the Mediterranean countries with insignificant contribution from countries at the central and northern parts of Europe.

The distribution of PSCF values for NH_3 is depicted in Figure 4.42. There is no very strong potential source area observed for NH_3 concentrations at Çubuk. Yellow legent in the map corresponds to PSCF values 0.1 to 0.3. Since highest 30% of NH_3 concentrations were used as polluted trajectories, the yellow legend indicates that distribution of polluted trajectory segments are very similar with the distribution of unpolluted trajectory segments. This may be either due to fairly uniform distribution of sources in Europe or very strong sources in the immediate vicinity of the station. Since all trajectories have to pass from the grid in which station is located, a very strong source in that grid contributes equally to all trajectories.

In earlier sections it was shown that the seasonal variation of NH_3 concentrations was not similar with the seasonal pattern observed in parameters that are known to be dominated by local sources, such as SO_2. Similarly, discussion $SO_4^{2-}/(SO_4^{2-} + SO_2)$ also suggested that NH_3 is not among the locally dominated species (NH_3 concentration is comparable in the samples with high and low SO_4^{2-} - to – total S ratio). Consequently, the homogeneity observed in the distribution of NH_3 PSCF values can not be explained by local sources and can be due to homogeneous distribution of NH_3 in Europe. The distribution of NH_3 emissions in Europe is given in Figure 4.43. Indeed, NH_3 emissions are homogenously distributed throughout the continent. Consequently, the distribution of PSCF values for NH_3 simply mimics the distribution of sources.

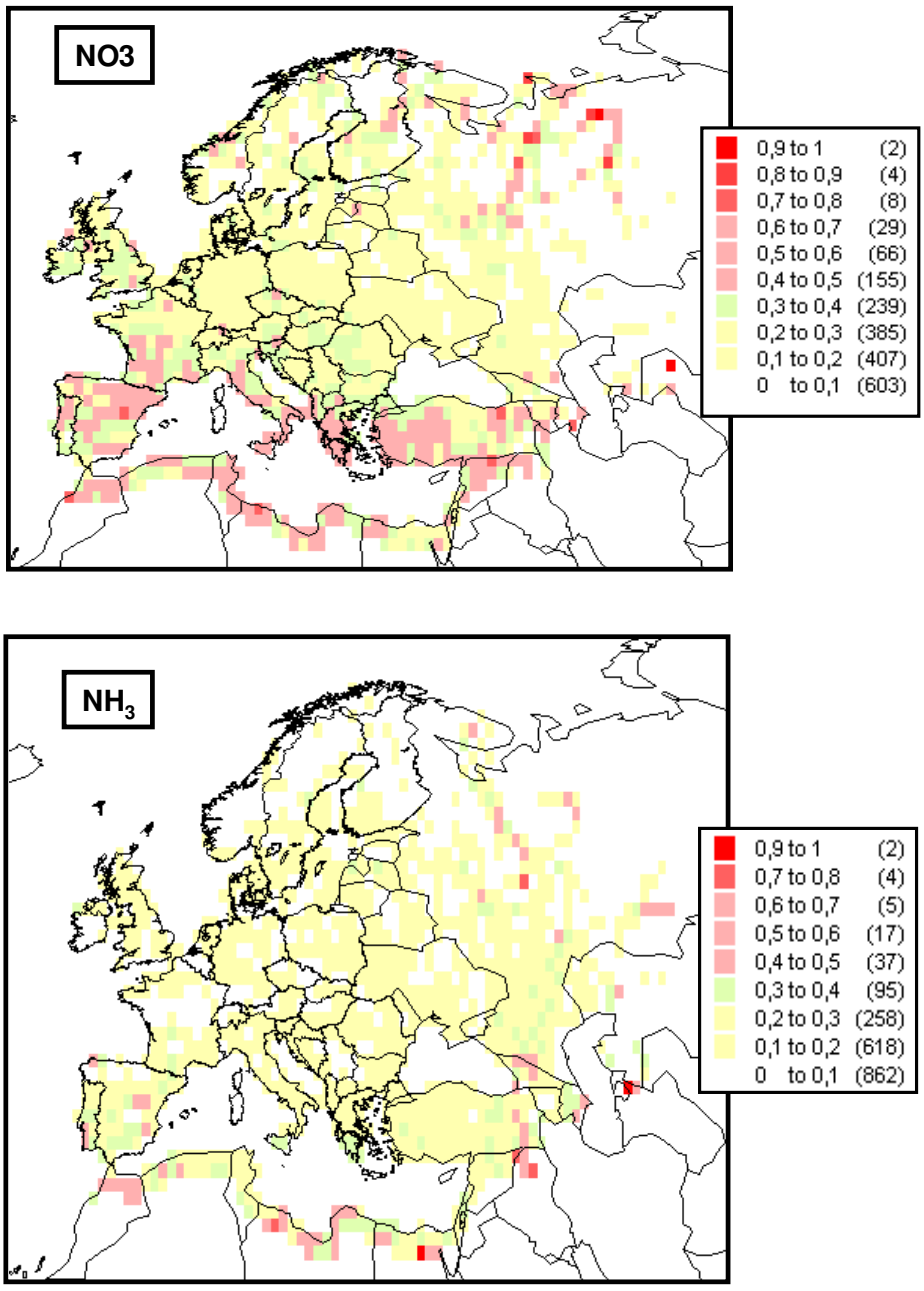

Figure 4.42. Distribution of PSCF values for NO_3 and NH_3

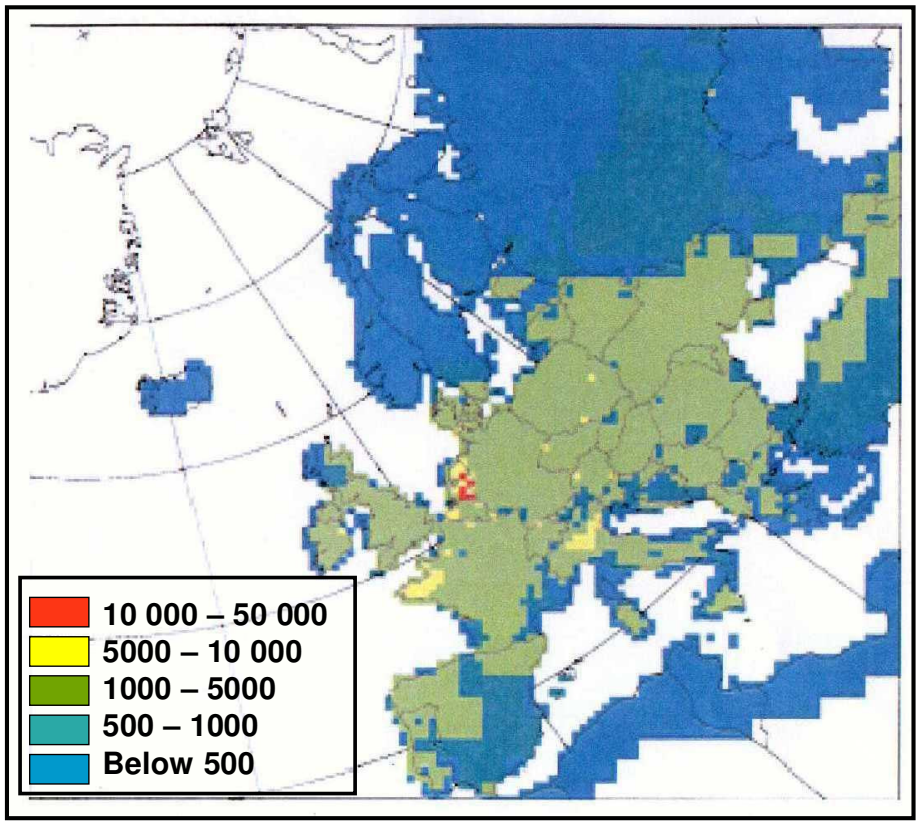

Figure 4.43. EMEP NH_3 emissions in 1995 (Berge et al., 1999)

Distributions of PSCF values for Pb and Cd are given in Figure 4.44. The distribution for Pb is very similar to the distribution observed in NH_3, but unlike NH_3, both its seasonal variation and significantly higher concentrations in samples with low SO_4^{2-} - to – total S ratio indicated that there is a strong Pb source which is very close to station (Ankara). Consequently observed homogeneity in the distribution of PSCF values can be due to contribution of local sources, rather than homogeneous distribution of Pb emission sources. Çubuk does not seem to be an appropriate location to investigate distant sources of Pb.

Unlike Pb distribution of PSCF values indicate that Cd has distant sources as in the case of SO_4^{2-} and NH_4^+. There are some regions with

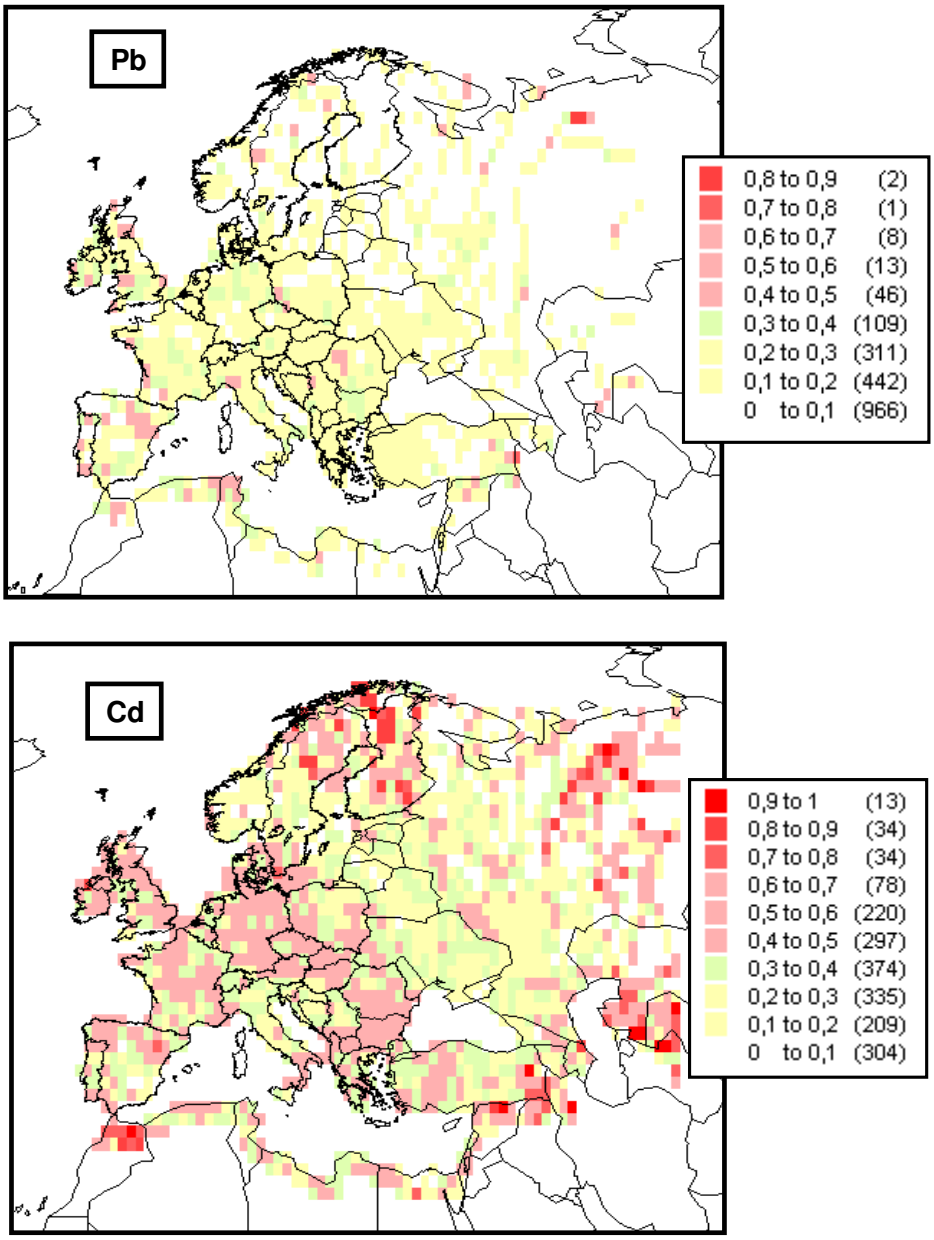

Figure 4.44. Distribution of PSCF values for Pb and Cd

higher than 70% probability to be a source region of Cd. These regions include central Russian Federation, a region to the east of the Caspian Sea, northern Morocco, a region to the north of the Finland and a region at southeast of Turkey. Non-ferrous metal production is the main source of Cd. High contribution of these source areas is due to the high metal production activities at these regions. Besides these regions, most of Balkan countries including Bulgaria, south of Romania, south of Herzegovina, Macedonia, Albania, most parts of Hungary and Slovakia; western and central Europe consisting of Germany, France, United Kingdom, regions in Spain, southeastern and southwestern Poland and most parts of Austria; north of Sweden and Finland and some regions located at Mediterranean coast of North Africa are found as the source regions of Cd with 40-70% probability.

4.4.6. Positive Matrix Factorization

Multivariate statistical techniques, such as factor analysis (Hopke, 1985), chemical mass balance (Miller et al., 1972) and principle component analysis (Thurston and Spengler, 1985), are applied in atmospheric studies in order to apportion the measured concentrations at a sampling site to their sources (Hopke, 1985). Among the multivariate statistical approaches factor analysis is known as the most commonly used technique (Hacısalihlioğlu et al., 1992; Rojas and Van Grieken, 1992; Molinaroli et al., 1999; Glavas and Moschonas, 2002; Heidam, 1984; Quin et al., 2002).

Recently, a new multivariate technique called Positive Matrix Factorization (PMF) (Paatero and Tapper, 1994) started to be applied to atmospheric data as a new approach to factor analysis. PMF has some advantages over factor analysis as PMF produces non-negative constraints to explain the sources and source strengths of the pollutants measured at the receptor site. Besides, factor analysis can not handle the missing and below detection data whereas PMF can do by adjusting

the corresponding error estimates. It is shown by Paatero and Tapper (1993) that factor analysis produces poor fits of the data matrix. PMF overcome this problem by using error estimates of the data matrix and free rotations. In PMF, one can adjust the error estimates of individual data points and make rotations in order to obtain the best fit. By the help of Q-value, distributions of weighted residuals and profiles of factor loadings it is possible to decide if the best fit is obtained or not.

In this study, first factor analysis is performed to determine the sources of the pollutants measured at Çubuk station by using the Statgraphics Software. Due to the limitations of factor analysis to handle missing values, only parameters with the highest data points, namely NO_2, SO_2, HNO_3, NH_3, SO_4^{2-}, NO_3^- and NH_4^+, were studied. Factor numbers in the factor analysis is determined by looking at the eigenvalues. Factors which have eigenvalues larger than unity have been retained in this study.

The result of factor analysis is given in Table 4.11. As can be seen from the table, factor analysis found out 3 factors, which have eigenvalues larger than unity. These factors explain a total 71.73 variance in the data set. It is seen that the first factor has high loadings of SO_4^{2-} and NH_4^+; the second factor NO_2, SO_2 and NO_3^- and the third factor HNO_3 and NH_3.

In this study, commercially available program software PMF2 (Paatero, 1998) is used in order to determine the factors and the contributions of these factors on the sources. In order to obtain the best least squares fit in PMF, the data matrix used in factor analysis and the factors found out by factor analysis are used as the starting point of PMF runs. So, in the first trial PMF is run for 7 variables consist of 666 samples with 3 factors.

Table 4.11. Varimax Rotated Factor Loadings Obtained from Factor Analysis

Parameters	Factor 1	Factor 2	Factor 3	Communality
SO_2	0.23	**0.68**	-0.13	0.53
NO_2	-0.08	**0.81**	0.13	0.68
HNO_3	0.35	-0.11	**0.74**	0.68
NH_3	-0.22	0.12	**0.83**	0.75
SO_4^{2-}	**0.90**	0.12	-0.05	0.82
NO_3^-	0.52	**0.65**	0.04	0.7
NH_4^+	**0.90**	0.14	0.09	0.83
% variance	36.23	18.39	17.11	71.73

The most important feature of PMF is that it gives an opportunity to the user to define the error estimates of individual data points of the data matrix. For the first trial the standard deviations of variables are assigned by using the methodology of the PMF by just putting the data matrices composed of one variable and 666 samples into the program and run it to obtain the standard deviation matrix of that variable. The parameters affecting standard deviation are the error models used and the corresponding error codes. In PMF2 there are 5 error models, namely error models -10, -11, -12, -13 and -14. Error model -10 can be used only for lognormal distributions. In this error model it is assumed that each data value X_{ij} comes from a lognormal distribution with a geometric mean equal to the fitted value Y_{ij} and log(geometric-standard-deviation) equals to V_{ij}, where

$$X = GF + E$$

and

$$Y = GF$$

It is further assumed that there is “measurement error” having standard-deviation equals to t_{ij} in each measured value X_{ij}. In this error model standard deviation matrix S_{ij} is computed as

$$S_{ij} = \sqrt{t_{ij}^2 + cv_{ij}^2 \left|Y_{ij}\right| \left(\left|Y_{ij}\right| + \left|X_{ij}\right|\right)}$$

where c equals to 0.5.

Error model -11 can be used for correspondence analysis. It is assumed that each data value X_{ij} comes from the Poisson distribution with a parameter μ_{ij}, where

$$\mu_{ij} = GF$$

In this error model PMF2 computes S_{ij} as

$$S_{ij} = \sqrt{\max\left(\left|\mu_{ij}\right|, 0.1\right)}$$

When the distributions of the data matrixes are not lognormal or Poisson then error models -12, -13 or -14 can be used. In error model -12 standard deviation matrix is computed as

$$S_{ij} = C1 + C2\sqrt{\left|X_{ij}\right|} + C3\left|X_{ij}\right|$$

where C1, C2 and C3 are error codes which take user defined values. The error code C1 should be chosen so that small values of X get a good standard deviation value. In environmental studies it is chosen as the detection limit. Similarly, C3 should be chosen so that the relative uncertainty of large values is reasonable. C3 takes values between 0.01 and 0.1, typically. Finally, the value of C2 is zero if the distribution of the data set is not Poisson (Paatero, 2002).

In error model -13, same standard deviation formula is computed except the fitted values Y replace X in this case. Finally, in error model -14 standard deviations are computed as

$$S_{ij} = C1 + C2\sqrt{\max\left(\left|X_{ij}\right|, \left|Y_{ij}\right|\right)} + C3 \max\left(\left|X_{ij}\right|, \left|Y_{ij}\right|\right)$$

In environmental studies error model -14 is recommended as in this error model larger of Xij and Yij is taken. So, the possibility of generating too small standard daviations would be avoided (Paatero, 2002).

In this study, error model -14 is used in the PMF2 runs. C1 is assigned as the standard deviation values given in Table 4.12. C2 value is taken as zero as the input data set is not Poisson distributed. In order to assign the C3 value that would be used in further runs C3 value of 0.01, 0.05 and 0.1 are tried. So, three runs were performed for all seven variables and the corresponding standard deviation arrays were obtained. Then they are put together to form the standard deviation matrix. The result files are investigated to decide which one to select.

The parameter Q is the main indicator of best fit as mentioned before. The theoretical value of Q is calculated by extracting the individual data points in the F matrix from the points in the data matrix. The data matrix is composed of 4662 data points formed by 7 variables and 666 samples and F matrix is composed of 21 data points formed by 7 variables and 3 factors. So, the theoretical value of Q is calculated as 4621. The Q values obtained from the PMF runs by using the standard deviation matrices formed with 0.01, 0.05 and 0.1 C3 values are 24568, 18251 and 13905, respectively. It is seen that when C3 values increase the corresponding Q values approach to the theoretical Q value although all of them are 3 to 6 times higher than the theoretical Q.

Factor loadings and histograms of weighted residuals of variables studied in PMF for standard deviations obtained for C3 value of 0.01, 0.05 and 0.1 are given in Tables 4.13, 4.14 and 4.15 and Figures 4.45, 4.46 and 4.47. As could be from these tables, factor loadings are the

Table 4.12. Detection Limits of the Parameters Measured

Variables	Detection Limits ($\mu g\ m^{-3}$)
SO_2	0.020
NO_2	1.050
HNO_3	0.056
NH_3	0.061
SO_4^{2-}	0.042
NO_3^-	0.094
NH_4^+	0.051
Na	0.011
Mg	0.005
K	0.007
Ca	0.060
V	0.0003
Cd	0.003
Pb	0.001

Table 4.13. Factor Loadings when C3 = 0.01

Variable	Factor 1	Factor 2	Factor 3
SO_2	**3.180**	0.008	0.006
NO_2	**0.202**	**4.371**	0.001
HNO_3	0.022	0.160	**0.217**
NH_3	0.000	**0.266**	0.104
SO_4^{2-}	0.034	0.000	**2.579**
NO_3^-	0.137	**0.202**	**0.340**
NH_4^+	0.038	0.045	**0.556**

Table 4.14. Factor Loadings when C3 = 0.05

Variable	Factor 1	Factor 2	Factor 3
SO_2	**3.158**	0.007	0.007
NO_2	**0.226**	**4.294**	0.001
HNO_3	0.016	0.167	**0.191**
NH_3	0.000	**0.269**	0.085
SO_4^{2-}	0.036	0.001	**2.464**
NO_3^-	0.110	**0.216**	**0.285**
NH_4^+	0.032	0.054	**0.602**

Table 4.15. Factor Loadings when C3 =0.1

Variable	Factor 1	Factor 2	Factor 3
SO_2	**3.175**	0.007	0.007
NO_2	**0.244**	**4.193**	0.001
HNO_3	0.015	**0.207**	**0.136**
NH_3	0.000	**0.308**	0.048
SO_4^{2-}	0.033	0.003	**2.230**
NO_3^-	0.089	**0.223**	**0.249**
NH_4^+	0.031	0.025	**0.683**

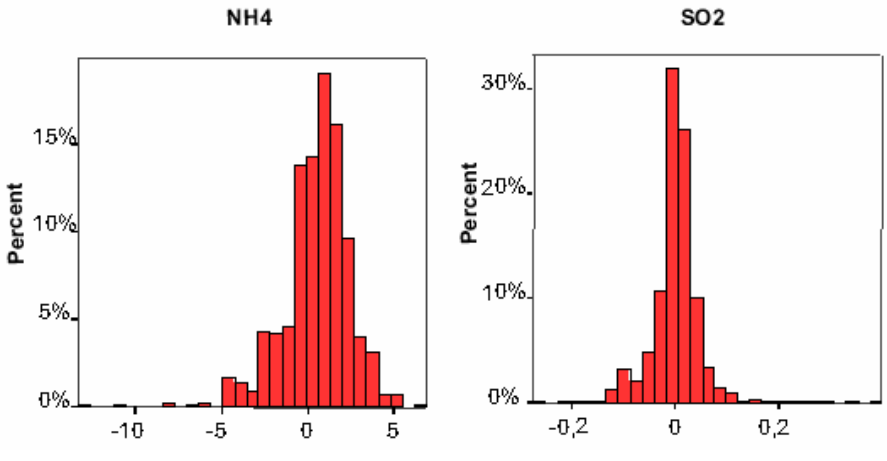

Figure 4.45. Histograms of Weighted Residuals of NH_4^+ and SO_2 Variables when C3 = 0.01

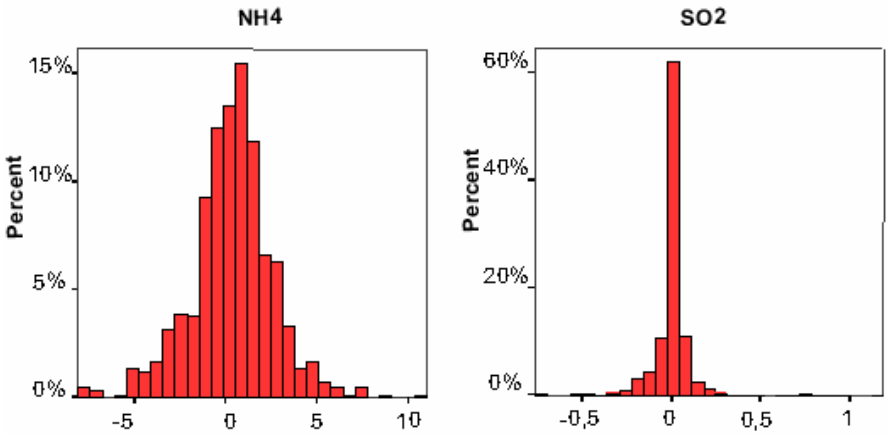

Figure 4.46. Histograms of Weighted Residuals of NH_4^+ and SO_2 Variables when C3 = 0.05

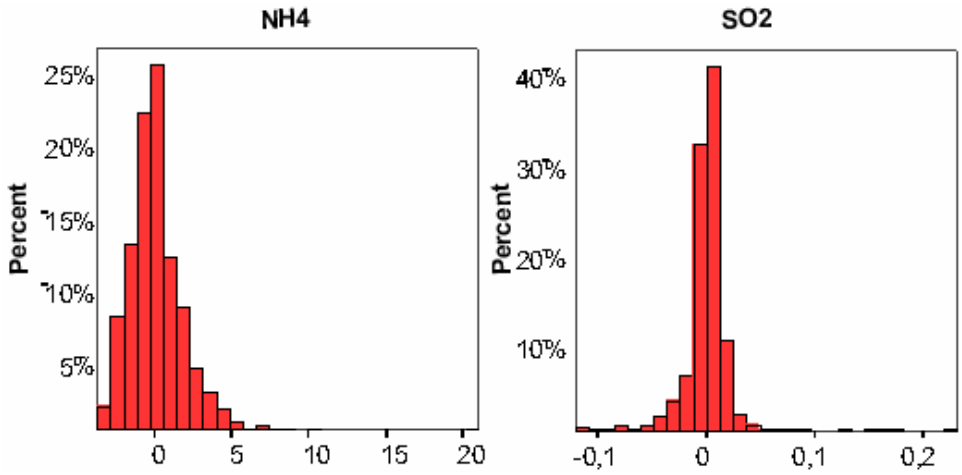

Figure 4.47. Histograms of Weighted Residuals of NH_4^+ and SO_2 Variables when C3 =0.1

same for 0.01 and 0.05 C3, whereas HNO_3 transported from factor 3 to factor 2 for 0.1 C3. It is seen from the histograms of weighted residuals that the distributions became narrower around 0 when C3 value gets bigger. So, it is decided to use 0.05 C3 for further runs of PMF.

As Q value for 0.05 C3 and 3 factors is approximately 5 times higher than the theoretical Q, 4 and 5 factors are tried to decrease Q. Theoretical Q for 4 and 5 factors are changed to 4634 and 4587, respectively as data points of loading matrix has changed. The Q values obtained for 4 and 5 factors are 10890 and 7132, respectively.

The factor loadings and histograms of weighted residuals are given in Tables 4.16 and 4.17 and Figures 4.48 and 4.49. It is seen from the Figures 4.48 and 4.49 that changing the number of factor did not affect the distributions of the weighted residuals. In contrast, as could be seen from Tables 4.16 and 4.17, 4 factors explain the factor loadings stronger than 3 factors. Whereas, in 5 factors run 2 factors are explained by only one variable. So, it is decided to use 4 factors in the following runs of the PMF.

Table 4.16. Factor Loadings for 0.05 C3 and 4 Factors

Variable	Factor 1	Factor 2	Factor 3	Factor 4
SO_2	0.006	**3.151**	0.004	0.009
NO_2	0.011	0.086	0.029	**4.465**
HNO_3	**0.533**	0.026	0.105	0.000
NH_3	**0.613**	0.000	0.000	0.067
SO_4^{2-}	0.001	0.001	**2.579**	0.005
NO_3^-	0.094	0.101	**0.293**	**0.160**
NH_4^+	0.132	0.020	**0.597**	0.003

Table 4.17. Factor Loadings for 0.05 C3 and 5 Factors

Variable	Factor 1	Factor 2	Factor 3	Factor 4	Factor 5
SO_2	**3.157**	0.007	0.004	0.005	0.005
NO_2	0.085	0.011	**4.470**	0.012	0.032
HNO_3	0.038	0.000	0.000	**0.513**	0.167
NH_3	0.000	0.101	0.021	**0.659**	0.000
SO_4^{2-}	0.000	**1.432**	0.000	0.000	**2.237**
NO_3^-	0.033	**1.291**	0.028	0.095	0.001
NH_4^+	0.027	0.259	0.009	0.124	**0.559**

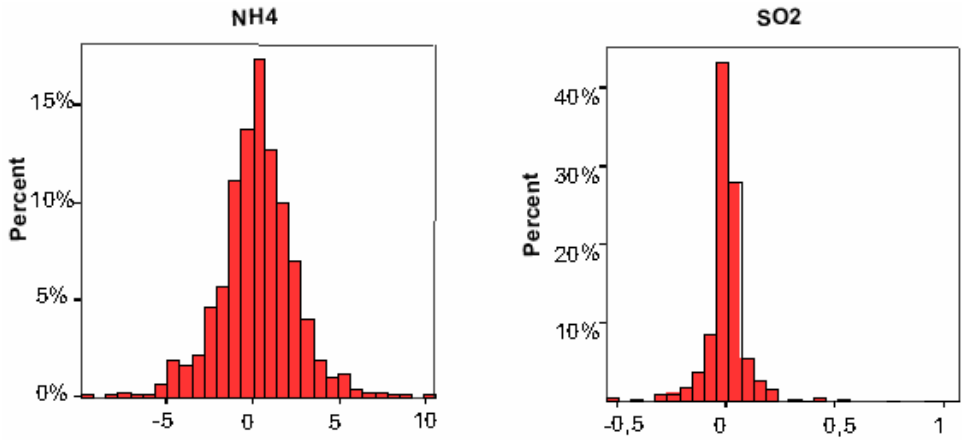

Figure 4.48. Histograms of Weighted Residuals of NH_4^+ and SO_2 Variables for 0.05 and 4 factors

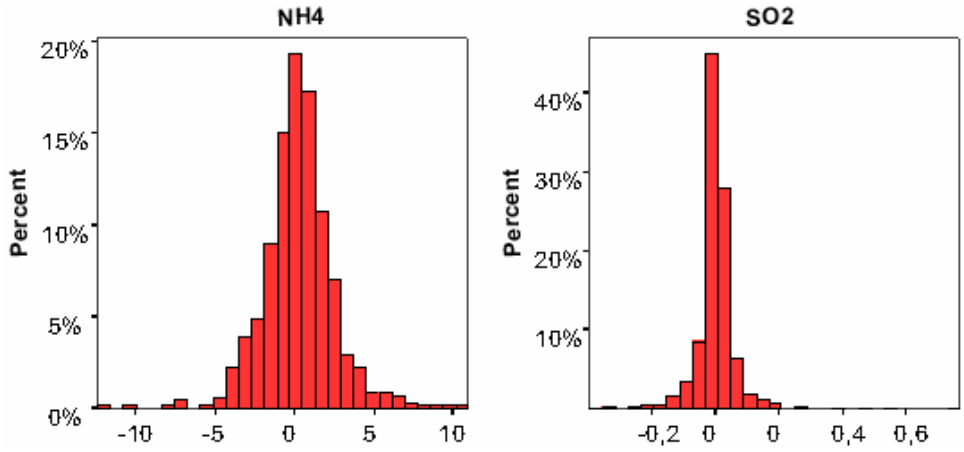

Figure 4.49. Histograms of Weighted Residuals of NH_4^+ and SO_2 Variables for 0.05 and 5 factors

So far, the data matrix used for factor analysis was studied to see how PMF results are changed according to the values assigned to the user-defined parameters. After that point, the original data matrix composed of 13 variables and 2360 samples were used as the input file of PMF.

As mentioned before the standard deviations were obtained by using the methodology of the PMF. Besides, the below detection limit values were assigned as what are they in the input file and the missing values were treated by PMF. However, as the missing values and the below detection data and the corresponding standard deviations inhibit the best least squares fit it is decided to use the methodology used by Polissar et al. (2001) to handle these parameters. In this method the following formulas were used for the concentrations and their corresponding standard deviations:

$X_{ij} = v_{ij}$ For determined values

$X_{ij} = d_{ij}/2$ For below detection limit values

$X_{ij} = z_{ij}$ For missing values

$\sigma_{ij} = u_{ij} + d_{ij}/3$ For determined values

$\sigma_{ij} = d_{ij}/2 + d_{ij}/3$ For below detection limit values

$\sigma_{ij} = 4z_{ij}$ For missing values

where v_{ij}, u_{ij}, d_{ij} and z_{ij} are the measured concentration, the analytical uncertainty, the analytical detection limit and the geometric mean of the concentrations measured, respectively.

The analytical uncertainty values given in Table 4.18 were obtained from EMEP/CCC-Report 6/2003 (Aas et al., 2003). As could be seen from this table analytical uncertainties were not available for V, Mg, Ca and K. So, in the first run of PMF the standard deviations of determined values of all 13 variables were calculated by using the methodology of PMF told before. The detection limits and geometric mean values of parameters measured used in PMF are given in Table 4.19 below.

Table 4.18. Analytical Uncertainty Values of Parameters Measured

Parameter	Analytical Uncertainty (%)
SO_2	2.85
NO_2	6.26
SO_4^{2-}	4.11
NO_3^-	5.73
HNO_3	16.87
NH_4^+	14.96
NH_3	7.74
Cd	1.60
Pb	3.60

Table 4.19. Detection limits and Geometric Mean Values of Parameters Measured

Variables	Detection Limits ($\mu g\ m^{-3}$)	Geometric Mean ($\mu g\ m^{-3}$)
SO_2	0.020	0.841
NO_2	1.050	2.229
HNO_3	0.056	0.250
NH_3	0.061	0.246
SO_4^{2-}	0.042	1.248
NO_3^-	0.094	0.288
NH_4^+	0.051	0.338
Pb	0.001	0.007
Cd	0.003	0.105
V	0.0003	0.001
Mg	0.005	0.099
Ca	0.060	0.367
K	0.007	0.174

In order to decide the number of factors that create best least squares fit, the PMF trials were started with 4 factors which is the factor number that give best fit for 7 variables and extended to 5 and 6 factors. The theoretical Q values for 4, 5 and 6 factors were 30628, 30615 and 30602 and the obtained Q values from PMF runs were 30648, 19838 and 10080, respectively. It is seen that the Q value obtained for 4 factors is nearly the same of theoretical Q and the others have Q values lower than the corresponding theoretical Q values. In order to decide which factor number gives the best least squares fit, factor loadings and histograms of weighted residuals were investigated. Tables 4.20, 4.21 and 4.22 and Figures 4.50, 4.51 and 4.52 gives the factor loadings and histograms of weighted residuals for 4, 5 and 6 factors, respectively. It is seen from these tables and figures that the increase of factor numbers makes the distributions of weighted residuals narrower near zero whereas at 6 factors some variables became only variables that

Table 4.20. Factor Loadings for 4 Factors

Variable	Factor 1	Factor 2	Factor 3	Factor 4
SO_2	**4.494**	0.002	0.005	0.003
NO_2	0.198	0.104	**8.272**	0.004
HNO_3	0.060	0.111	0.000	**0.622**
NH_3	0.000	0.000	**0.293**	**0.473**
SO_4^{2-}	0.030	**3.357**	0.032	0.003
NO_3^-	**0.323**	**0.278**	**0.209**	0.081
NH_4^+	0.022	**0.866**	0.019	0.061
Pb	0.001	0.001	0.003	0.002
Cd	0.065	0.092	0.039	0.027
V	0.000	0.000	0.000	0.000
Mg	0.012	0.002	0.002	**0.187**
Ca	0.000	**0.295**	0.001	**0.417**
K	0.089	0.000	0.006	**0.254**

Table 4.21. Factor Loadings for 5 Factors

Variable	Factor 1	Factor 2	Factor 3	Factor 4	Factor 5
SO_2	0.004	0.003	**4.476**	0.015	0.003
NO_2	**5.625**	0.041	0.062	0.020	0.061
HNO_3	0.000	**0.202**	0.080	0.000	**0.474**
NH_3	0.000	0.000	0.000	0.177	**0.575**
SO_4^{2-}	0.003	**3.208**	0.002	**1.083**	0.001
NO_3^-	0.018	0.085	0.076	**1.227**	0.009
NH_4^+	0.016	**0.840**	0.057	**0.237**	0.033
Pb	0.001	0.000	0.001	0.002	0.003
Cd	**0.254**	0.003	0.009	0.003	0.026
V	0.000	0.000	0.000	0.000	0.000
Mg	0.001	0.003	0.009	0.004	**0.203**
Ca	0.001	0.001	0.000	**0.308**	**0.509**
K	0.001	0.002	0.103	0.001	**0.272**

Table 4.22. Factor Loadings for 6 Factors

Variable	Factor 1	Factor 2	Factor 3	Factor 4	Factor 5	Factor 6
SO_2	0.005	**4.313**	0.004	0.004	0.005	0.005
NO_2	0.032	0.048	**5.635**	0.045	0.012	0.046
HNO_3	0.034	0.028	0.003	0.002	0.001	**0.872**
NH_3	**0.712**	0.006	0.002	0.001	0.012	0.002
SO_4^{2-}	0.059	0.045	0.004	**3.567**	0.012	0.001
NO_3^-	0.020	0.031	0.016	0.023	**1.004**	0.005
NH_4^+	0.000	0.000	0.001	**0.781**	0.085	**0.220**
Pb	0.004	0.001	0.001	0.000	0.001	0.001
Cd	0.032	0.011	**0.248**	0.001	0.001	0.009
V	0.000	0.000	0.000	0.000	0.000	0.000
Mg	0.168	0.000	0.001	0.000	0.019	0.080
Ca	**0.818**	0.001	0.002	0.142	0.001	0.004
K	0.162	0.001	0.001	0.001	0.084	**0.173**

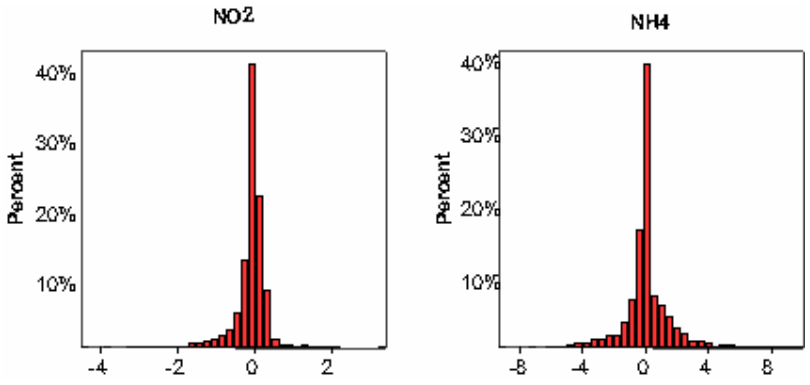

Figure 4.50. Histograms of Weighted Residuals of NO_2 and NH_4^+ Variables for 4 Factors

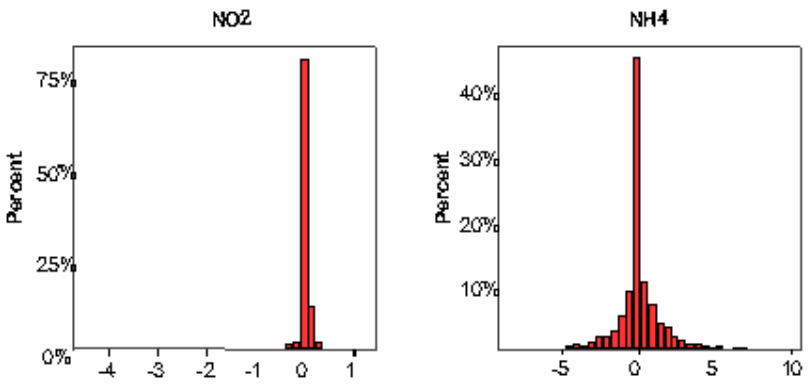

Figure 4.51. Histograms of Weighted Residuals NO_2 and NH_4^+ Variables for 5 Factors

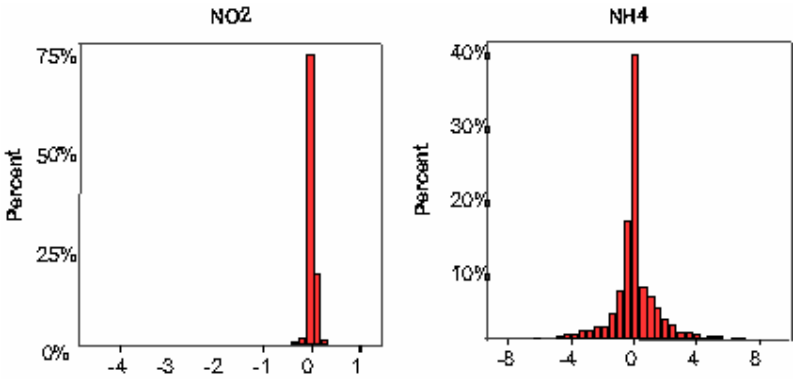

Figure 4.52. Histograms of Weighted Residuals NO_2 and NH_4^+ Variables for 6 Factors

explain the corresponding factor. So, it is decided to select 5 factors for the next trial.

One of the important features of the PMF is that its ability to make user defined free rotations instead of the varimax rotation in factor analysis. One of the methods to perform rotations in PMF is to assign F-peak value between 0 and 1. In this study F-peak values 0.1, 0.4 and 0.8 were tried to obtain best fit. As 5 factors is the number of factors selected in the previous trial, the theoretical Q is 30615 for these PMF

runs. The Q-values for F-peak values 0.1, 0.4 and 0.8 were 19832, 19860 and 20169.So, it is seen that increase of F-peak value increases the Q-value. It is suggested by the developers of the program that the increase of Q due to F-peak value is acceptable in tens. The original Q-value for 5 factors was 19838; so, F-peak value of 0.8 is not acceptable. As could be seen from Tables 4.23 and 4.24 and Figures 4.53 and 4.54, the factor loadings have changes whereas the histograms of weighted residuals have not been changed significantly. Because the factor loadings are more pronounced for F-peak 0.4 it is decided to use this value in the following PMF runs.

Table 4.23. Factor Loadings for F-peak Value of 0.1

Variable	Factor 1	Factor 2	Factor 3	Factor 4	Factor 5
SO_2	0.006	0.005	**6.782**	0.019	0.004
NO_2	**8.530**	0.054	0.061	0.027	0.054
HNO_3	0.000	**0.280**	**0.120**	0.000	**0.635**
NH_3	0.000	0.000	0.000	0.235	**0.767**
SO_4^{2-}	0.004	**4.493**	0.003	**1.408**	0.001
NO_3^-	0.021	0.116	**0.114**	**1.628**	0.010
NH_4^+	0.024	**1.177**	0.085	0.308	0.045
Pb	0.001	0.000	0.001	0.003	0.004
Cd	**0.385**	0.003	0.013	0.003	0.034
V	0.000	0.000	0.000	0.000	0.000
Mg	0.002	0.004	0.014	0.004	**0.273**
Ca	0.001	0.001	0.001	**0.404**	**0.680**
K	0.002	0.003	**0.153**	0.001	**0.364**

Table 4.24. Factor Loadings for F-peak Value of 0.4

Variable	Factor 1	Factor 2	Factor 3	Factor 4	Factor 5
SO_2	0.006	0.005	**7.940**	0.023	0.004
NO_2	**10.274**	0.022	0.014	0.019	0.012
HNO_3	0.000	0.213	**0.139**	0.000	**0.832**
NH_3	0.000	0.000	0.000	**0.374**	**0.788**
SO_4^{2-}	0.017	**5.856**	0.006	0.087	0.006
NO_3^-	0.002	**0.212**	**0.112**	**2.083**	0.001
NH_4^+	0.008	**1.506**	0.085	0.014	0.065
Pb	0.001	0.000	0.001	0.004	0.004
Cd	**0.481**	0.001	0.005	0.001	0.024
V	0.000	0.000	0.000	0.000	0.000
Mg	0.002	0.002	0.007	0.004	**0.307**
Ca	0.001	0.001	0.001	**0.529**	**0.702**
K	0.002	0.002	**0.149**	0.001	**0.411**

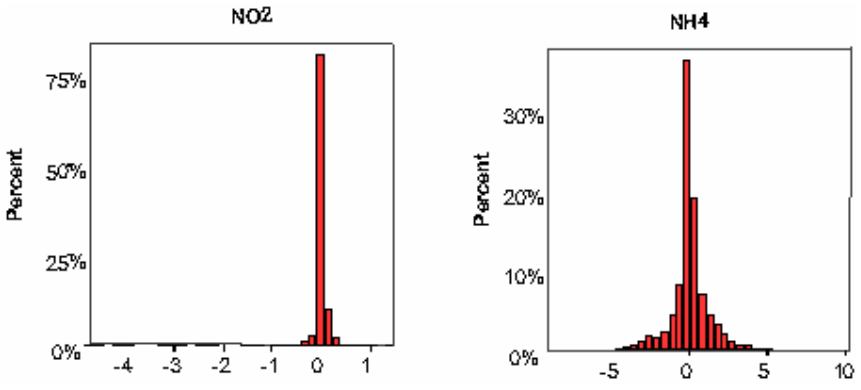

Figure 4.53. Histograms of Weighted Residuals of NO_2 and NH_4^+ Variables for F-peak Value of 0.1

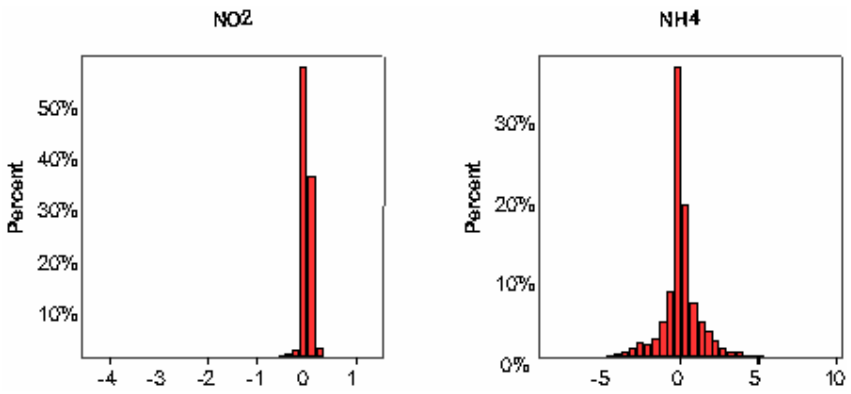

Figure 4.54. Histograms of Weighted Residuals of NO_2 and NH_4^+ Variables for F-peak Value of 0.4

In order to test how analytical uncertainties affect the PMF results the analytical uncertainties given in Table 4.18 were used as the standard deviations of determined values. With using the new standard deviation input matrix, PMF was run for 4, 5, 6, 7 and 8 factors. The theoretical Q values were 30628, 30615, 30602, 30589 and 30576 and the obtained Q values were 100773, 65871, 36892, 18631 and 8564 for 4, 5, 6, 7 and 8 factors, respectively. It seen that the most appropriate Q value is obtained for 6 factors. 6 factors has been found as the factor number that creates bet least squares fit by looking at the factor loadings given in Tables 4.25-4.29.

Table 4.25. Factor Loadings for 4 Factors

Variable	Factor 1	Factor 2	Factor 3	Factor 4
SO_2	**9.241**	0.002	0.004	0.003
NO_2	0.000	**4.051**	**4.477**	0.000
HNO_3	**0.116**	**0.348**	**0.182**	0.000
NH_3	0.000	**0.157**	**0.806**	0.000
SO_4^{2-}	0.065	**7.311**	0.000	**0.103**
NO_3^-	**0.456**	**0.216**	0.000	**0.693**
NH_4^+	**0.118**	**1.418**	0.035	0.063
Pb	0.000	0.000	0.061	0.000
Cd	0.000	0.001	0.000	**0.934**
V	0.000	0.000	0.000	0.000
Mg	**0.148**	0.012	0.003	0.052
Ca	**0.228**	**0.484**	**0.169**	**0.244**
K	**0.232**	0.002	**0.229**	**0.121**

Table 4.26. Factor Loadings for 5 Factors

Variable	Factor 1	Factor 2	Factor 3	Factor 4	Factor 5
SO_2	0.001	0.018	**10.166**	0.004	0.006
NO_2	**3.839**	0.000	**1.778**	**3.293**	0.000
HNO_3	0.039	**0.189**	**0.116**	**0.459**	0.000
NH_3	0.000	**0.993**	0.010	**0.171**	0.000
SO_4^{2-}	0.000	0.000	0.000	**6.170**	**1.864**
NO_3^-	0.095	0.028	0.073	0.001	**1.489**
NH_4^+	0.008	0.047	0.052	**1.280**	**0.388**
Pb	0.000	0.061	0.000	0.000	0.002
Cd	**0.980**	0.003	0.000	0.000	0.005
V	0.000	0.000	0.000	0.000	0.000
Mg	0.004	0.009	0.001	0.001	**0.229**
Ca	0.004	**0.250**	0.001	**0.139**	**0.756**
K	0.074	**0.232**	0.057	0.001	**0.204**

Table 4.27. Factor Loadings for 6 Factors

Variable	Factor 1	Factor 2	Factor 3	Factor 4	Factor 5	Factor 6
SO_2	0.005	0.009	**8.864**	0.005	0.006	0.006
NO_2	**14.434**	0.001	**0.440**	0.005	0.002	**0.231**
HNO_3	**0.179**	0.045	0.000	**0.508**	**0.102**	0.000
NH_3	**0.392**	**0.844**	0.000	0.000	0.000	0.000
SO_4^{2-}	0.002	0.058	0.015	0.001	**5.511**	0.024
NO_3^-	0.032	0.003	0.004	0.008	**0.123**	**2.166**
NH_4^+	0.002	0.000	0.018	**0.188**	**1.032**	0.058
Pb	0.000	0.061	0.001	0.000	0.000	0.007
Cd	0.000	0.000	0.001	**1.052**	0.000	0.008
V	0.000	0.000	0.000	0.000	0.000	0.000
Mg	0.002	0.010	0.000	0.002	**0.284**	0.006
Ca	0.081	**0.171**	0.000	0.005	**0.528**	**0.531**
K	0.020	**0.217**	0.001	0.007	**0.367**	0.001

Table 4.28. Factor Loadings for 7 Factors

Variable	Factor 1	Factor 2	Factor 3	Factor 4	Factor 5	Factor 6	Factor 7
SO_2	0.006	**8.979**	0.005	0.004	0.006	0.006	0.008
NO_2	**13.827**	0.052	0.010	0.012	0.074	0.009	0.047
HNO_3	**0.153**	0.000	**0.143**	**0.516**	0.000	0.065	0.000
NH_3	0.001	0.008	**1.344**	0.001	0.038	0.001	0.005
SO_4^{2-}	0.000	0.000	0.000	0.001	0.000	**5.649**	**0.841**
NO_3^-	0.002	0.005	0.001	0.001	**1.847**	0.002	0.076
NH_4^+	0.019	0.059	0.028	**0.113**	**0.116**	**1.277**	0.000
Pb	0.000	0.000	0.001	0.000	0.001	0.000	0.065
Cd	0.000	0.000	0.000	**1.046**	0.005	0.000	0.010
V	0.000	0.000	0.000	0.000	0.000	0.000	0.000
Mg	0.024	0.000	0.060	0.002	**0.189**	0.065	0.000
Ca	**0.353**	0.002	**1.107**	0.004	0.003	0.003	0.010
K	0.001	0.001	**0.290**	0.003	0.003	**0.331**	0.085

Table 4.29. Factor Loadings for 8 Factors

Variable	Factor 1	Factor 2	Factor 3	Factor 4	Factor 5	Factor 6	Factor 7	Factor 8
SO_2	0.006	**8.963**	0.007	0.005	0.005	0.005	0.005	0.004
NO_2	**12.318**	0.027	0.024	0.013	0.021	0.014	0.021	0.016
HNO_3	0.001	0.001	**0.124**	**0.878**	0.000	0.000	0.000	**0.229**
NH_3	0.003	0.003	**1.611**	0.002	0.004	0.004	0.003	0.002
SO_4^{2-}	0.006	0.005	0.023	0.003	**7.249**	0.007	0.007	**0.108**
NO_3^-	0.003	0.003	0.002	0.002	0.003	0.002	**1.859**	0.003
NH_4^+	0.000	0.001	0.000	**0.714**	**0.728**	**0.299**	0.002	0.000
Pb	0.000	0.000	0.000	0.000	0.000	0.065	0.000	0.000
Cd	0.001	0.001	0.001	0.001	0.001	0.002	0.001	**0.998**
V	0.000	0.000	0.000	0.000	0.000	0.000	0.000	0.000
Mg	0.001	0.001	0.029	**0.273**	0.001	0.001	0.027	0.002
Ca	**0.367**	0.001	0.001	**0.792**	0.001	**0.114**	0.001	0.003
K	0.001	0.001	**0.324**	**0.233**	0.001	**0.036**	0.089	0.003

For 6 factors, it is seen that there is no Pb and V source either factors. So, it is decided to extract these variables from the data matrix. For the remaining 11 variables and 6 factors the theoretical Q is calculated as 25894 and the Q-value obtained from the last PMF run is 20705. The resultant factor loadings are given in Table 4.30.

Table 4.30. Factor Loadings for Variables other than Pb and V

Variable	Factor 1	Factor 2	Factor 3	Factor 4	Factor 5	Factor 6
SO_2	0.007	**7.749**	0.005	0.005	0.006	0.005
NO_2	**12.292**	**0.121**	0.008	0.010	0.095	0.012
HNO_3	**0.149**	0.000	0.056	**0.113**	0.000	**0.424**
NH_3	0.001	0.007	0.001	**1.016**	0.035	0.001
SO_4^{2-}	0.003	0.032	**5.973**	0.046	0.015	0.002
NO_3^-	0.002	0.004	0.002	0.004	**1.673**	0.001
NH_4^+	0.001	0.001	**1.037**	0.000	**0.117**	**0.173**
Cd	0.000	0.000	0.000	0.000	0.005	**0.903**
Mg	0.033	0.000	0.001	**0.280**	0.019	0.001
Ca	**0.199**	0.001	**0.518**	**0.507**	0.001	0.003
K	0.005	0.001	0.001	**0.357**	**0.184**	0.003

There is no further run is performed in PMF2 exercise. So, PMF reveals 6 factors for variables other than Pb and V with the factor loadings given in Table 4.30.

Factor profiles for the 6 factor PMF solution (concentrations of measured parameters in each factor) is given in Figure 4.55, together with the explained variance by each parameter (EV). The EV is a qualitative term and shows how much of the variance is explained by each parameter in that particular factor. It is used for confirmation of sources, but not for source identification.

Factor 1 identified by the PMF has high NO_2 concentration in it and moderate contributions from HNO_3, Mg and Ca. The NO_2 is emitted to the atmosphere from motor vehicles and from combustion of fossil fuel from both industries and space heating. This factor can not be related

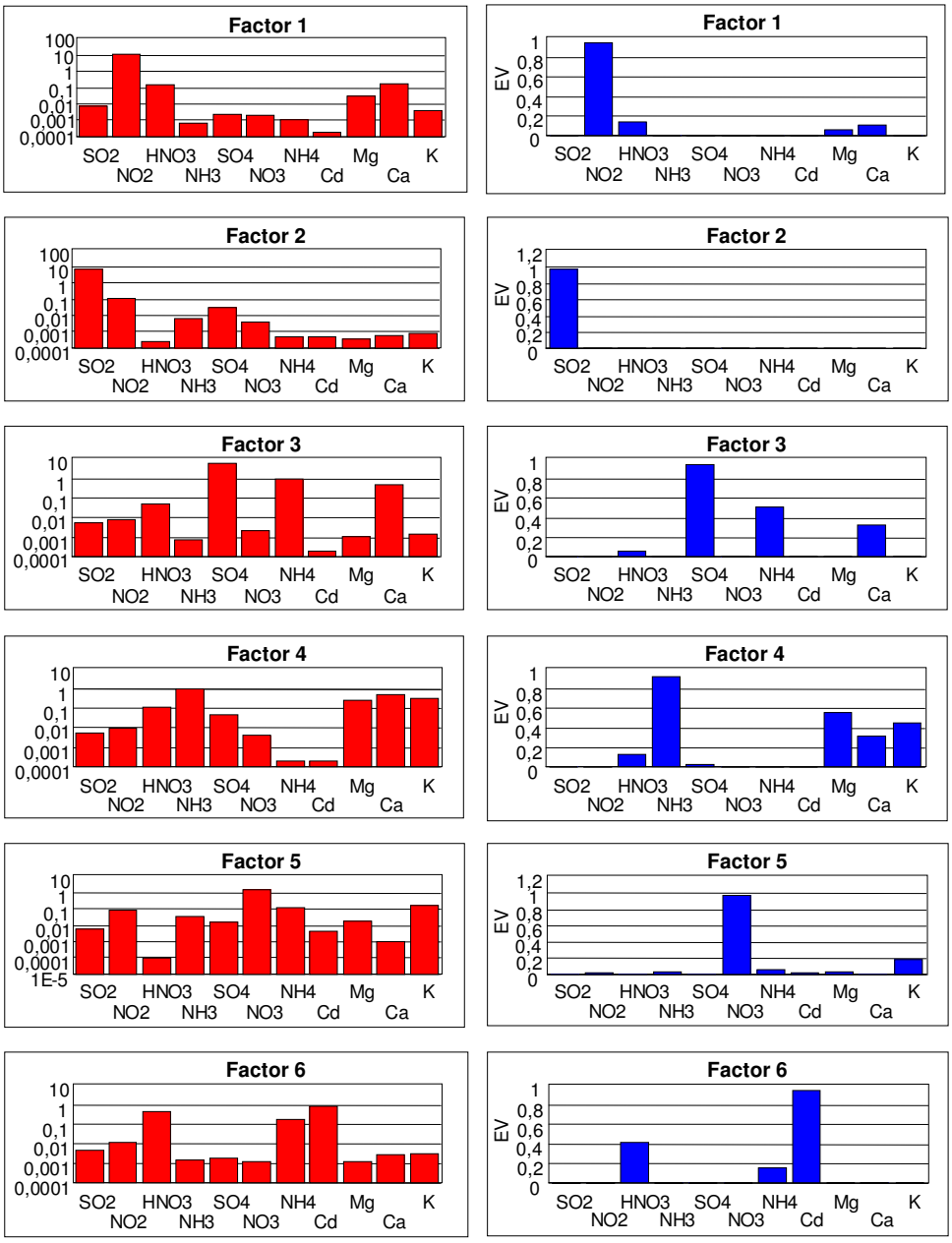

Figure 4.55. Factor Loadings and Explained Variations

with space heating because any factor that is related to space heating should also contain high concentrations of SO_2, and concentration of SO_2 is very small in this factor. This factor can be related with motor vehicle emissions. The main source of Mg, Ca and K in the atmosphere is the resuspension of soil dust. These parameters are frequently observed to be associated with motor vehicle factors in source apportionment studies, because transport of traffic related pollutants to the receptor also brings road dust to the sampler and separation of road dust from motor vehicle emissions require the availability of many crustal and traffic markers which are not measured in this study (Kim et al., 2003; Liu et al., 2003; Lee et al., 1999). Normally one would expect Pb concentration to be strongly correlated with this factor. However, Pb is not correlated with this factor. Actually Pb is not significantly correlated with any of the parameters measured in this study. This may indicate an analytical problem in Pb measurements. Monthly variation of Factor 1 scores are depicted in Figure 4.56. The factor 1 scores do not show a well defined seasonal pattern shown by the NO_2 concentrations as discussed in Section 4.2.2. Winter concentrations are slightly higher than summer concentrations, but the cycle is not well defined. This lack of seasonal pattern also supports the motor vehicle source for this factor, because unlike emissions from combustion for heating, motor vehicle emissions do not show a significant difference between summer and winter seasons. Factor 1 should represent a relatively local source in the atmosphere, because N chemistry is fairly rapid and NO_2 oxidizes to NO_3 within a day.

Factor 2 has high concentrations of SO_2 and also includes NO_2, NH_3, SO_4^{2-}, NO_3^- associated with it. This factor is identified as mixed urban factor. The SO_2 and NO_2 are the main components of this factor. The presence of SO_4^{2-} and NO_3^- may be due to oxidation of precursor gases

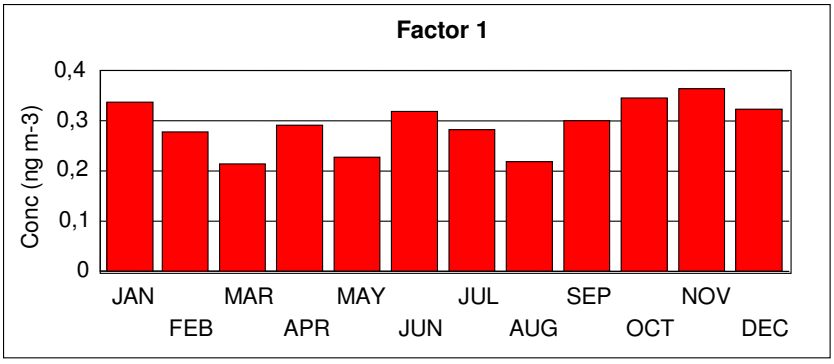

Figure 4.56. Monthly variation of Factor 1 scores

during transport. No matter how close the transport distance is, some of the SO_2 and NO_2 convert to SO_4^{2-} and NO_3^- ions. Since the concentrations of SO_4^{2-} and NO_3^- in this factor are an order of magnitude smaller than their corresponding precursors the transport distance can not be very long and factor should represent a local component. The seasonal variation of Factor 2 scores are depicted in Figure 4.57. Avery clear seasonal pattern with approximately a factor of 5 to 6 higher concentrations in winter confirms the local nature and urban nature of this component. The source of this component should be local, because (1) any distance source can not result in such higher concentrations in winter season, because no matter how high the emissions are, pollutants are scavenged out in winter by more frequent rains and winter concentrations and winter concentrations approaches to summer concentration, as discussed previously, (2) if the sources of pollutants in this factor are not close to the station, then one would expect higher concentrations of SO_4^{2-} and NO_3^- associated with it. Since SO_4^{2-} and NO_3^- are formed by oxidation of SO_2 and NO_x in the atmosphere, then SO_2 and NO_2 concentrations decrease and concentrations of SO_4^{2-} and NO_3^- increase with transport time. Concentrations of SO_4^{2-} and NO_3^- are approximately an order of magnitude smaller than those of SO_2 and NO_2 indicating a local source.

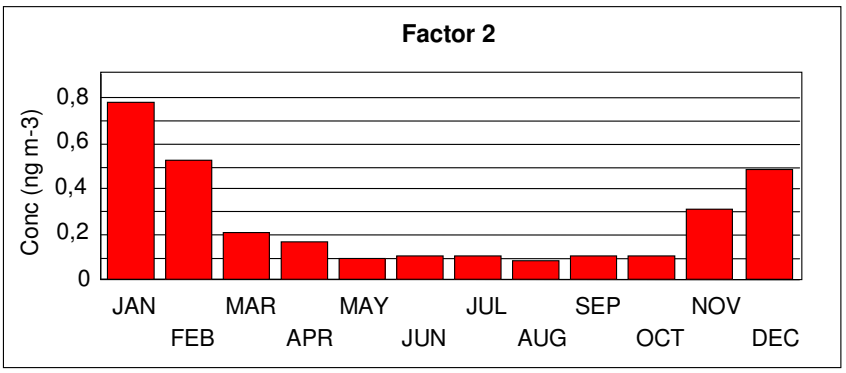

Figure 4.57. Monthly variation of Factor 2 scores

A large difference between summer and winter concentrations also indicate that Factor 2 is related with urban emissions. The SO_2 and NO_2 are also emitted from combustion of fossil fuels in point sources, such as industries and power plants. However, one would expect more uniform concentrations in summer and winter if the receptor is affected from such point sources. Observed large difference between summer and winter concentrations is typical pattern in urban areas. Based on this argument, Factor 2 was identified as mixed urban factor.

Factor 3 includes high concentrations of SO_4^{2-}, NH_4^+, Ca. The factor also includes fair amount of HN_3 and lesser concentrations of SO_2 and NO_2. This is a neutralized SO_4^{2-} factor representing both $(NH_4)_2SO_4$ and $CaSO_4$ in the atmosphere. Factor 3 is a long range transport factor and SO_4^{2-} and other parameters associated with this factor do not have local sources close to station, because SO_4^{2-} concentration in Factor 3 is approximately 3 orders of magnitude higher than SO_2 concentration, indicating that almost all of the SO_2 is converted to SO_4^{2-}. The monthly variation of factor 3 scores are depicted in Figure 4.58. Factor 3 scores do not show a significant difference between the summer and winter seasons, which was also the case in monthly variation of SO_4^{2-} concentrations discussed previously. The PSCF values for Factor 3 were calculated using the highest 40% of the factor score

concentrations as the polluted data set. The distribution of PSCF values are given in Figure 4.59. The distribution of PSCF values in the figure is very similar with the distribution of PSCF values calculated using SO_4^{2-} concentrations. This observed similarity in both distribution of PSCF values and monthly variation of factor scores with those calculated using SO_4^{2-} concentrations indicates that SO_4^{2-} observed at the central Anatolia is largely accounted by this factor. Consequently, it can be concluded that although contribution of local sources are substantial to observed levels of most of the parameters measured in this study, SO_4^{2-} measured at the central Anatolia are transported from distant sources and contribution of local sources are not significant.

Factor 4 is an interesting factor. It includes high concentrations of NH_3, Ca, Mg and K, moderate concentrations of HNO_3 and SO_4^{2-} and small concentrations of SO_2, NO_2 and NO_3. Although there is both natural and anthropogenic species in this factor, variance in factor 4 is explained by NH_3, Ca, K, and Mg and contribution of other parameters to EV is negligible. The seasonal variation in Factor 4 scores are given

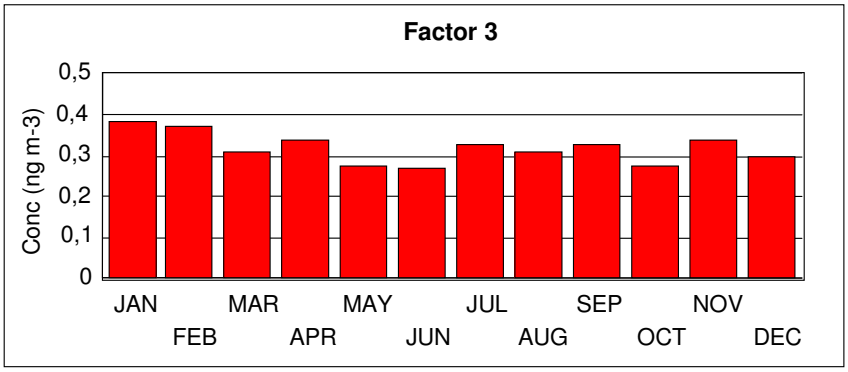

Figure 3.58. Monthly variation of Factor 3 scores

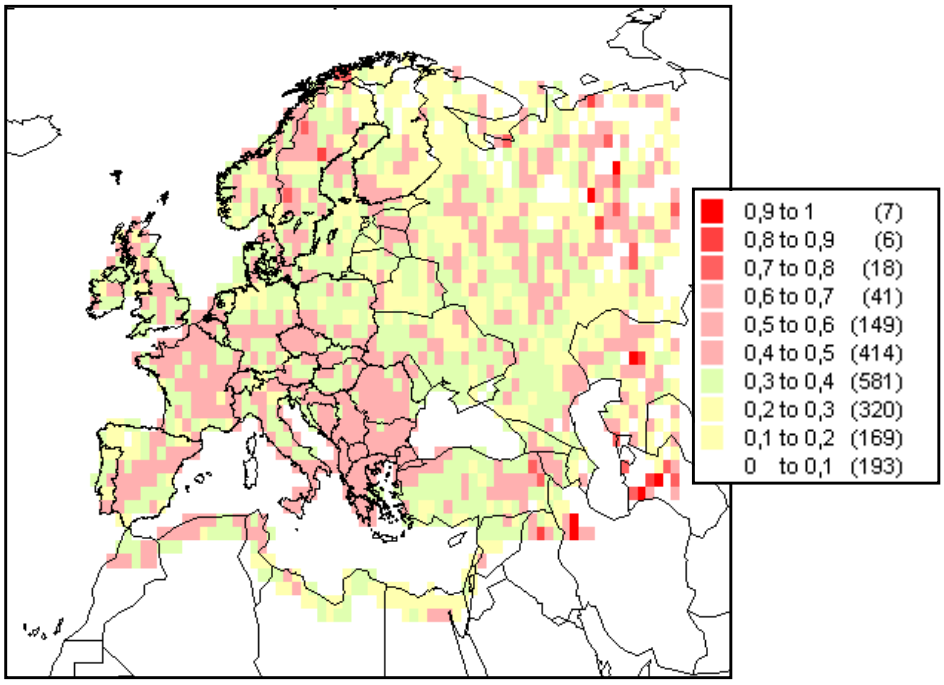

Figure 3.59.Distribution of PSCF Values Calculated for Factor 3 Scores

in Figure 4.60. This factor has higher concentrations in summer, which is similar with the seasonal patterns observed in concentrations of NH_3, Ca, Mg and K concentrations, but not in the concentrations of other species found in this factor. Consequently, Factor 4 is primarily determined by these 4 parameters and their observed concentrations are accounted for by this factor. Factor 4 is identified as soil component in the atmosphere. The weak correlation of various anthropogenic species such as, SO_2, NO_2, SO_4^{2-}, NO_3^-, NH_4^+ etc is probably due to mixing of an anthropogenic component with soil component.

Such mixing is frequently observed in factor analysis applications in air pollution studies and can be due to a real mixing process or an artifact. If there is a strong anthropogenic source relatively close to sampling point, then anthropogenic and crustal parameters can occur in the same

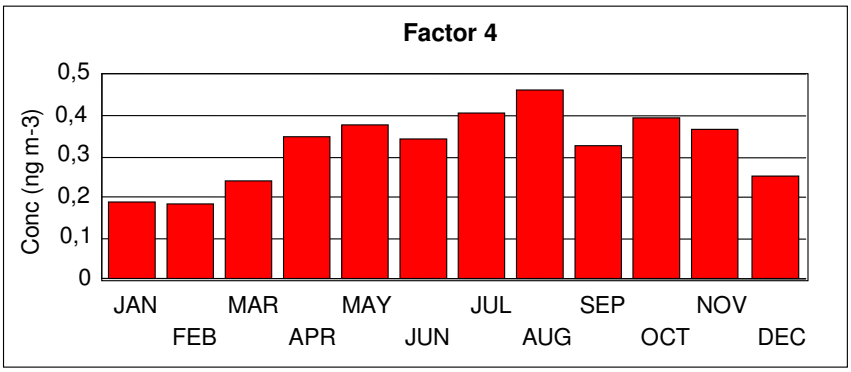

Figure 4.60. Monthly Variation of Factor 4 Scores

factor, because winds blowing from that source brings in both crustal material and anthropogenic emissions. However, in this study observed mixing of anthropogenic and soil related parameters is probably an artifact due to lack of adequate crustal markers. In source apportionment studies, litophilic elements such Al, Si, Fe, Sc, are used as marker elements for soil, because (1) their main source in the atmosphere is the crustal material and (2) their concentrations do not change significantly from one soil type to another. However in this study none of these crustal markers were measured. Calcium, Mg and K were used as soil indicator elements. Soil is not the only source of these elements (for example Ca is known to be emitted from cement industry and other industries where soil is processed and K is a well known component in biomass burning). Furthermore, Ca, K and Mg concentration in soil is a strong function of mineralogy. We believe that the mixing of anthropogenic parameters with crustal component is due to lack of proper crustal markers.

However, presence of NH_3 in Factor 4 should be evaluated separately, because it is not a minor component in this factor (EV value is very high). The presence of NH_3 in this factor is probably real and can not be explained by the lack of crustal markers. The presence of NH_3 in

crustal factor suggests a very local source of NH_3. This is confirmed by the distribution of PSCF values for Factor 4, which shows a strong source region within Turkey, covering most of the western half of the country. There are two important sources of NH_3 in the atmosphere. One of these is the animal manure and the other one is fertilizer use. Since animal farming is not very widespread in Turkey, NH_3 volatilization from fertilizer applications is expected to be the main source of NH_3. Higher NH_3 concentrations in summer and a wide area source region observed in PSCF calculations supports this hypothesis, because NH_3 volatilization is expected to be higher in summer due to both more extensive application N-containing fertilizers in spring and summer and higher temperatures, which enhances volatilization from soil. Consequently, Factor 4 is probably a soil-fertilizer use factor representing resuspension of soil and fertilizer applications within Turkey.

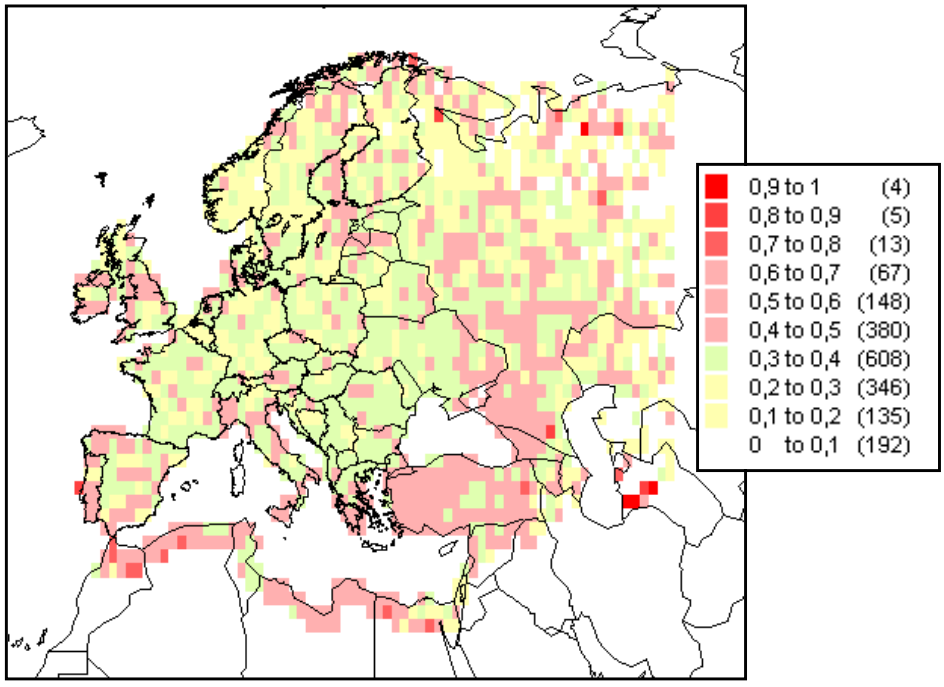

Figure 4.61. Distribution of PSCF Values Calculated for Factor 4 Scores

Factor 5 are not very clear at this point. Factor 5 includes primarily NO_3^- and in lesser concentrations NH_4^+, NO_2, NH_3, SO_4^{2-}, and K. Although most of the measured parameters are included in the factor, variance is explained mostly by NO_3^-. That is why this factor is named as NO_3^- factor. The temporal variation of Factor 5 scores are given in Figure 4.62. Scores show a very clear trend with approximately a factor 2 higher values in winter season. The distribution of PSCF values for Factor 5 closely resemble the distribution of PSCF values calculated using NO_3^- concentrations. Where the sources are more local relative to those for Factor 3 (long range transported neutralized SO_4^{2-} factor). However, this is not a local factor, because $SO_4^{2-}/(SO_2 + SO_4^{2-})$ ratio in this factor is 0.7 indicating several day long stay in the atmosphere.

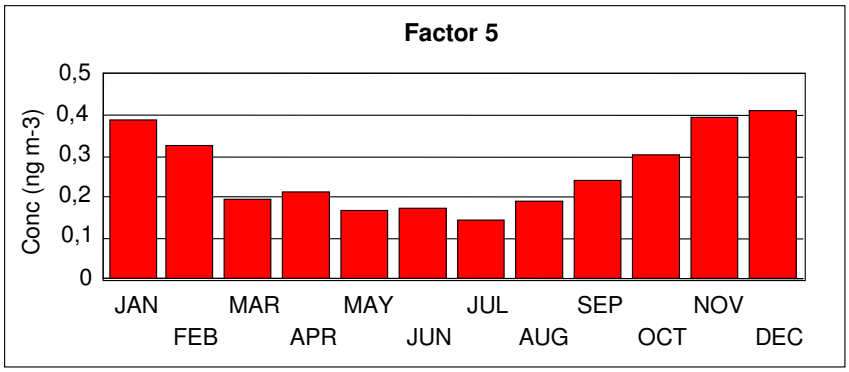

Figure 4.62. Monthly Variation of Factor 5 Scores

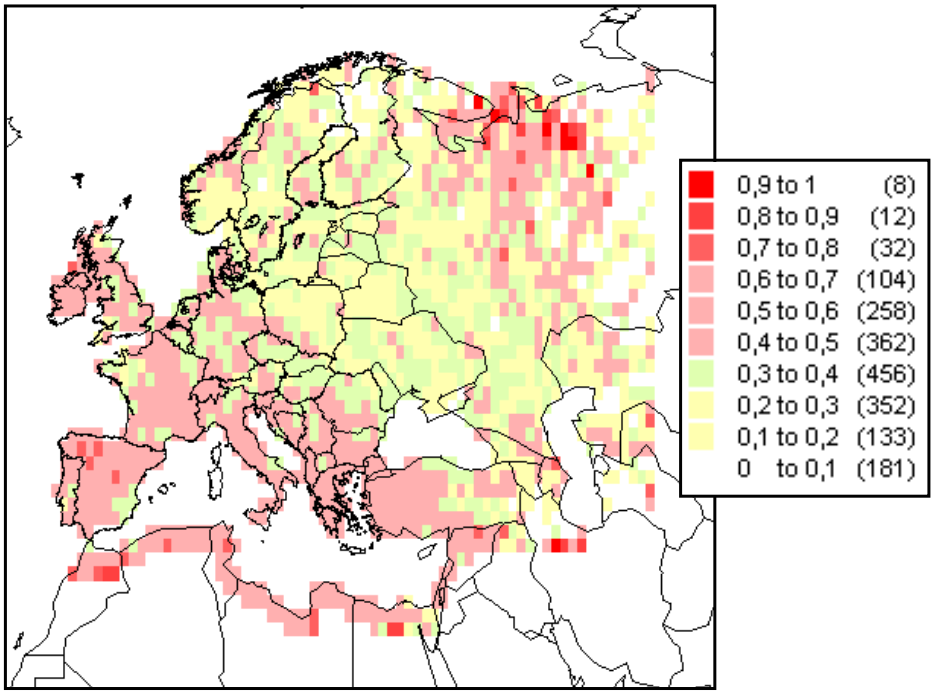

Figure 4.63. Distribution of PSCF Values Calculated for Factor 5 Scores

Factor 6 is composed of NH_4^+, HNO_3 and Cd. The variance in the factor is explained mostly by Cd. As pointed earlier the component represented by this factor is not clear.

The PMF results showed that composition of the atmosphere in the Central Anatolia can be explained by 6 components. Four of these components are identified and related to sources, but 2 were not identified. The main reason for the difficulty encountered in assigning sources to factors is the very few parameters measured in this study. Trace elements which are excellent tracers for various source types were not available. Most of the parameters measured in this study are not conservative (go through chemical processes during their transport in the atmosphere) which makes the interpretation of sources difficult. In any case the PMF appeared as promising approach to identify

sources and source regions with much higher resolution than that can be obtained using conventional factor analysis, particularly when trace element data are available.

CHAPTER 5

CONCLUSION

Concentrations of elements and ions measured in samples collected between February 1993 and December 2000 at a rural site in Central Anatolia were investigated.

In order to determine the pollution level of Central Anatolia concentrations measured at Çubuk station were compared with the data obtained from other EMEP stations and stations located at Turkey. The comparison revealed that Central Anatolia has lower pollution level than European countries except for SO_2. SO_2 concentrations were found to be higher than most of the stations in the European countries indicating that Çubuk station is under strong influence of local emissions, most probably Ankara.

Concentrations measured at Çubuk station were also compared with data obtained from Antalya, Amasra and Uludağ stations. Results of this comparison indicates that concentrations measured at high altitude stations, namely Çubuk and Uludağ stations, have much lower concentration values than coastal stations located at Antalya and Amasra. For anthropogenic elements this indicates that there should be different transportation mechanisms. In order to understand these mechanisms and the differences between them, a monitoring program that include modeling and measurements at high altitudes should be performed. In contrast to anthropogenic elements, concentrations of

natural elements Mg, Ca and K are higher in coastal stations due to the marine contribution on the concentrations.

Concentrations of elements and major ions measured at Çubuk station were found to show high episodic and seasonal variations. Such high variations in concentrations can be explained by variations in the source strengths, transport patterns and meteorological events. It is fairly known that anthropogenic elements are long range transported to Turkey. So as the sources of anthropogenic elements are located thousands of kilometers away from the station, the variations of source strengths can not have any impact on the concentrations measured. Indeed, high variations of concentrations of these elements and ions are due to the variations of transport patterns and local and distant rain events. Contrary to anthropogenic elements, temporal variations of concentrations of natural elements depend on the source strengths and local rain events.

Dry deposition fluxes of parameters measured at Çubuk station were calculated by multiplying the concentrations measured with the dry deposition velocity values found by the literature survey. Dry deposition fluxes calculated can be put into descending order as SO_2, Ca, HNO_3, K, Mg, NH_3, NO_2, SO_4^{2-}, NH_4^+, NO_3^-, Cd, V and Pb. Concentrations, particles sizes and/or dry deposition velocities are the determining factors of this order. Dry deposition fluxes of all parameters have comparable values with the wet deposition fluxes. This is due to the extremely low annual rainfall at Central Anatolia.

Correlations between parameters indicate that crustal elements correlate well between each other due to the same source they have. For anthropogenic elements the situation is somehow different. SO_4^{2-}, NO_3^-, NH_4^+, SO_2, NO_2 and HNO_3 elements and ions correlate well due to similar chemical reactions they undergo. Whereas, other anthropogenic elements like Pb and Cd do not show any correlation

with other elements and ions as they do not participate in atmospheric chemistry (they are emitted on particles, they remain on particles through atmospheric transport and eventually they deposit on particles).

Enrichment factor calculations have revealed that sulfate, Pb and Ca are highly enriched in the aerosol (with EF_c's ranging between 100 for Pb and 10 000 for Cd) in Çubuk indicating that contribution of soil on their measured concentrations is not significant. Enrichment factors of V, Mg, Ca and K, on the other hand, are all less than 10, suggesting dominant contribution of soil component in aerosols on their observed concentrations. This pattern is not unusual and commonly observed in most of the studies performed in the Mediterranean region.

In order to determine if SO_4^{2-} is long range transported to Central Anatolia $SO_4^{2-}/(SO_2 + SO_4^{2-})$ ratio is calculated. Average value of $SO_4^{2-}/(SO_2 + SO_4^{2-})$ ratio is found as 0.54 ± 0.29 indicating approximately half of the SO_2 is oxidized to SO_4^{2-} by the time air masses are intercepted at Çubuk station. Calculations of conversion rates correspond to locate the sources of SO_4^{2-} between 1-2 day trajectory distance away. This distance extends to part of the Balkan countries, but not beyond them, suggesting that Central Anatolia are affected primarily from source within Turkey and Balkan Countries and not affected as much from distant sources. The estimation of location of sources based on SO_4^{2-}-to-total S ratio is a very crude approximation, as it bases on conversion rate, which changes significantly depending on the solar flux and pollution level in the air mass, but it at least provides information if the station is affected from very local sources or the SO_4^{2-} observed is transported from sources that are not in the immediate vicinity of the station. The ratio observed in this study indicates that contribution of distant sources is more important than the contribution of local sources on observed SO_4^{2-} levels.

SO_4^{2-}/NO_3^- calculated in this study is used as tracer for air masses originating from Eastern and Western parts of the Europe. SO_4^{2-}/NO_3^- ratio for all years between 1977 and 2000 is calculated as 1.3 and 3.4 for Western and Eastern Europe, respectively. The same ratio for Çubuk station is calculated as 3.7 indicating that Çubuk is receipt of SO_4^{2-} from Eastern European countries. There is not considerable difference in the SO_4^{2-}/NO_3^- ratios before and after 1995 in the Western Europe (average ratio before and after 1995 is 1.2 and 1.3, respectively) but there are significant differences in the Eastern Europe. The ratio is 3.8 before 1995 and 2.7 after 1995. This indicates that the reductions in Western Europe were completed before 1995, but in the Eastern Europe SO_4^{2-} reductions started later and SO_4^{2-} levels are still decreasing. High variation of SO_4^{2-}/NO_3^- ratio calculated in Çubuk for before and after 1995 (4.2 and 3.2 before and after 1995, respectively) supports the idea that SO_4^{2-} is long range transported to Central Anatolia from Eastern Europe.

Positive Matrix Factorization (PMF) is applied to Çubuk data in order to quantitatively identify the sources of pollutants measured at the station. PMF analysis revealed 6 source groups, namely motor vehicle source, mixed urban factor, long range transport factor, soil factor, NO_3^- factor, Cd factor. Last two components can not be identified due to few parameters measured in this study.

To identify the source regions of pollutants in Central Anatolia Potential Source Contribution Function (PSCF) is used. Distribution of PSCF values showed that main sources of SO_4^{2-} and NH_4^+ are observed in the western parts of Turkey, Balkan countries and Central and Western Europe. PSCF values calculated for NO_3^- indicates that main source regions are located around the Mediterranean Sea. There is no very strong potential source area observed for NH_3 concentrations at Çubuk due to fairly uniform distribution of sources in Europe. Similarly, PSCF values calculated for Pb do not indicate any potential source area due

to high contribution of local sources on Pb concentrations measured at station. Like SO_4^{2-} and NH_4^+ main source areas of Cd are located far away from Çubuk. The most probable source areas are located at central Russian Federation, Balkan countries, western and central Europe, north of Sweden and Finland and some regions located at Mediterranean coast of North Africa.

5.1. Recommendations for Future Research

This study presents the results of the statistical analysis of the aerosols and gaseous pollutants data obtained from Çubuk station. Since being an EMEP station, air data measurements at Çubuk station is done according to EMEP procedures. Besides its benefits, such as the high quality data obtained by means of data quality assurance studies conducted by Chemical Coordinating Center of EMEP, it limits the parameters to be measured. And also due to economic shortcomings no further measurement of other species is performed at the station.

At the station, trace elements which are excellent tracers for various source types have not been measured. Measurement of trace elements in the future will significantly increase the usefulness of data, particularly for source region apportionment.

Persistent organic pollutants (POPs) are organic compounds that are stable for long period of time in the atmosphere and harmful to the environment. Due to their atmospheric stability, they can be transported over long distances. These organic compounds are not being measured at Çubuk station for the time being, but their sampling and measurements are recommended, because data on atmospheric levels and transport of POPs are lacking in Turkey.

Measurement of other trace elements and organics are highly recommended to understand the composition of the atmosphere and

the sources of the pollutants in a better manner. In this regard, these pollutants (specially the ones that are difficult to be analyzed such as mercury) can be studied as short campaigns. One or two year data sets have statistical significance and can be used in composition and source apportionment studies.

REFERENCES

Aas W., Hjellbrekke A., Schaug J. (2003). Data quality 2001, quality assurance, and field comparisons, EMEP/CCC-Report 6/2003.

Al-momani I. F., Tuncel S., Eler U., Ortel E., Sirin G., Tuncel G. (1995). Major Ion Composition of Wet and Dry Deposition in the Eastern Mediterranean Basin, **The Science of the Total Environment**, **164**, 75-85.

AMAP (1998). AMAP Assessment Report: Arctic Pollution Issues. Arctic Monitoring and Assessment Programme (AMAP), Oslo, Norway.

Anderson N., Strader R., Davidson C. (2003). Airborne Reduced Nitrogen: Ammonia Emissions from Agriculture and Other Sources, **Environment International**, **29**, 277-286.

Arimoto R., Duce R.A., Ray B.J., Unni C.K. (1985). Atmospheric Trace Elements at Enewetak Atoll: 2. Transport to the Ocean by Wet and Dry Depositions, **Journal of Geophysical Research**, **90**, 2391-2408.

Avila A., Alarcon M., Queralt I. (1998). The Chemical Composition of Dust Transported in Red Rains-Its Contribution to the Biochemical Cycle of a Holm Oak Forest in Catolina (Spain), **Atmospheric Environment, 32, 2,** 179-191.

Bailey P.D., Gough C.A., Millock K. And Chadwick M. J. (1996). Prospects for the Joint Implementation of Sulphur Emission Reductions in Europe, **Energy Policy**, **24 (6)**, 507-516.

Bardouki H., Liakakou H., Economou C., Sciare J., Smolik J., Ždimal V., Eleftheriadis K., Lazaridis M., dye C., Mihalopoulos N. (2003). Chemical Composition of Size-Resolved Atmospheric Aerosols in the Eastern Mediterranean During Summer and Winter, **Atmospheric Environment, 37**, 195-208.

Barrett K., Schaug J., Bartonova A., Semb A., Hjellbrekke A., Hanssen J.E. (2000). A Contribution from CCC to the Reevaluation of the Observed Trends in Sulphur and Nitrogen in Europe 1978–1998, EMEP/CCC-Report 7/2000, EMEP Chemical Co-ordinating Centre.

Bergametti G., Dutot A. L., Buart-Menard P., Losno R., Remoudaki E. (1989). Seasonal Variability of Elemental Composition of Atmospheric

Aerosol Particles over the Northwestern Mediterranean. **Tellus, 41b**, 353-361.

Berge E., Bartnicki J., Olendrzynski K., Tsyro S. G. (1999) Long-term trends in emissions and transboundary transport of acidifying air pollution in Europe, **Journal of Environmental Management**, **57**, **1**, 31-50.

Chabas A., Lefévre R. A. (2000). Chemistry and microscopy of atmospheric particulates at Delos (Cyclades-Greece), **Atmospheric Environment, 34**, 225-238.

Charron A., Plaisance H., Sauvage S., Coddeville P., Galloo J., Guillermo R. (2000). A Study of the Source-receptor Relationships Influencing the Acidity of Precipitation Collected at a Rural Site in France, **Atmospheric Environment**, **34**, 3665-3674.

Charron A., Harrison R. M. (2003). Primary Particle Formation From Vehicle Emissions During Exhaust Dilution in the Roadside Atmosphere, **Atmospheric Environment**, **37**, 4108-4119.

Cheng M.D., Hopke P.K., Barrie L., Rippe A., Olson M., Landsberger S. (1993). Qualitative Determination of Source Regions of Aerosol in Canadian High Arctic, **Environmental Science & Technology**, **27, 10**, 2063-2071.

Cheng M.D., Gao N., Hopke P.K. (1996). Source Apportionment Study of Nitrogen Species Measured in Southern California in 1987 **Journal of Environmental Engineerıng-Asce, 122**, **3**, 183-190.

Cheng M.D., Lin C.J. (2001). Receptor Modeling for Smoke of 1998 Biomass Burning in Central America, **Journal of Geophysical Research-Atmospheres, 106 (D19),** 22871-22886.

Chester R., Baxter G.G., Behairy A.K.A., Connor K., Cross D., Elderfield H., Pandgam R.C. (1977). Soil-sized Eolian Dusts from the Lower Tropoposphere of the Eastern Mediterranean, **Marine Geology**, **32**, 141-154.

Chester R., Sharples E. J., Sanders G.S. (1984). Saharan Dust Incursion over the Tyrrhenian Sea, **Atmospheric Environment**, **18**, 929-935.

Chow J.C., Watson J.G., Houck J.E., Pritchett L.C., Rogers C.F., Frazier C.A., Egami R.T., Ball B.M. (1994). A Laboratory Resuspension Chamber to Measure Fugitive Dust Size Distributions and Chemical Compositions, **Atmospheric Environment, 28, 21**, 3463–3481.

Cipriano, R.J., Blanchard, D.C., Hogan, A.W., Lala, G.G. (1983). On the Production of Aitken Nuclei from Breaking Waves and Their Role in the Atmosphere. **Journal of the Atmospheric Sciences, 40**, 469–479.

Çetin B. (2002). Elemental Tracers for Saharan Dust, M. Sc. Thesis, Department of Environmental Engineering, Middle East Technical University, Ankara.

Danatalos D., Glavas S., Kambezidis H. (1995). Atmospheric Nitric Acid Concentrations in a Mediterranean Site, Patras, Greece, **Atmospheric Environment**, **29**, **No.15**, 1849-1852.

Danatalos D., Glavas S. (1999). Gas Phase Nitric Acid, Ammonia and Related Particulate Matter at a Mediterranean Coastal Site, Patras, Greece, **Atmospheric Environment**, **33**, 3417-3425.

Despiau S., Cougnenc S., Resch F. (1995). Concentrations and Size Distributions of Aerosol Particles in Coastal Zone, **Journal of Aerosol Science, 27, 3**, 403-415.

Duce R.A., Merrill J.T., Atlas E.L., Buat-Menard P., Hicks B.B., Miller J.M., Prospero J.M., Arimoto R., Church T.M., Ellis W., Galloway J.N., Hansen L., Jickells T.D., Knap A.H., Reinhardt K.H., Schneider B., Soudine A., Tokos J.J., Tsunogai S., Wollast R., Zhou M. (1991) The Atmospheric Input of Trace Species to the World Ocean, **Global Biogeochemical Cycles, 5,** 193–259.

Dulac, F., Buart-Menard P., Arnold M., Ezat U., Martin D. (1987). Atmospheric Input of Trace Metals to the Western Mediterranean Sea: 1. Factors Controlling the Variability of Atmospheric Concentrations, **Journal of Geophysical Research**., **92**, 8437-8453.

Duyzer J. (1994). Dry Deposition of Ammonia and Ammonium Aerosols over Heatland, **Journal of Geophysical Research**, **99**, **D9**, 18757-18763.

Elsom D. (1987). Atmosperic Pollution - Causes, Effects and Control Policies, Basil Blackwell Inc.

EMEP Manual for Sampling and Chemical Analysis, NILU CCC 1/95,1996. Norweigan Institude for Air Research, Norway.

Erdman, L.K., Sofiev, M.A., Subbotin, S.R., Dedkova, I.S., Afinogenova, O.G., Cheshukina, T.V., Pavlovskaya, L., Soudine, A. (1994). Assessment of Airborne Pollution of the Mediterranean Sea by Sulphur and Nitrogen Compounds and Heavy Metals in 1991. MAP Technical Report Series No. 85, UNEP/WMO, Athens.

Erduran M.S.,. Tuncel S.G. (2001). Gaseous and Particulate Air Pollutants in the Northeastern Mediterranean Coast, **The Science of The Total Environment, 281, 1-3,** 205-215.

Faber E., Moran C., Garzon G., Poggenburg J., Teschner M. (2003). Continuous Gas Monitoring Fumarolic Gases at the Galeras Volcano, Colombia; First Evidence, **Journal of Volcanology and Geothermal Research, 125,** 13–23.

Finlayson-Pitts B. J., Ezell M. J., Pitts Jr. J. N. (1989). **Nature**, **337**, 241.

Gangoiti G., Millan M.M., Salvador R., Mantilla E. (2001) Long-range Transport and Re-circulation of Pollutants in the Western Mediterranean During the Project Regional Cycles of Air Pollution in the West-Central Mediterranean Area, **Atmospheric Environment**, **35**, **36**, 6267-6276.

Ganor E., Levin Z., Van Grieken R. (1997). Composition of Individual Aerosol Particles Above the Israelian Mediterranean Coast During the Summer Time, **Atmospheric Environment, 32, 9,** 1631-1642.

Ganor E., Foner H. A., Bingemer H. G., Udisti R., Setter I. (2000). Biogenic Sulfate Generation in the Mediterranean Sea and Its Contribution to Sulfate Anomaly in the Aerosol Over Israel and the Eastern Mediterranean, **Atmospheric Environment**, **34**, 3453-3462.

Gao N., Cheng M.D., Hopke P.K. (1993). Potential Source Contribution Function Analysis and Source Apportionment of Sulfur Species Measured At Rubidoux, Ca During The Southern California Air-Quality Study, 1987, **Analytica Chimica Acta**, **77, 2**, 369-380.

Gao N., Hopke P.K., Reid N.W. (1996). Possible Sources for Some Trace Elements Found in Airborne Particles and Precipitation in Dorset, Ontario **Journal of the Air & Waste Management Association, 46**, **11**, 1035-1047.

Gebhart K.A., Malm W.C. (1994). Examination of the Effects of Sulfate Acidity and Relative Humidity on Light Scattering at Shenandoah National Park, **Atmospheric Environment, 28**, 841-849.

Glavas S., Moschonas N. (2002). Origin of Observed Acidic-Alkaline Rains in a Wet-Only Precipitation Study in a Mediterranean Coastal Site, Patras, Greece, **Atmospheric Environment**, **36**, **19**, 3089-3099.

Gordon, G. E. (1980). Receptor Models. **Environmental Science and Technology**, **14**, 972.

Grousset F. E., Quetel C. R., Thomas B., Donald D. F. X., Lambert C. E., Guillard F., Monaco A. (1995). Anthropogenic vs. Lithogenic Origins of Trace Elements (As, Cd, Pb, Rb, Sb, Sc, Sn, Zn) in Water Column

Particles: Northwestern Mediterranean Sea, **Marine Chemistry, 48**, 291-310.

Guerzoni S., Molinaroli E., Chester R. (1996). Saharan Dust Inputs to the Western Mediterranean Sea: Depositional Patterns, Geochemistry and Sedimentological Implications, **Deep-Sea Research II**, **44**, **No. 3-4**, 654-657.

Guerzoni S., Chester R., Dulac F., Herut B., Loÿe-Pilot M., Measures C., Migon C., Molinaroli E., Moulin C., Rossini P., Saydam C., Ziveri P. (1999). The Role of the Atmospheric Deposition in the Biochemistry of the Mediterranean Sea", **Progress in Oceanography, 44,** 147-190.

Guieu C., Chester R., Nimmo M., Martin J. M., Guerzoni S., Nicolas E., Mateu J., Keyse S. (1996). Atmospheric Input of Dissolved and Particulate Metals to the Northwest Mediterranean, **Deep-Sea Research II, 44, No. 3-4**, 655-674.

Güllü, G. (1996). Long Range Transport of Aerosols, Ph D. Thesis, Department of Environmental Engineering, Middle East Technical University, Ankara.

Güllü G. H., Ölmez İ., Tuncel G. (2000). Temporal Variability of Atmospheric Trace Element Concentrations over the Eastern Mediterranean Sea, **Spectromica Acta Part B 55**, 1135-1150.

Hacisalihlioğlu, G., Eliyakut, F., Ölmez, İ., Balkas, T. I., and Tuncel, G. (1992). Chemical Composition of Particles in the Black Sea Atmosphere, **Atmospheric Environment**, **26A/17**, 3207-3218.

Havránek V., Maenhaut W., Ducastel G. Hanssen J. E. (1996). Mass Size Distributions for Atmospheric Trace Elements at the Zeppelin Background Station in Ny Ålesund, Spitsbergen, **Nuclear Instruments and Methods in Physics Research Section B: Beam Interactions with Materials and Atoms, 109-110,** 465-470

Heidam N.Z. (1979). The Components of the Arctic Aerosol, **Atmospheric Environment, 18,** 329-343.

Hernandez E., Rua A., Mendez R., Gimeno L. (1996). Finding Regions of Influence on SO_2 and SO_4^{2-} Daily Concentration Measurements at Four Sites in Spain **Annales Geophysicae-Atmospheres Hydrospheres and Space Sciences, 14**, **8**, 853-863.

Herut B., Nimmo M., Medway A., Chester R., krom M. D. (2001). Dry Atmospheric Inputs of Trace Metals at the Mediterranean Coast of Israel (SE Mediterranean): Sources and Fluxes, **Atmospheric Environment, 35**, 803-813.

Hjellbrekke A.G., Data Report 1999, Acidifying and Eutrophying Compounds: Part 2: Monthly and Seasonal Summaries, EMEP/CCC-Report 2/2001.

Hjellbrekke A.G., Data Report 2001, Acidifying and Eutrophying Compounds EMEP/CCC-Report 3/2003.

Holsen T.M., Noll K.E., Fang G.C., Dry Deposition and Particle-Size Distributions Measured During The Lake-Michigan Urban Air Toxics Study, **Environ. Sci. Technol., 27, 7,** 1327-1333.

Hopke P.K. (1985). Receptor Modeling in Environmental Chemistry, 155-197, John Wley, New York.

Hopke P.K., Gao N., Cheng M.D. (1993) Combining Chemical and Meteorological Data to Infer Source Areas of Airborne Pollutants, **Chemometrics and Intelligent Laboratory Systems**, **19, 2**, 187-199.

Hopke P.K., Barrie L.A., Li S.M., Cheng M.D., Li C., Xie Y. (1995). Possible Sources and Preferred Pathways for Biogenic and Non-Sea-Salt Sulfur for the High Arctic, **Journal of Geophysical Research-Atmospheres, 100**, **D8**, 16595-16603.

Kallos G., Kotroni V., Lagouvardos K., Papadopoulos A. (1998) On the Long-Range Transport of Air Pollutants from Europe to Africa, **Geophysical Research Letters, 25**, **5**, 619-622.

Karakaş S. (1995). Determination of Major Ions in Uludağ National Park, M. Sc. Thesis, Department of Environmental Engineering, Middle East Technical University, Ankara.

Karakaş S.Y., Tuncel S. G. (1997). Chemical Characteristics of Atmospheric Aerosols in a Rural Site of Northwestern Anatolia, **Atmospheric Environment, 31, 18,** 2933-2943.

Karakaş D. (1999). Determination of the European Contribution on the Aerosol Composition İN the Black Sea Basin and Investigation of Transport Mechanisms, M. Sc. Thesis, Department of Environmental Engineering, Middle East Technical University, Ankara.

Kim K.H., Choi G.H., Kang C.H., Lee J.H., Kim J.Y., Youn Y.H., Lee S.R. (1999). The Chemical Composition of Fine and Coarse Particles in Relation with the Asian Dust Events, **Atmospheric Environment, 37**, **6**, 735-765.

Kouvakaris G., Mihalopoulos N. (2002). Seasonal Variation of Dimethylsulphide in the Gas Phase and of Methanesulphate and Non-Sea-Salt Sulphate in the Aerosol Phase in the Eastern Mediterranean Atmosphere, **Atmospheric Environment**, **36**, 929-938.

Kouvarakis G., Bardouki H.,Mihalopoulos N. (2002). Sulfur Budget above the Eastern Mediterranean: Relative Contribution of Anthropogenic and Biogenic Sources. **Tellus**, **54B**, 201-212.

Krupa S. V. (2003). Effects of Atmospheric Ammonia (NH_3) on Terrestrial Vegetation: A Review, **Environmental Pollution,124, 2,** 179-221.

Kubilay, N., Saydam, A. C. (1995). Trace Elements in Atmospheric Particulates Over the Eastern Mediterranean; Concentrations, Sources, and Temporal Variability", **Atmospheric Environment**, **29**, **No 17**, 2289-2300.

Kubilay N., Koçak M., Çokacar T., Oğuz T. (2002). Influence of Black Sea and local Biogenic Activity in the Eastern Mediterranean Atmosphere, **Global Biochemical Cycles, 16, No. 4**, 1079.

Kuloglu, E., Oztas N.B., Tuncel G. (2001). Size Separation and Dry Deposition Fluxes of Particles and the Size Dependent Solubility of Metals in the Eastern Mediterranean Basin, Second International Symposium on Air Quality Management at urban, Regional and Global Scales, Proceedings, Istanbul , Turkey, 448-455.

Kuloglu, E. (1997). Size Separation and Dry Deposition Fluxes of Particles in the Eastern Mediterranean Basin, M.Sc. Thesis, Middle East Technical University, Ankara, Turkey.

Latha K.M., Badarinath K.V.S. (2004). Studies on Satellite and Ground-Based Measurements of Aerosols Over Urban Environment**, Journal of Quantitative Spectroscopy and Radiative Transfer, 84, 2,** 207-213.

Lee D.S., Dollard G.J., Derwent R.G., Pepler S. (1999). Observations on Gaseous And Aerosols Components of the Atmosphere and Their Relationships, **Water Air and Soil Pollution**, **113**, **1-4**, 175-202.

Lin C.J., Cheng M.D., Schroeder W.H. (2001). Transport Patterns and Potential Sources of total Gaseous Mercury Measured in Canadian High Arctic in 1995, **Atmospheric Environment, 35, 6,** 1141-1154.

Liu W., Hopke P. K., Han Y. J., Yi S. M., Holsen T. M., Cybart S., Kozlowski K., Milligan M. (2003). Application of Receptor Modeling to Atmospheric Constituents at Potsdam and Stockton, NY, **Atmospheric Environment, 37 (36),** 4997-5007.

Lucey D., Hadjiiski L., Hopke P. K., Scudlark J.R. , Church T. (2001). Identification of Sources of Pollutants in Precipitation Measured at the mid-Atlantic US Coast Using Potential Source Contribution Function (PSCF), **Atmospheric Environment, 35 (23)**, 3979-3986.

Lupu A. Maenhaut W. (2002). Application and Comparison of Two Statistical Trajectory Techniques for Identification of Source Regions of Atmospheric Aerosol Species**, Atmospheric Environment, 36,Issues 36-37**, 5607-5618.

Luria M., Peleg M., Sharf G., Tov-Alper D. S., Spitz N., Ami Y. B., Gawaii Z., Lifschitz B., Yitzchaki A., Seter I. (1996). Atmospheric Sulfur Over the East Mediterranean Region. **Journal of Geophysical Research 101**, **20**, 25917-25930.

Malm W.C. Johnson C.E., Bresch J.F. (1986). Application of Principal Component Analysis for Purposes of Identifying Sourc-Receptor Relationships. In Receptor Methods for Source Apportionment (Edited by T.G. Pace), Publication TR-5. Air Pollution Control Association, Pittsburg, PA.

Martin M., Plaza J., Andres M.D., Bezares J.C., Millan M.M. (1991) Comparative-Study of Seasonal Air Pollutant Behavior in a Mediterranean Coastal Site - Castellon (Spain), **Atmospheric Environment Part A-General Topics**, **25**, **8**, 1523-1535.

Mason, B. (1966). Principles of Geochemistry, 3rd ed. Wiley, New York.

Mather T.A., Allen A.G., Davison B.M., Pyle D.M., Oppenheimer C., McGonigle A.J.S. (2004). Nitric Acid from Volcanoes, **Earth and Planetary Science Letters**, **218**, 17-30.

Matvev V., Dayan U., Tass I., Peleg M. (2002). Atmospheric Sulfur Flux Rates to and from Israel, **The Science of the Total Environment, 291**, 143-154.

Meagher J. F., Stockburger L., Bailey E. M., Huff O. (1978). The Oxidation of Sulfur Dioxide to Sulfate Aerosols in the Plume of a Coal-Fired Power Plant, **Atmospheric Environment (1967), 12, 11,** 2197-2203.

Migon C., Alleman L., Leblond N., Nicolas E., Evolution of Atmospheric Lead over the Northwestern Mediterranean Between 1986 and 1992, **Atmospheric Environment Part A-General Topics 1993, 27, Iss 14**, 2161-2167.

Migon C., Journel B., Nicolas E. (1996). Measurement of Trace Metal Wet, Dry and Total Atmospheric Fluxes over the Ligurian Sea, **Atmospheric Environment**, **31**, **No. 6**, 889-896.

Migon C., Gentilli B., Journel B. (2000). Statistical Analysis of the Concentrations of Twelve Metals in the Ligurian Atmospheric Aerosol, **Oceanologica Acta, 23, No. 1**, 37-45.

Migon C., Sandroni V., Béthoux J.P. (2001). Atmospheric Input of Anthropogenic Phosphorus to the Northwest Mediterranean under Oligotrophic Conditios, **Marine Environment Research, 52**, 413-426.

Millan M. M., Artisano B., Alonso L., Navazo M., Castro M. (1991) The Effect of Meso-Scale Flows on Regional and Long Range Transport in the Western Mediterranean, **Atmospheric Environment**, **25A**, 949-963.

Miller M.S., Friedlander S.K., Hidy G.M. (1972). A Chemical Element Balance for the Pasadena Aerosol, **Journal of Colloid Interface Science**, **39**, 165-176.

Miller, J. M., Moody, J. L., Harris, J. M., Gaudry, A. (1993). A 10-year Trajectory Flow Climatology for Amsterdam Island, 1980-1989. **Atmospheric Environment**, **27**, 1909-1916.

Molinaroli E., Pistolato M., Rampazzo G., Gurzoni S. (1999). Geochemistry of Natural and Anthropogenic Fall-Out (Aerosol and Precipitation) Collected from the NW Mediterranean: Two Different Multivariate Statistical Approaches, **Applied Chemistry, 14**, 423-432.

Narcisi B. (2000). Late Quaternary Eolian Deposition in Central Italy, **Quaternary Research, 54**, 246-252.

Okay C., Akkoyunlu B. O., Tayanç M. (2002). Composition of Wet Deposition in Kaynarca, Turkey, **Environmental Pollution**, **118**, 401-410.

Olivier J. G. J., Bouwman A. F., Van der Hoek K. W., Berdowski J. J. M. (1998). Global Air Emission Inventories for Anthropogenic Sources of NO_x, NH_3 and N_2O in 1990, **Environmental Pollution**, **102**, **S1**, 135-148.

Paatero P. (1998). User's Guide for Positive Matrix Factorization Programs PMF2 and PMF3, Part 1: Tutorial

Paatero P. (1999). The Multilinear Engine – a Table-driven Least Squares Program for Solving Multilinear Problems, Including the n-way Parallel Factor Analysis Model, **Journal of Computational and Graphical Statistics**, **8**, **No. 4**, 854-888.

Paatero P. (2002). User's Guide for Positive Matrix Factorization Programs PMF2 and PMF3, Part 2: Reference

Paatero, P., Tapper, U. (1993). Analysis of Different Models of Factor Analysis as Least Squares Fit Problem. **Chemometrics and Intelligent Laboratory Systems**, **18**, 183-194.

Paatero, P., Tapper, U. (1994). Positive Matrix Factorization: a non-negative factor model with optimal utilization of error estimates of data values. **Environmetrics**, **5**, 111-126.

Pakkanen T.A. (1996). Study of Formation of Coarse Particle Nitrate Aerosol, **Atmospheric Environment, 30, 14,** 2475-2482.

Plaisance H., Coddeville P., Roussel L., Guillermo R. (1996). A Qualitative Determination of the Source Locations of Precipitation Constituents in Morvan, France, E**nvironmental Technology,17**, **9**, 977-986.

Plaisance H., Galloo J.C., Guillermo R. (1997). Source Identification and Variation in the Chemical Composition of Precipitation at Two Rural Sites in France, **Science of the Total Environment, 206**, **1**, 79-93.

Polissar A.V., Hopke P. K., Poirot R.L. (2001). Atmospheric Aerosol over Vermont: Chemical Composition and Sources, **Environmental Science & Technology, 35, 23,** 4604-4621.

Quin, Y., Oduyemi, K., Chan, L. Y. (2002). Comparative testing of PMF and CFA models. **Chemometrics and Intelligent Laboratory Systems**, **61**, 75-87.

Ramadan Z., Eickhout B., Song X., Buydens L.M.C., Hopke P.K. (2003). Comparison of Positive Matrix Factorization and Multilinear Engine for the Source Apportionment of Particulate Pollutants, **Chemometrics and Intellicent Laboratory Sysytems**, **66**, 15-28.

Ranmar D.O., Matveev V., Dayan U., Peleg M., Kaplan J., Gertler A.W., Luria M., Kallos G., Katsafados P., Mahrer Y. (2002) Impact of Coastal Transportation Emissions on Inland Air Pollution over Israel: Utilizing Numerical Simulations, Airborne Measurements, and Synoptic Analyses, **Journal Of Geophysical Research-Atmospheres**, **107**, **17**, art. no. 4331.

Remoudaki E., Bergametti G., Losno R. (1991). On the Dynamic of The Atmospheric Input of Copper and Manganese into the Western Mediterranean Sea, **Atmospheric Environment**, **25A**, **No. 3** / **4**, 733-744.

Rojas C.M., Van Grieken R.E. (1992). Electron Microscope Characterization of Individual Aerosol Particles Collected by Aircraft Above the Southern Bight of the North Sea, **Atmospheric Environment, 26A,** 1231-1237.

Rojas M.C., Injuk J., Grieken E.V., Laane R.W. (1993). Dry and Wet Deposition Fluxes of Cd, Cu, Pb and Zn into the Southern Bight of the North Sea, **Atmospheric Environment**, **27**, 251-259.

Sandroni-V Migon-C. (1997). Significance of Trace-Metal Medium-Range Transport in the Western Mediterranean, **Science of the Total Environment, 196, Iss 1**, 83-89

Sanz M. J., Carratalá A., Gimeno C., Millán M. M. (2002). Atmospheric Nitrogen Deposition on the East Coast of Spain: Relevance of Dry Deposition in Semi-arid Mediterranean Region, **Environmental Pollution, 118**, 259-272.

Seibert, P., Kromp-Kolb, H., Baltensperger, U., Jost, D. T. and Schwikowski, M. (1994). Trajectory Analysis of High-Alpine Air Pollution Data In: Gryning, S.-E. and Millan, M.M. Editors, Air Pollution Modelling and its Application X Plenum Press, New York, pp. 595–596

Singels R., Sutton M. A., Weston K. J. (1998). A Multi-Layer Model to Describe the Atmospheric Transport and Deposition of Ammonia in Great Britain, **Atmospheric Environment, 32, 3**, 393-399.

Spokes, L.J., Yeatman S.G., Cornell S.E., Jickells T.D. (2000). Nitrogen Deposition to the Eastern Atlantic Ocean. The importance of South-Easterly Flow, **Tellus*,*52B**, 37-49.

Stohl, A. (1996). Trajectory Statistics—A New Method to Establish Source–receptor Relationships of Air Pollutants and its Application to the Transport of Particulate Sulfate in Europe. **Atmospheric Environment, 30**, 579–587.

Takahashi A., Sato K., Wakamatsu T., Fujita S. (2001). Atmospheric Deposition of Acidifying Components to a Japanese Cedar Forest, **Water, Air, and Soil Pollution, 130**, 571-576.

Tassi F., Vaselli O., Capaccioni B., Macias J. L., Nencetti A., Montegrossi G., Magro G (2003). Chemical Composition of Fumarolic Gases and Spring Discharges from El Chichòn Volcano, Mexico: Causes And Implications Of The Changes Detected Over The Period 1998–2000, **Journal of Volcanology and Geothermal Research, 123**, **Iss.1-2**, 105-121.

Taylor, R. (1972) Abundance of Chemical Elements in the Continental Crust: A new Table, **Geochim. Cosmochim. Acta, 28,** 1273.

Thurston, G. D., Spengler J. D. (1985). A Quantitative Assessment of Source Contributions to Inhalable Particulate Matter Pollution in Metropolitan Boston. **Atmospheric Environment**, **19**, 9-25.

Tohno S., Takano T., Kasahara M. (2001). Simultaneous Determination of Gas and Particulate Dry Deposition onto Conditioned Surrogate Surfaces, **Water, Air, and Soil Pollution, 130**, 535-540.

Tov D.A., Peleg M., Matveev V., Mahrer Y., Seter I., Luria M. (1997) Recirculation of Polluted Air Masses over The East Mediterranean Coast, Atmospheric Environment, 31, 10, 1441-1448.

Tuncer B., Bayar B., Yesilyurt C., Tuncel G. (2001). Ionic Composition of Precipitation at the Central Anatolia, **Atmospheric Environment, 35**, 5989-6002.

Varrica D., Aiuppa A., Dongarra G. (2000). Volcanic and Anthropogenic Contribution to Heavy Metal Content in Lichens from Mt. Etna and Vulcano Island (Sicily), **Environ. Poll***.,* **108,** 153–162.

Vega E., Reyes E., Sánchez G., Ortiz E., Ruiz M., Chow J., Watson J., Edgerton S. (2002). Basic statistics of $PM_{2.5}$ and PM_{10} in the atmosphere of Mexico City**, The Science of The Total Environment, 287, Iss. 3,** 167-176.

Vinogradova A.A. (1996). Elemental Composition of Atmospheric Aerosol of the Eastern Arctic Regions, **Izvestiya Akademii Nauk Fizika Atmosfery I**, **32**, **Iss 4**, 479-486.

Vitousek P.M., Aber J.D., Howarth R.W., Likens G.E., Matson P.A., Schindler D.W., Schlesinger W.H., Tilman D.G. (1997). Human Alteration of the Global Nitrogen Cycle: Sources and Consequences, **Ecological Applications, 7,** 737–750.

Waldman J.M., Liang C.S.K., Kitto A., Kourtakis P., Alien G., Burton R., Wilson W.E. (1993). Exposures to acid aerosols and Gases in Schools and Youth Centers of Philadelphia, Measurements of Toxic and Related Air Pollutants, AWMA, Pittsburg, 727-732.

Wanger A., Peleg M., Sharf G., Mahrer Y., Dayan U., Kallos G., Kotroni V., Lagouvardos K., Varinou M., Papadopoulos A., Luria M. (2000) Some Observational and Modeling Evidence of Long-Range Transport of Air Pollutants from Europe Toward the Israeli Coast, **Journal of Geophysical Research-Atmospheres**, **105**, **6**, 7177-7186.

Wedephol K. H. (1969). Handbook of Geochemistry, Springer-Verlag, Berlin.

White W.H. (1990). The Components of Atmospheric Light Extinction: A Survey of Ground-level Budgets, **Atmospheric Environment**, **24A**, 2673-2679.

Yin D., Jiang W., Roth H., Giroux E. (2004). Improvement of Biogenic Emissions Estimation in the Canadian Lower Fraser Valley and Its Impact on Particulate Matter Modeling Results, **Atmospheric Environment**, **38**, 507-521.

Zeng Y.S., Hopke P.K. (1994). Comparison of the Source Locations and Seasonal Patterns for Acidic Species in Precipiitation and Ambient Particles in Southern Ontorio, Canada, **Science of the Total Environment, 143, 2-3**, 245-260.

Zhuang H., Chan C.K., Fang M. Wexler A.S. (1999) Size Distributions of Particulate Sulfate, Nitrate, and Ammonium at a Coastal Site in Hong Kong, **Atmospheric Environment, 33, 6**, 843-853.

APPENDIX A

MATERIALS AND METHODS

1. Sampling Site

Site selection is an important step in establishing sampling station. As Çubuk II station is an EMEP station site selection is done according to the criteria developed in the EMEP program. Site selection for all of the approximately 100 stations in the EMEP program were based on the same criteria.

According to the general requirements, sampling site must be at least 50 km away from the large pollution sources (towns, power plants, major motorways), 100 m away from the small scale domestic heating with coal, fuel oil or wood, 100 m away from minor roads, 500 m away from the main roads, 2 km away from the application of manure, stabling of animals, and 500 m away from the grazing by domestic animals on fertilized pasture with taking into consideration of the meteorological and topographic conditions, and quantity of emissions from the sources. Sampling site must also be representative of a larger area and the size of this area depends on the spatial resolution in the concentration and deposition fields and the variability of the air and precipitation quality.

By taking into account the above requirements a German Technical Committee, a consulting group from the Turkish Meteorological Institute and the Ministry of Environment worked in corporation in the site selection process. Consequently, the station is established in Central

Anatolia region of Turkey at approximately 50 km away from the city of Ankara and 12 km away from Çubuk town (33.10 longitude east of Greenwich and 40.10 latitude north of Equator).

Sampling station is a rectangular cabin with a surface area of 12 m^2. It consists of as air intake, a high volume sampler, a precipitation meter and a stack filter unit which are placed on a gravel platform with a height of 2.50 m, 2.00 m, 1.60 m, and 2.00 m, respectively above the ground level. In the station, meteorological parameters are also measured for inter-comparison purposes. The general appearance of the station is depicted in Figure A.1.

The station is established in 1992 and it collects air and precipitation samples since 1993. In this study, the aerosol and gaseous pollutants samples collected between 10 February, 1993 and 31 December, 2000 were interpreted.

Figure A.1. The site view of the Çubuk station

2. Sampling Procedures

Gaseous pollutants, namely, HNO_3, NH_3, SO_2 and NO_2 were collected using a filterpack. In this method samples were collected onto cellulose filters impregnated with solutions, which specifically adsorbs one of these gases. These impregnated filters are placed in series behind an inert Teflon filter which removes particles.

In this study, KOH impregnated filter was used to collect HNO_3 and SO_2 from atmosphere. Similarly filters impregnated with citric acid and NaI were used to collect NH_3 and NO_2, respectively.

2.1. Preparation of Filters

Cellulose filters may contain small amount of impurities which have to be removed from the filters before sampling of pollutants. The cleaning process may be omitted if the filter blanks from a new batch of filters are lower than the requirements given in Table A.1, otherwise filters are cleaned by passing through a cleaning solution.

Table A.1. Recommended Requirements

Parameter	Recommended Requirements
SO_4^{2-}	Better than 0.01 µg S/ml
NO_3^-	" " 0.01 µg N/ml
NH_4^+	" " 0.01 µg N/ml

Following the cleaning, filters which will be used for collection of NH_3, HNO_3 and SO_2 samples are rinsed with 20 liters of water. Then 1.0 M KOH and 10% glycerol in methanol and 1.0 M citric acid impregnation solutions are dripped on the filters. Impregnated filters are dried in the air for half an hour and put into plastic bags. The bags for acid impregnated and alkaline impregnated filters are stored in different desiccators which have citric acid or KOH at the bottom, respectively.

2.2. Sample collection

2.2.1. Collection of gaseous parameters

The impregnated filters were placed in series in a “stack filter unit”. Stack filter unit consists of an air intake, a filter pack, a pump and a gas meter which are connected in series along the sampling line. Pollutants enter the sampling line via cylindrical 15 cm wide and 25 cm high air intake. This air intake reduce the sampling efficiency for particles larger than 10 µm in diameter, such as soil dust particles, large sea spray droplets, large pollen, and fog droplets. The filter pack is connected to the sampling line with an airtight seal. It is placed outdoor only sheltered by the air intake. Figure A.2 shows filter pack with two impregnated filters. In this study, filter pack with three impregnated filters (two alkaline and one acid impregnated) were used to collect NH_3, HNO_3 and SO_2 samples.

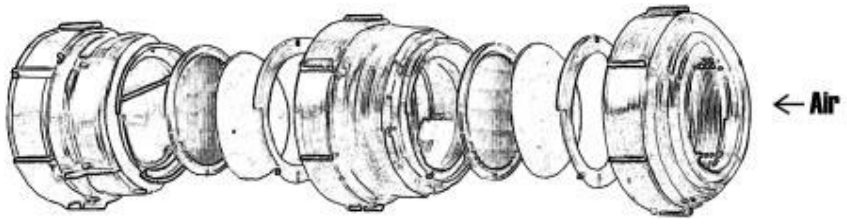

Figure A.2. Filter pack with two impregnated filters

Air volume, sampling rate, and flow velocity through the filters are respectively 20 m^3, 15 l/min., and 15 cm/s. Sampling volume is recorded dry bellows-type gas meter. The pump used is a membrane pump that have capacity to allow 15 l/min. against a pressure difference of 10-20 kPa (0.1 atm.), which is the typical pressure drop across two filters.

Sampling system for NO_2 collection with iodine absorption method includes an air intake (inverted funnel), prefilters, an absorption system, a gas meter and a pump. Ambient air with a flow rate of about 0.5 L min^{-1} is drawn through an air intake and a glass filter impregnated with sodium iodide (NaI) and sodium hydroxide (NaOH). Prefilters inert to NO_2 are placed in front of the absorption system in order to remove particulate matter and are replaced every week. Absorption system is composed of a 4 mm thick sintered glass filter 25 mm in diameter with a porosity of 40–60 μm enclosed in a glass bulb as shown in Figure 2.3. Nitrogen dioxide is absorbed in the filter and the iodide reduces NO_2 to nitrite (NO_2^-).

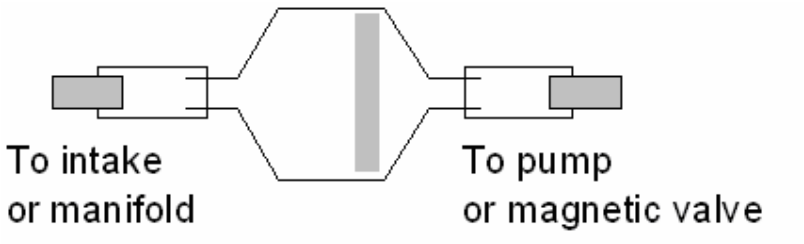

Figure A.3. Sintered glass filter in a glass bulb

Sampling period is 24 hr for all samples. Filter packs and teflon filters are transported to the sampling site in plastic bags. In order to prevent any contamination, filter packs are mounted and dismounted in the laboratory only and air tight protection covers are mounted in both ends of the filter pack. Each filter pack is tagged with the site code in the laboratory before it is sent to the sampling site. Exposed filter packs abd teflon filters are transferred to the laboratory in a collection vessel. Exposed filter packs are opened in the laboratory and both exposed impregnated filters and teflon filters are kept in the refrigerator and they are kept away from sun light till the analysis takes place.

2.2.2. Collection of atmospheric particles

Atmospheric particle (aerosol) samples were collected using a Digitel, model DHA-80 Hi-Volume Sampler. PTFE (Teflon) filters having diameters 47mm and pore size 2 um were used for sampling.

As in the filterpacks**,** sampling period is 24 hr for particles. Filters are placed every Monday and they are removed from the samplers every Monday, Wednesday, and Thursday by the technicians. On Mondays, "Weekly Field Journal" is filled out to control emissions around the site and at each visit "Daily Field Journal" is filled out to record filter codes, starting and stopping time of sampling.

Blank filters are placed to the samplers every Monday in order to record any contamination of filters during the transport to and from the site and during the days that filters waited at the site.

3. Sample Handling

3.1. Preparation of Samples to Analysis

The impregnated cellulose filters requires careful treatment not to loosen fibres, which will cause problems during the analysis. Alkaline impregnated filters are extracted with hydrogen peroxide extraction solution and acid impregnated filters are extracted with nitric acid extraction solution the day they are removed from the filter packs. Before analysis it is necessary to wait a few hours to allow any fibres in the solution to settle.

NaI impregnated filters are extracted with 0.001 M solution of triethanolamine in deionized water. Extraction solution is added to glass bulb and the bulb is shaken for 15 min. for complete extraction.

Cellulose filters used in high volume samplers are cut into smaller pieces before extraction. These pieces are then extracted with

concentrated nitric acid in a Teflon bomb. The bomb is kept at 150^{o}C for 6 hours and then cooled to room temperature before analysis.

3.2. Analysis of Samples

Samples collected at Çubuk II station are measured by analytical techniques given in Table A.2 in the laboratories of Ministry of Health Refik Saydam Hygiene Center.

Table A.2. Analytical Techniques used in the determination of measured species

Parameter Measured	Analytical Tecnique
SO_2, SO_4^{2-}, NO_3^-, NH_3, HNO3	Dionex/DX 100 Ion Chromotograpy
NO_2	Spectrophotometric nitrite determination
$NH_3 + NH_4^+$	Spectrophotometric Indophenol Blue method
Pb, Cd, V, Mg, Ca, K	Perkin Emler 1100 B Atomic Absorbtion Spectroscopy coupled with HGA 700 Atomization Unit

3.2.1. Determination of Sulfur Dioxide, Sulfate, Nitrate, Ammonium and Nitric Acid by Ion Chromotography

A small volume of the sample, typically less than 0.5 ml, is introduced into the injection system of an ion chromatograph. The sample is mixed with an eluent and pumped through a guard column, a separation column, a suppressor device and a detector, normally a conductivity cell.

The separation column is an ion exchange column which has the ability to separate the ions of interest. The separation column is often preceded by a shorter guard column of the same substrate as in the

separation column to protect the separation column from overloading and particles. Different types of separation columns, eluents and suppression devices have to be used for anions and cations respectively. Each ion is identified by its retention time within the separation column. The sample ions are detected in the detection cell, and the signals produced (chromatograms) displayed on a strip chart recorder or a PC equipped with the necessary software for measurement of peak height or area.

The ion chromatograph is calibrated with standard solutions containing known concentrations of the ions of interest. Calibration curves are constructed from which the concentration of each ion in the unknown sample is determined (EMEP Manual for Sampling and Chemical Analysis, 1996)

Sulfur dioxide, sulfate, nitrate, ammonium and nitric acid samples are analyzed with Dionex/DX-100 model spectrophometer with a flow rate of 200 ml/min. 0.002M Na_2CO_3 is used as the eluent and 1g/lt Merck standart solution is used in the analysis.

3.2.2. Determination of NO_2, NH_3, NH_4^+ by Spectrophotometry

NO_2 samples has been anaylzed with iodine method. In this method, nitrite (NO_2^-) and sulphanilamide form a diazo compound in acid solution which by a coupling reaction with NEDA, N-(1-naphthyl)-ethylenediamine-dihydrochloride, gives a red azo dye which is measured spectrophotometrically at 540 nm.

NH_3 and NH_4^+ are determined by spectrophotometric indophenol blue method. In an alkaline solution (pH 10.4-11.5) ammonium ions react with hypochlorite to form monochloramine. In the presence of phenol and an excess of hypochlorite, the monochloramine will form a blue colored compound, indophenol, when nitroprusside is used as catalyst.

The total concentration of ammonium and ammonia is determined by spectrophometrically at 630 nm measuring indophenol.

Unicam Philips Spectrophotometer is used for all parameters measured.

3.2.2. Determination of Pb, Cd, V, Mg, Ca, K by GF-AAS

Mg, Ca, K are determined by an atomic adsorption spectrophotometer. A small volume of sample is placed inside the sample compartment of the AAS, which then is heated by applying a voltage across its ends. The analyte is dissociated from its chemical bonds and the fraction of analyte atoms in the ground state will absorb portions of light from an external light source passing through it. The attenuation of the light beam is measured. As the analyte atoms are created and diffuse out of the tube, the absorption raises and falls in a peak-shaped signal. Beer-Lamberts law describes the relation between the measured attenuation and concentration of analyte. In order to determine Pb, Cd and V, atomic absorption spectrophotometer is coupled with a graphite atomization unit by locating a graphite tube in the sample compartment of the AAS.

In the analysis, Perkin Emler 1100 B Atomic Absorbtion Spectroscopy and HGA 700 Atomization Unit is used. The hollow cathode lamp for elements to be analyzed are placed and activated. After a 15 min warming period Mg, Ca, K, Pb, Cd, and V elements are determined at 285.2 nm, 422.7 nm, 766.5 nm, 217.0 nm, 228.8 nm and 319.6, respectively.

4. Data Quality Assurance

An EMEP Quality Assurance manager at the Chemical Coordinating Center and a National Quality Assurance manager of Turkey are

responsible for implementing harmonized quality assurance system, including documentation of standards and reference materials.

The overall goal of the quality assurance activities is to provide data which meet following EMEP Data Quality Objectives;

- 10% accuracy or better for oxidised sulphur and oxidised nitrogen in single analysis in the laboratory,
- 15–25% uncertainty for the combined sampling and chemical analysis,
- 90% data completeness of the daily values,
- 30% accuracy in annual average.

4.1. Field Operations

Field journeys in order to checks the quality of the field operations in general are conducted at every week, month, and year. In these journeys, sample locations, site surroundings, and changes since the last visit are noted and the equipment and instruments for sampling are checked and calibrated.

For gaseous and aerosol air pollutants accurate volume readings are most important for the resulting measurements accuracy, and the volume meters may need frequent calibration. The accuracy of an air volume meter should be better than 5%.

Weekly field blank samples are used to check possible sample contamination or sampling errors. A field blank sample is a sample which has been prepared, handled, and analyzed as a normal sample in every way, except that it has not intentionally been exposed, and therefore should not contain the substance to be determined. Detection limits for the measurements are calculated from field blanks as given in Section 4.2.

4.1. Determination of Accuracy

Chemical Coordinating Center of EMEP is the responsible for organizing the annual laboratory comparison exercises in order to determine the accuracy of a chemical analysis in the laboratory. It is, however, in principle not possible to assess the accuracy in air concentration measurements carried out at a site when accuracy is defined as the deviation from the true, and unknown, concentration. Even the comparability of the data is a severe problem with a widespread monitoring network involving a large number of different sampling methods and laboratories. It is, however, possible to determine the systematic errors (bias) relative to a reference measurement system and also to determine the precision of the measurements.

The systematic errors (bias) relative to a reference measurement system is determined by a parallel sampling between two systems. In this regard, the samples forwarded by EMEP are analyzed at the laboratories of the Ministry of Health Refik Saydam Hygiene Center. The results of the analysis are then forwarded back to Chemical Coordinating Center and compared with that of another laboratory in the EMEP Network.

The basis for an estimation of the measurement precision is a parallel sampling with two identical measurement devices following identical sampling and analytical procedures. The modified median absolute difference (M.MAD) which is the measure of precision used in this study. It is an estimator of the spread in the data which becomes equivalent to the standard deviation for normal distributions. In the latter case about 68 per cent of the data will be within one standard deviation from the average. The M.MAD is based on the median of the differences between the corresponding measurements which will be insensitive to the presence of a few extreme values.

4.2. Calculation of Detection Limit

The differences between measurements made on normal exposed samples and field blanks are used as the data interpreted in this study. The blank values are aggregated to interannual averages before used to correct measurement results.

Field blanks are also used in the detection limit calculations. Unexpected high blank values are not used for the corrections of measurements and calculations of detection limits. The related measurement results are flagged as less accurate than normal.

The detection limit can be calculated as follows:

$$L_d = 3.0 \cdot S_b$$

where S_b is the standard deviation defined as

$$S_b = \left(\frac{1}{N-1} \sum_{i=1}^{N} (C_i - \overline{C})^2 \right)$$

where N is the number of field blanks, C_i is the concentration of the relevant substance in the ith field blank and $\overline{C}$ is the field blank average after elimination of “extreme” blank values.

Calculated data points should be greater than the detection limits; however, in some cases they are found to be lower. In such situations, data user is able to take these data into account by keeping in mind their limitation.